

**ENVIRONMENTAL CHANGE AND ATMOSPHERIC  
CONTAMINATION ACROSS CHINA AS INDICATED  
BY LAKE SEDIMENTS  
(Joint Project Q741)**

**DATA REPORT FOR YEAR 1: JIANGSU**

Neil Rose <sup>1</sup>	Cai Shuming <sup>2</sup>
Peter Appleby <sup>3</sup>	Du Yun <sup>2</sup>
Helen Bennion <sup>1</sup>	Yi Chaolu <sup>2</sup>
John Boyle <sup>4</sup>	Yu Lizhong <sup>5</sup>
Dai Xue Rong <sup>5</sup>	

- 1. Environmental Change Research Centre, University College London, 26 Bedford Way, London, WC1H 0AP. UK.*
- 2. Institute of Geodesy & Geophysics, Chinese Academy of Sciences, 54 Xu Dong Road, Wuchang (430077), Hubei, P.R. of China*
- 3. Environmental Radioactivity Research Centre, Department of Mathematical Sciences, University of Liverpool, P.O.Box 147, Liverpool, L69 3BX, UK*
- 4. Department of Geography, University of Liverpool, P.O.Box 147, Liverpool, L69 3BX, UK*
- 5. Department of Geography, East China Normal University, Shanghai 200062, P.R. of China*

**October 2000**

## Contents

1. Introduction
2. Sites and sampling
3. Radiometric results Peter Appleby
4. Microfabric properties for Tai 1 Chaolu Yi
5. Grainsize analysis for Taihu and Chenghu Chaolu Yi
6. Environmental magnetic measurements (I) Du Yun
7. Magnetic measurements (II);  
Nitrogen and phosphorus analyses Dai Xue Rong
8. Sediment geochemistry John Boyle
9. Sediment lithostratigraphy  
and diatom analysis Helen Bennion
10. Spheroidal carbonaceous particles Neil Rose

## 1. Introduction

### 1.1. Project aims

In China, anthropogenic impact from changes in water quality, land-use and atmospheric deposition vary both spatially and temporally. There is a gradient across the country from the populous lowlands in the east, where considerable long-term impact on water bodies has resulted from centuries of agricultural and aquacultural practices superimposed by more recent, rapid industrial growth; to the mountainous west where many areas remain minimally impacted and any anthropogenic impact is restricted to long-range transport of atmospheric pollutants and change in climate. Currently, however, there is little information on temporal trends in atmospheric deposition.

The importance of water resources in China cannot be overestimated and therefore determining the extent, rate and direction of change in water quality is a national priority. In the absence of long-term monitoring programmes, lake sediments remain the only way whereby this information can be retrospectively determined at the necessary temporal scale to ascertain whether the causes of any detriment in quality are as a result of natural changes, or due to agricultural or industrial impacts.

Therefore, *the aim of this research programme is to use lake sediments from three regions of China to determine the extent to which impacts to lakes have changed through time and the causes of these changes.*

The project focuses on an east - west transect along the Yangtse River. The Middle and Lower Reaches of the Yangtse are undergoing exceptionally rapid economic and industrial development and this region is receiving a great deal of attention as the Three Gorges Dam undergoes construction. The three areas in which lakes are to be studied in this proposal are:

1. **Jiangsu Province in east China north of Shanghai.** Lowland sites. Lakes in this area are likely to have been impacted by long-term agriculture and may therefore may have become eutrophic. Atmospheric deposition may also be significant from local and regional industrial sources.
2. **The upper reaches of the Yangtse River, in Sichuan and Yunnan Provinces.** Lakes at 1-2000m. Lakes in this area may have been impacted by agriculture, but where possible sites will be selected where direct impact is minimal. Lakes may therefore be mesotrophic but sources of atmospherically derived industrial pollutants are likely to be remote.
3. **The Tibetan Plateau.** Lakes at 4 - 5000m. 'Control' sites in a pristine area with minimal human influence. Sediment cores from these sites will be used to determine background levels of atmospherically deposited contaminants. Oligotrophic (low nutrient) sites on sensitive geology (low acid neutralising capacity e.g. granites) will be selected where possible.

By including earlier collaborative work between the participating institutes (funded by the Royal Society and the Chinese Academy of Sciences) on the lake sediment records on the Jiangnan Plain and research currently being undertaken on lakes in the Shennongjia region in western Hubei (NNFSC funded), this study will produce a transect of lakes from five regions providing a unique database on the historical impact of human activity on the freshwater environment.

### 1.2. Year 1.

The aims of Year 1 were to collect sediment cores from the Jiangsu region near Shanghai and return the samples to Wuhan, Shanghai, Liverpool and London for screening to select the best sites and cores, followed by more detailed analysis on those selected. These analyses were undertaken by all participants, with colleagues from Wuhan visiting the UK in early 1999 in order to pursue more detailed analysis. The field sampling of this first area took place in October 1998, with Dr Helen Bennion (UCL) and Dr Peter Appleby (Liverpool) visiting the Shanghai region. This work was coordinated by Prof Cai Shuming (Wuhan) and Prof. Yu Lizhong (Shanghai).

### 1.3. This report

This report contains the data obtained from the analyses of the sediment cores collected in the Jiangsu Region. It is intended, primarily, for circulation within the project group in order that all participants

have access to all the data, and all have the same versions of that data. The reports that follow are simply a compilation of the data reports produced by the analysts. Only the interpretations of the analysts are included and no attempt has been made to bring together analyses or to draw overall conclusions. That will be the purpose of papers derived from this and subsequent reports.

## Acknowledgements

We would like to acknowledge the financial support of the Royal Society and the Chinese Academy of Sciences without whom this project would not have been possible.

## 2. Sites and sampling

Table 1 - Summary table of core locations- October 1998

Coring site	Latitude	Longitude	Water depth
<u>Lake sediment cores:</u>			
TAI 1	31° 27.562' N	120° 08.924' E	??
TAI 2	31° 29.365' N	120° 11.030' E	2.8 m
TAI 3	31° 18.110' N	120° 03.030' E	2.8 m
TAI 4	31° 19.917' N	120° 04.791' E	2.5 m
GEHU 1	31° 31.882' N	119° 48.331' E	1.7 m
CHEN 1	31° 14.675' N	120° 48.794' E	2.3 m
CHEN 2	31° 13.683' N	120° 52.004' E	2.5 m
<u>Soil cores:</u>			
THS 1	31° 25.372' N	120° 07.575' E	
THS 2	31° 25.204' N	120° 07.606' E	
THS 3 and 4	31° 10.403' N	119° 54.839' E	

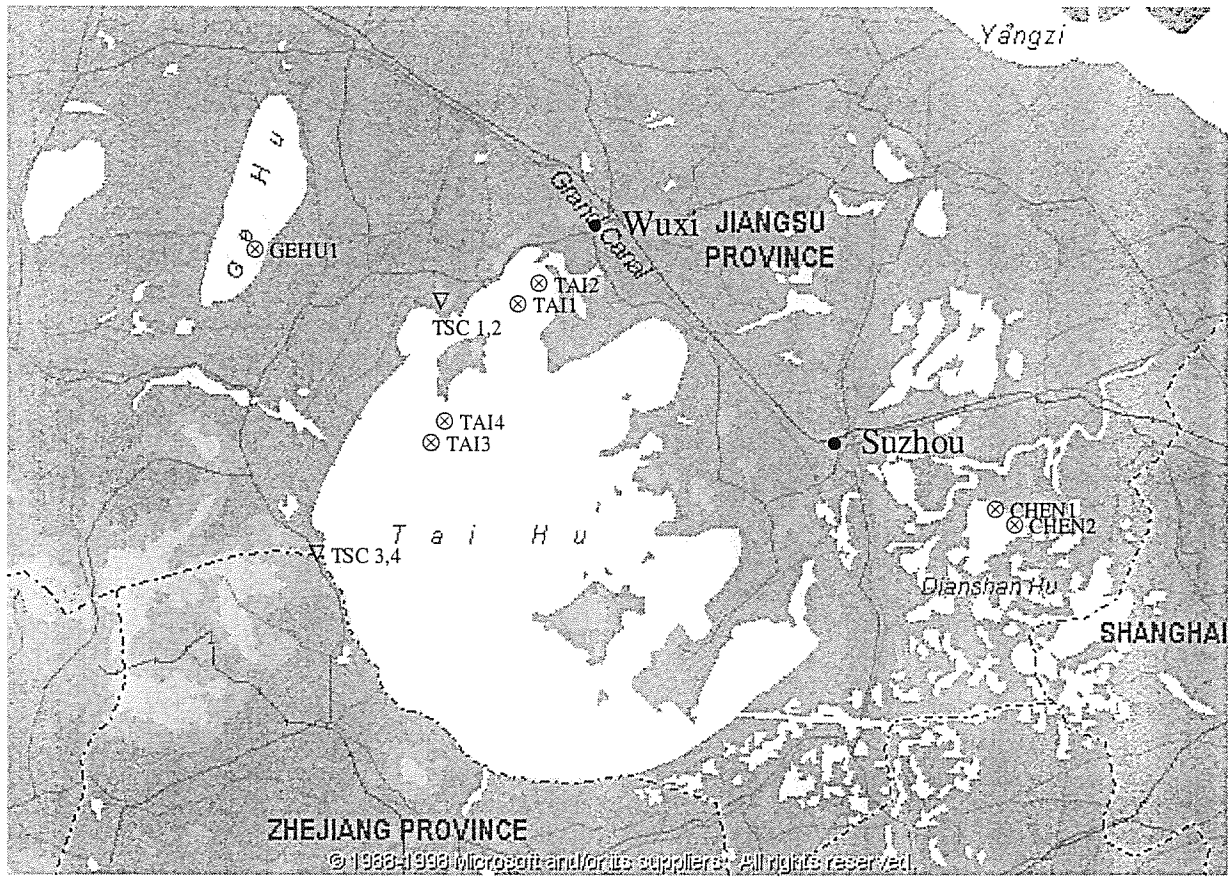
Table 2 - Summary of core codes- collected October 1998:

Site name	Short cores	Length	Long cores	Soil cores
Tai Hu	TAI 1S	0-30cm	TAI 1-1L TAI 1-2L	THS 1 THS 2
	TAI 2S	0-19cm	TAI 2-1L TAI 2-2L	THS 3 THS 4 (duplicate THS3)
	TAI 3S	0-20cm	TAI 3-1L TAI 3-2L	
	TAI 4S	0-25cm	TAI 4-1L only	
Ge Hu	GEHU 1S	0-20cm	GEHU 1-1L only	
Cheng Hu	CHEN 1S	0-15cm	CHEN 1-1L CHEN 1-2L	
	CHEN 2S	0-28cm	CHEN 2-2L only	

### Footnote

Note that long cores coded with a suffix "-1" were kept in the tubes and those coded with "-2" were sectioned in the field

Figure 1. Map showing core locations



### 3. Radiometric Results from Jiangsu Province

P.G.Appleby  
Environmental Radioactivity Research Centre  
University of Liverpool

#### 1. Atmospheric Deposition of Radionuclides

Good estimates of the atmospheric deposition of fallout radionuclides are essential to their use as tools in deciphering lake sediment records, both for dating and as a tracer for identifying the main pathways by which atmospheric pollutants are delivered to the sediments. There are very few reliable data on  $^{210}\text{Pb}$  and  $^{137}\text{Cs}$  fallout for China and the objective of this part of the program was to determine atmospheric fluxes in the three regions of China in which lake sediments will be studied. This report presents results from the Year 1 field trip to Jiangsu Province, east China.

#### Methods

Fallout was determined via the accumulated inventories in soil cores collected from 3 sites adjacent to Taihu. As far as could be determined they were from undisturbed locations selected according to the criteria:

1. there should have been no major soil disturbance for at least 30 years, and preferably longer,
2. soil types should be of a type that inhibits radionuclide migration through the soil column,
3. they should be on open level ground not subject to erosion or flooding by surface waters,
4. the soils should be relatively compact and saturated (so as to minimise in situ  $^{222}\text{Rn}$  escape),
5. the soil depth should be sufficient contain the entire fallout inventory.

The locations of the cores sites are shown in Figure 1 and Table 1.

At each site sharpened plastic tubes were driven into the soil taking care to avoid compaction. The tubes were then dug out and the soil extruded at 2 cm sections down to 12 cm and thereafter at 3cm. The *in situ* volume of each core slice was recorded, and the dry bulk density determined by drying overnight at 40°C. The dried samples from cores TSC1, TSC2, TSC4 were analysed for fallout  $^{210}\text{Pb}$ ,  $^{137}\text{Cs}$  and  $^{241}\text{Am}$  by gamma spectrometry (Appleby *et al.* 1986) at the University of Liverpool ERRC to determine the fallout inventories. Core TSC3 is being analysed at East China Normal University.

Table 1 Locations of Taihu soil cores

Core	Latitude	Longitude
THS 1	31° 25.37' N	120° 07.58' E
THS 2	31° 25.20' N	120° 07.61' E
THS 3 and 4	31° 10.40' N	119° 54.84' E

#### Results

Figure 2 shows radionuclide concentrations versus depth (measured as  $\text{gDM cm}^{-2}$ ). Table 2 gives the unsupported  $^{210}\text{Pb}$  and  $^{137}\text{Cs}$  inventories of each soil core calculated by numerical integration of the concentration versus depth profiles and the mean  $^{210}\text{Pb}$  flux required to sustain the  $^{210}\text{Pb}$  inventory. The  $^{137}\text{Cs}$  inventory is also expressed in nominal terms that discount the effect of radioactive decay since deposition from the atmosphere. These values are independent of the sampling date. Also shown are the (normalised)  $^{137}\text{Cs}/^{210}\text{Pb}$  inventory ratios.

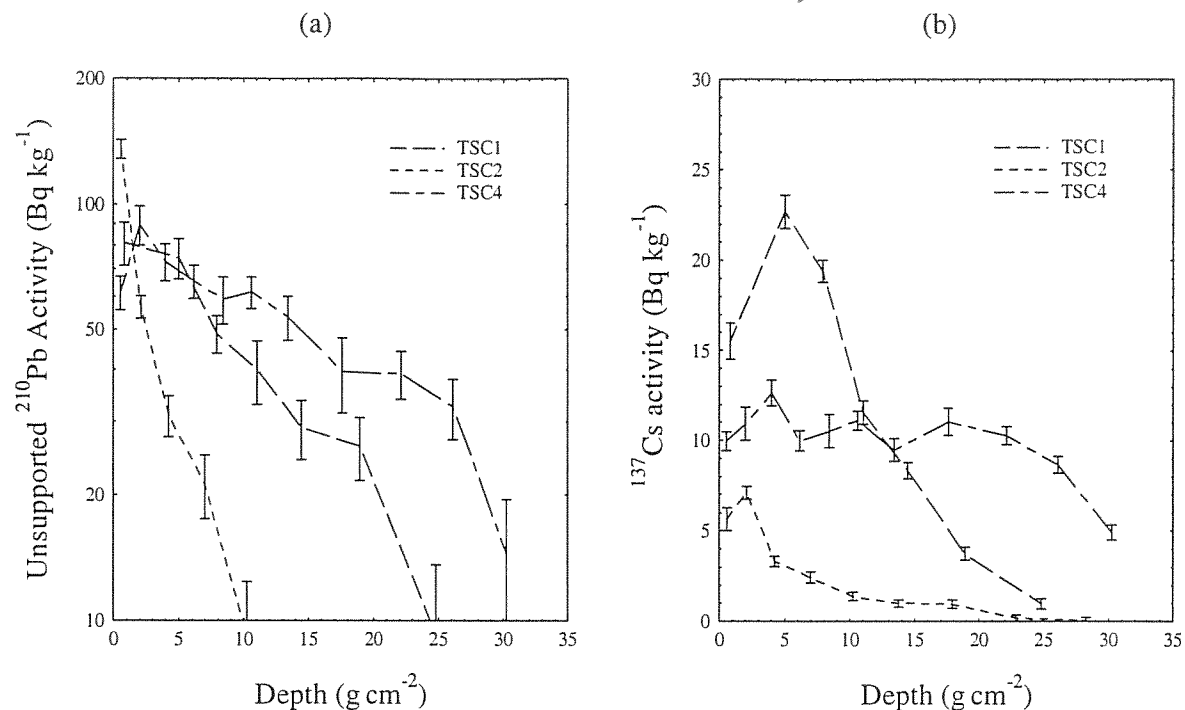


Figure 2 Fallout radionuclides in Taihu soil cores showing (a) unsupported  $^{210}\text{Pb}$  and (b)  $^{137}\text{Cs}$  activity versus depth.

The radionuclide profiles suggest that the soils have been relatively stable for a number of decades. Concentrations decline fairly regularly with depth though there are significant differences between individual cores. For  $^{210}\text{Pb}$  the depths containing 90% of the total inventory range from 13 cm ( $17 \text{ g cm}^{-2}$ ) in TSC2 to 26 cm ( $31 \text{ g cm}^{-2}$ ) in TSC4. There are similar differences in the  $^{137}\text{Cs}$  90% penetration depths which range from 13 cm in TSC2 to 23 cm in TSC4.

$^{210}\text{Pb}$  inventories in the three cores vary by a factor of 3 and represent  $^{210}\text{Pb}$  fluxes ranging from  $177\text{-}540 \text{ Bq m}^{-2} \text{ y}^{-1}$ . The mean value of  $352 \text{ Bq m}^{-2} \text{ y}^{-1}$  is comparable to other data from China and Japan and represents at this stage the best estimate of  $^{210}\text{Pb}$  fallout in Jiangsu.  $^{137}\text{Cs}$  inventories are usually more varied than those of  $^{210}\text{Pb}$  due to the greater mobility of this radionuclide. Values in the Taihu cores range from  $1170\text{-}6800 \text{ Bq m}^{-2}$  with a mean of  $4760 \text{ Bq m}^{-2}$ . This is comparable with the expected value at this latitude of  $3000\text{-}5500 \text{ Bq m}^{-2}$  based on global studies of  $^{137}\text{Cs}$  fallout and again represents at this stage the best estimate of  $^{137}\text{Cs}$  fallout in Jiangsu.

Table 2 Radionuclide Inventories and Fluxes from Taihu Soil Cores

Core	$^{210}\text{Pb}$ Inventory		Flux		$^{137}\text{Cs}$ Inventory		Nominal $^{137}\text{Cs}$ $^{210}\text{Pb}$ Ratio	
	$\text{Bq m}^{-2}$	$\pm$	$\text{Bq m}^{-2} \text{ y}^{-1}$	$\pm$	$\text{Bq m}^{-2}$	$\pm$		
TSC1	11475	740	357	23	2810	85	6320	0.55
TSC2	5680	350	177	11	520	30	1170	0.21
TSC4	16790	1090	523	34	3020	80	6800	0.41
Mean	11310		352		2120		4760	0.42

## 2. Radiometric Dating of Lake Sediment Cores

### Methods

Four sediment cores were collected from Taihu, two from Chenghu and one from Gehu using a Glew core of tube diameter 7 cm. Details of the cores and their locations are given in Figure 1 and Table 3. The cores were sectioned at 1 cm intervals and subsamples from each section sent to the University of Liverpool ERRC for  $^{210}\text{Pb}$ ,  $^{226}\text{Ra}$  and  $^{137}\text{Cs}$  and  $^{241}\text{Am}$  analysis by gamma spectrometry. The cores were all screened for the quality of their records of fallout radionuclides and three, TAI1, TAI4 and CHEN2 chosen for more detailed studies. These were dated by  $^{210}\text{Pb}$  and  $^{137}\text{Cs}$  using the methods described in Appleby & Oldfield 1978 and Appleby 1998.

Table 3 Locations of Jiangsu sediment cores

Coring site	Latitude	Longitude	Water depth
TAI 1	31° 27.56' N	120° 08.92' E	
TAI 2	31° 29.38' N	120° 11.03' E	2.8 m
TAI 3	31° 18.11' N	120° 03.03' E	2.8 m
TAI 4	31° 19.94' N	120° 04.79' E	2.5 m
GEHU 1	31° 31.88' N	119° 48.33' E	1.7 m
CHEN 1	31° 14.68' N	120° 48.79' E	2.3 m
CHEN 2	31° 13.68' N	120° 52.00' E	2.5 m

### Results

The results of the radiometric measurements are given in Tables 4-6 and shown graphically in Figures 3.i-5.i. Table 7 summarises a number of parameters from each dated core. Radiometric chronologies are shown in Tables 8-10 and Figures 3.ii-5.ii.

#### *Taihu core TAI1*

##### *Lead-210 Activity*

$^{210}\text{Pb}$  activity declines irregularly with depth (Figure 3.i(a)). There is little net decline in the top 20 cm of the core and the maximum value occurs at a depth of 14.5 cm. Unsupported concentrations decline abruptly below 25 cm (Figure 3.i(b)) and equilibrium with the supporting  $^{226}\text{Ra}$  is apparently reached in the basal sample at 30 cm.

##### *Artificial Fallout Radionuclides*

The  $^{137}\text{Cs}$  activity versus depth profile (Figure 3.i(c)) has a relatively well resolved peak between 18-25 cm that most likely records the 1963 fallout maximum from the atmospheric testing of nuclear weapons. The presence of this peak together with the sharp decline in concentrations above c.18 cm suggests that the irregular  $^{210}\text{Pb}$  record is not due to mixing.

##### *Core Chronologies*

Figure 3.ii compares CRS model  $^{210}\text{Pb}$  dates with the 1963 date inferred from the  $^{137}\text{Cs}$  stratigraphy. There is a significant discrepancy between the two methods, the  $^{210}\text{Pb}$  chronology placing 1963 at a depth of c.15.5 cm. This is almost certainly due to an incomplete recovery of the  $^{210}\text{Pb}$  inventory. Revised  $^{210}\text{Pb}$  dates calculated using the  $^{137}\text{Cs}$  date as a reference point (also shown in Figure 3.ii) suggest a mean accumulation rate of  $0.30 \text{ g cm}^{-2} \text{ y}^{-1}$  ( $0.41 \text{ cm y}^{-1}$ ) between 1952-86, increasing during the past decade to  $0.52 \text{ g cm}^{-2} \text{ y}^{-1}$  ( $0.88 \text{ cm y}^{-1}$ ). Since the mean post-1963  $^{210}\text{Pb}$  flux ( $760 \text{ Bq m}^{-2} \text{ y}^{-1}$ , see Table 7), is more than twice the atmospheric flux, these values almost certainly reflect intensive sediment focussing at the core site. Primary sedimentation rates are probably less than half the above values.



Extrapolation of the  $^{210}\text{Pb}$  chronology dates the base of the core at 30 cm to c.1934. Detailed results are given in Table 8.

### **Taihu core TAI4**

#### *Lead-210 Activity*

$^{210}\text{Pb}$  activity again declined irregularly with depth (Figure 4.i(a)). There is little net decline in the top 7 cm of the core though beneath this depth concentrations of fallout  $^{210}\text{Pb}$  decline abruptly (Figure 4.i(b)) and only traces were detected in the deeper layers.

#### *Artificial Fallout Radionuclides*

The  $^{137}\text{Cs}$  activity versus depth profile (Figure 4.i(c)) has a relatively well resolved peak between 5-8 cm that most likely records the 1963 fallout maximum from the atmospheric testing of nuclear weapons. The presence of this peak together with the greatly reduced concentrations in the top 5 cm suggests that the irregular  $^{210}\text{Pb}$  record is not due to mixing.

#### *Core Chronologies*

Figure 4.ii compares CRS model  $^{210}\text{Pb}$  dates with the 1963 date inferred from the  $^{137}\text{Cs}$  stratigraphy. There is again a discrepancy, though less so than in TAI1. The  $^{210}\text{Pb}$  chronology places 1963 at between 5-5.5 cm. Corrected  $^{210}\text{Pb}$  dates were calculated using the  $^{137}\text{Cs}$  date as a reference point. The results are shown in Figure 4.ii and Table 9. The mean post-1963 sedimentation rate is calculated to be  $0.13 \text{ g cm}^{-2} \text{ y}^{-1}$  ( $0.19 \text{ cm y}^{-1}$ ). Since the mean  $^{210}\text{Pb}$  flux during this period (Table 7) is comparable to the atmospheric flux, these values may provide a better estimate of primary sedimentation rates in Taihu. It is uncertain whether the episode of very rapid sedimentation in the early 1950s is a real event or an artifact of the calculations arising from the incompleteness of the  $^{210}\text{Pb}$  record.

### **Chenghu core CHEN2**

#### *Lead-210 Activity*

There was little net change in  $^{210}\text{Pb}$  activity throughout the core. Concentrations in the basal sample (28 cm) were still well in excess of the supporting  $^{226}\text{Ra}$  (Figure 5.i(a,b)).

#### *Artificial Fallout Radionuclides*

The  $^{137}\text{Cs}$  activity versus depth profile (Figure 5.i(c)) has a relatively well resolved peak between 18-23 cm that most likely records the 1963 fallout maximum from the atmospheric testing of nuclear weapons. The presence of this peak together with the sharp decline in concentrations above 18 cm suggests that the irregular  $^{210}\text{Pb}$  record is not due to mixing.

#### *Core Chronologies*

Because of the incompleteness of the  $^{210}\text{Pb}$  record it was necessary to use the 1963  $^{137}\text{Cs}$  date as a reference point at the outset. The results of these calculations are shown in Figure 5.ii and Table 10. Sedimentation rates during 1960-96 appear to have been relatively constant, with a mean value of  $0.40 \text{ g cm}^{-2} \text{ y}^{-1}$  ( $0.59 \text{ cm y}^{-1}$ ). Values may have been slightly lower during the 1960s. Extrapolation of the chronology dates the base of the core at 28 cm to c.1946. The mean post-1963  $^{210}\text{Pb}$  flux (Table 7), a little higher than the atmospheric flux. These results may thus reflect a moderate degree of sediment focussing at the core site.

### **References**

- Appleby, P.G., 1998. Dating recent sediments by  $^{210}\text{Pb}$ : Problems and solutions. Proc. 2nd NKS/EKO-1 Seminar, Helsinki, 2-4 April 1997, STUK, Helsinki, pp7-24.
- Appleby, P.G., P.J.Nolan, D.W.Gifford, M.J.Godfrey, F.Oldfield, N.J.Anderson & R.W.Battarbee, 1986.  $^{210}\text{Pb}$  dating by low background gamma counting. *Hydrobiologia*, **141**:21-27.
- Appleby, P.G. & F.Oldfield, 1978. The calculation of  $^{210}\text{Pb}$  dates assuming a constant rate of supply of unsupported  $^{210}\text{Pb}$  to the sediment. *Catena*, **5**:1-8

Table 4 Fallout radionuclide concentrations in Taihu sediment cores

## (a) Core TAI1

Depth		$^{210}\text{Pb}$						$^{137}\text{Cs}$	
cm	g cm <sup>-2</sup>	Total		Unsupported		Supported		Bq kg <sup>-1</sup>	±
		Bq kg <sup>-1</sup>	±	Bq kg <sup>-1</sup>	±	Bq kg <sup>-1</sup>	±		
2.5	1.3	185.0	12.8	135.7	13.0	49.3	2.4	9.4	1.8
4.5	2.5	155.7	10.6	105.5	10.9	50.2	2.5	13.2	2.2
8.5	5.0	172.4	7.7	128.1	7.8	44.3	1.5	9.8	0.9
10.5	6.3	159.8	10.2	111.2	10.4	48.6	2.3	10.5	1.7
14.5	9.1	208.3	13.0	167.1	13.3	41.2	2.6	16.7	2.0
20.5	13.1	124.7	7.8	78.3	8.0	46.5	1.9	39.3	2.0
24.5	16.7	100.9	9.5	55.5	9.7	45.3	1.8	32.6	1.7
29.5	21.5	43.1	5.5	0.2	5.6	42.9	1.3	3.0	0.8

## (b) Core TAI2

Depth		$^{210}\text{Pb}$						$^{137}\text{Cs}$	
cm	g cm <sup>-2</sup>	Total		Unsupported		Supported		Bq kg <sup>-1</sup>	±
		Bq kg <sup>-1</sup>	±	Bq kg <sup>-1</sup>	±	Bq kg <sup>-1</sup>	±		
2.5	1.4	166.5	9.9	117.2	10.0	49.2	1.8	7.6	1.3
6.5	3.9	166.1	9.9	118.0	10.0	48.1	1.8	7.7	1.1

## (c) Core TAI3

Depth		$^{210}\text{Pb}$						$^{137}\text{Cs}$	
cm	g cm <sup>-2</sup>	Total		Unsupported		Supported		Bq kg <sup>-1</sup>	±
		Bq kg <sup>-1</sup>	±	Bq kg <sup>-1</sup>	±	Bq kg <sup>-1</sup>	±		
2.5	1.2	211.1	16.9	154.9	17.2	56.2	3.1	4.3	2.2
6.5	4.1	32.0	6.0	-18.5	6.2	50.4	1.6	0.6	0.7

## (d) Core TAI4

Depth		$^{210}\text{Pb}$						$^{137}\text{Cs}$	
cm	g cm <sup>-2</sup>	Total		Unsupported		Supported		Bq kg <sup>-1</sup>	±
		Bq kg <sup>-1</sup>	±	Bq kg <sup>-1</sup>	±	Bq kg <sup>-1</sup>	±		
0.5	0.2	159.7	11.0	106.4	11.3	53.3	2.8	6.7	2.4
2.5	1.5	176.0	9.5	121.5	9.7	54.6	1.9	4.9	1.2
4.5	2.9	150.7	7.2	98.3	7.4	52.4	1.6	10.2	0.9
6.5	4.5	139.8	7.5	92.5	7.7	47.3	1.8	16.3	1.6
8.5	6.2	48.1	6.4	7.6	6.5	40.5	1.2	1.2	0.7
10.5	8.0	52.6	7.4	17.8	7.6	34.8	1.7	0.9	1.1
15.5	12.8	37.5	3.7	-3.1	3.9	40.6	1.1	0.0	0.0

Table 5 Fallout radionuclide concentrations in Chenghu sediment cores

## (a) Core CHEN1

Depth		$^{210}\text{Pb}$						$^{137}\text{Cs}$	
cm	$\text{g cm}^{-2}$	Total		Unsupported		Supported		Bq $\text{kg}^{-1}$	$\pm$
		Bq $\text{kg}^{-1}$	$\pm$	Bq $\text{kg}^{-1}$	$\pm$	Bq $\text{kg}^{-1}$	$\pm$		
2.5	1.8	84.8	8.3	44.1	8.5	40.7	1.8	1.3	1.2
6.5	5.0	85.5	7.9	38.7	8.1	46.8	1.6	1.2	0.9

## (b) Core CHEN2

Depth		$^{210}\text{Pb}$						$^{137}\text{Cs}$	
cm	$\text{g cm}^{-2}$	Total		Unsupported		Supported		Bq $\text{kg}^{-1}$	$\pm$
		Bq $\text{kg}^{-1}$	$\pm$	Bq $\text{kg}^{-1}$	$\pm$	Bq $\text{kg}^{-1}$	$\pm$		
0.5	0.3	111.3	12.8	52.9	13.0	58.3	2.6	2.0	1.9
2.5	1.3	139.8	12.8	81.6	13.2	58.3	3.0	2.0	2.0
4.5	2.4	147.1	10.3	97.0	10.6	50.1	2.2	1.0	1.4
6.5	3.8	115.5	9.3	64.0	9.6	51.5	2.4	0.7	1.8
8.5	5.2	107.2	8.0	60.5	8.3	46.7	1.9	1.7	0.9
10.5	6.6	101.3	8.7	56.6	8.9	44.7	1.8	0.9	1.1
15.5	10.4	100.3	9.4	52.4	9.5	47.9	1.8	0.5	1.0
20.5	14.2	86.9	9.1	36.0	9.3	50.9	1.9	5.3	1.2
25.5	18.2	94.9	7.6	52.2	7.8	42.7	1.6	1.6	1.0
27.5	19.8	103.6	8.1	56.4	8.2	47.2	1.6	1.0	0.9

Table 6 Fallout radionuclide concentrations in Gehu sediment core

Depth		$^{210}\text{Pb}$						$^{137}\text{Cs}$	
cm	$\text{g cm}^{-2}$	Total		Unsupported		Supported		Bq $\text{kg}^{-1}$	$\pm$
		Bq $\text{kg}^{-1}$	$\pm$	Bq $\text{kg}^{-1}$	$\pm$	Bq $\text{kg}^{-1}$	$\pm$		
2.5	1.5	72.6	34.7	8.5	8.6	37.8	1.5	0.5	0.8
6.5	4.7	58.8	22.2	5.6	5.7	36.6	1.2	1.0	0.5

Table 7 Fallout parameters for Jiangsu sediment cores

	$^{210}\text{Pb}$			$^{137}\text{Cs}$	$^{137}\text{Cs}/^{210}\text{Pb}$
	Surface conc Bq $\text{kg}^{-1}$	Inventory Bq $\text{m}^{-2}$	Flux Bq $\text{m}^{-2}\text{y}^{-1}$	Inventory Bq $\text{m}^{-2}$	Ratio
TAI1	185	19067	761	9715	0.51
TAI4	160	5896	223	1334	0.23
CHEN1	111	12574	392	861	0.07
Fallout		11150	347	2095	0.42

Table 8  $^{210}\text{Pb}$  chronology of Taihu core TAI1

Depth		Chronology			Sedimentation Rate		
cm	$\text{g cm}^{-1}$	Date AD	Age y	$\pm$	$\text{g cm}^{-2} \text{y}^{-1}$	$\text{cm y}^{-1}$	$\pm$ (%)
0.0	0.00	1998	0				
2.0	1.02	1996	2	1	0.53	0.97	15
4.0	2.17	1994	4	2	0.60	1.00	16
6.0	3.41	1992	6	2	0.56	0.89	16
8.0	4.68	1989	9	2	0.47	0.73	16
10.0	6.00	1987	11	2	0.46	0.68	18
12.0	7.39	1983	15	3	0.38	0.56	20
14.0	8.80	1978	20	4	0.30	0.44	24
16.0	10.14	1974	24	5	0.30	0.45	24
18.0	11.45	1969	29	6	0.30	0.46	24
20.0	12.77	1965	33	7	0.30	0.40	24
22.0	14.45	1959	39	9	0.30	0.35	24
24.0	16.25	1953	45	11	0.30	0.31	24
26.0	18.3	1947	51		0.30	0.31	
28.0	20.2	1940	58		0.30	0.31	
30.0	22.0	1934	64		0.30	0.31	

Table 9  $^{210}\text{Pb}$  chronology of Taihu core TAI4

Depth		Chronology			Sedimentation Rate		
cm	$\text{g cm}^{-1}$	Date AD	Age y	$\pm$	$\text{g cm}^{-2} \text{y}^{-1}$	$\text{cm y}^{-1}$	$\pm$ (%)
0.0	0.00	1998	0				
1.0	0.57	1995	3	2	0.19	0.30	19
2.0	1.22	1991	7	2	0.15	0.24	21
3.0	1.88	1986	12	3	0.14	0.20	23
4.0	2.56	1981	17	4	0.13	0.18	26
5.0	3.29	1975	23	6	0.11	0.15	32
6.0	4.09	1967	31	8	0.09	0.12	40
7.0	4.92	1961	37	11	0.25	0.29	59
8.0	5.77	1956	42	13	0.58	0.67	88
9.0	6.65	1953	45	15	0.63	0.72	97
10.0	7.55	1951	47	16	0.40	0.44	84

Table 10  $^{210}\text{Pb}$  chronology of Chenghu core CHEN2

Depth		Chronology			Sedimentation Rate		
cm	$\text{g cm}^{-1}$	Date AD	Age y	$\pm$	$\text{g cm}^{-2} \text{y}^{-1}$	$\text{cm y}^{-1}$	$\pm$ (%)
0.0	0.0	1998	0				
2.0	1.1	1996	2	2	0.52	0.96	21
4.0	2.2	1994	4	2	0.37	0.63	17
6.0	3.4	1990	8	2	0.44	0.66	19
8.0	4.8	1987	11	2	0.46	0.66	19
10.0	6.2	1984	14	2	0.44	0.61	21
12.0	7.7	1981	17	3	0.41	0.55	23
14.0	9.2	1977	21	3	0.38	0.50	25
16.0	10.8	1973	25	4	0.35	0.45	27
18.0	12.3	1968	30	5	0.35	0.45	31
20.0	13.9	1964	34	6	0.35	0.45	36
22.0	15.4	1959	39	8	0.35	0.44	40
24.0	17.0	1955	43	11	0.35	0.44	44
26.0	18.6	1950	48	14	0.35	0.45	49
28.0	20.1	1946	52		0.35	0.45	

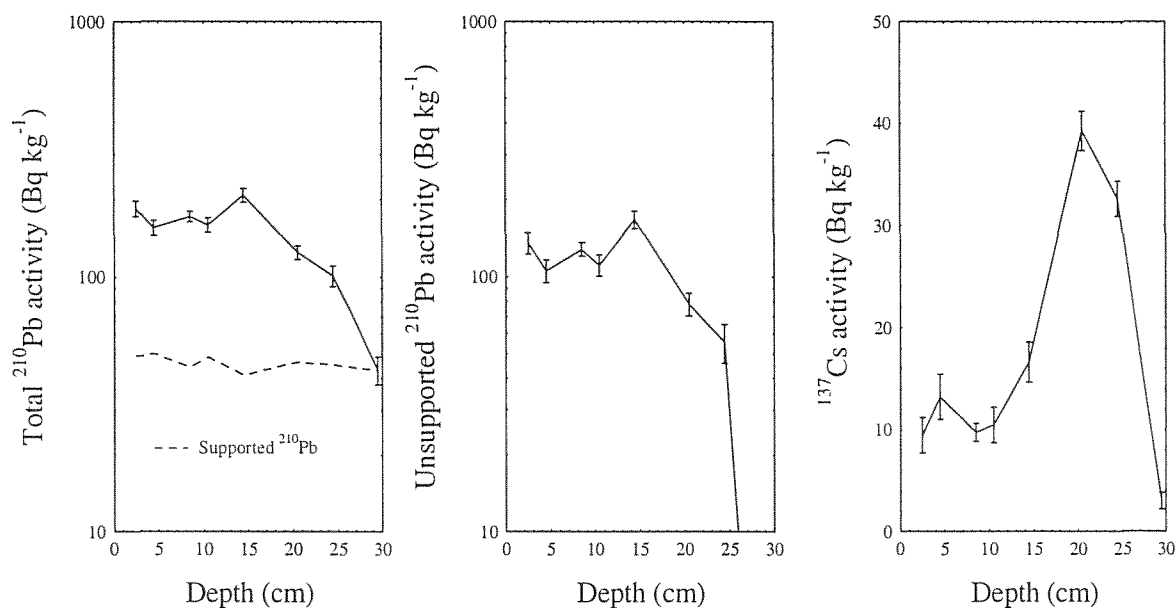


Figure 3.i Fallout radionuclide concentrations in Taihu core TAI1 showing (a) total and supported  $^{210}\text{Pb}$ , (b) unsupported  $^{210}\text{Pb}$ , (c)  $^{137}\text{Cs}$ .

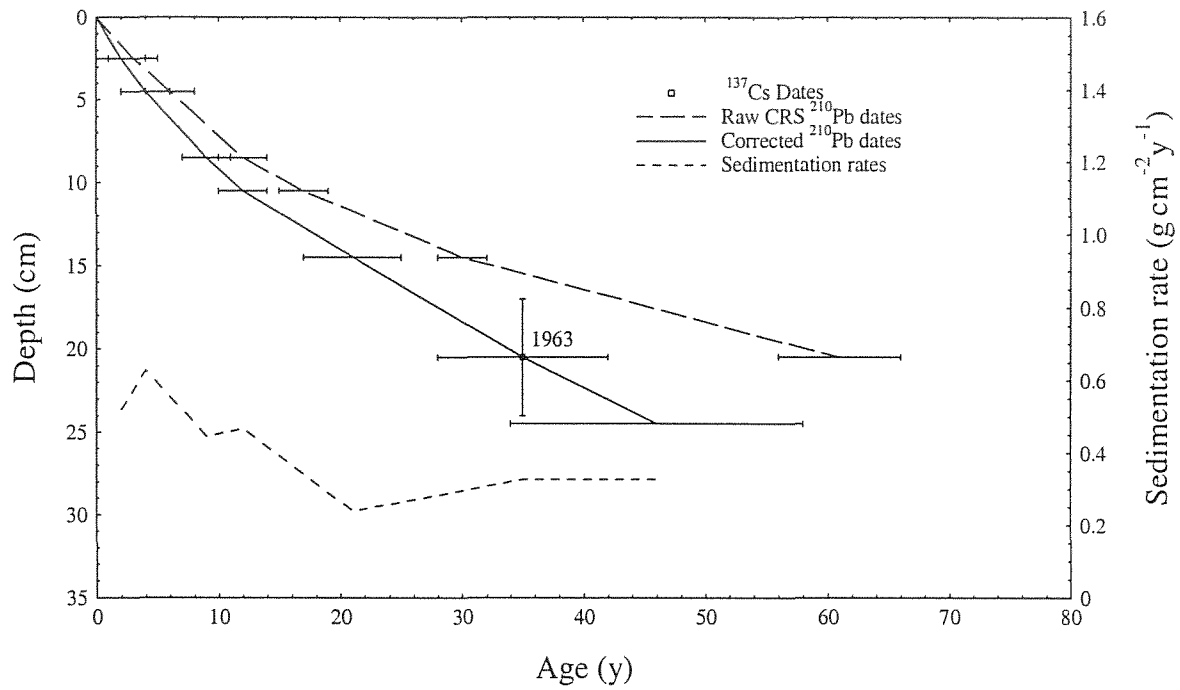


Figure 3.ii Radiometric chronology of Taihu core TAI1 showing CRS model  $^{210}\text{Pb}$  dates together with the 1963 depth determined from the  $^{137}\text{Cs}$  stratigraphy. Also shown are corrected  $^{210}\text{Pb}$  dates and sedimentation rates calculated using the  $^{137}\text{Cs}$  date as a reference point.

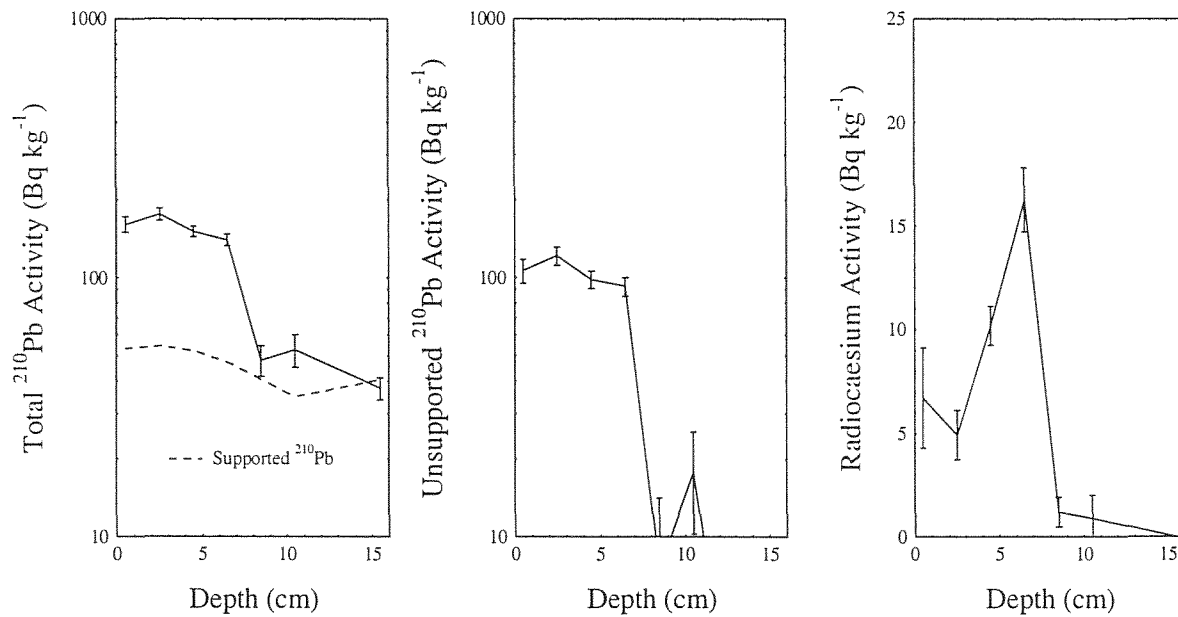


Figure 4.i Fallout radionuclide concentrations in Taihu core TAI4 showing (a) total and supported  $^{210}\text{Pb}$ , (b) unsupported  $^{210}\text{Pb}$ , (c)  $^{137}\text{Cs}$ .

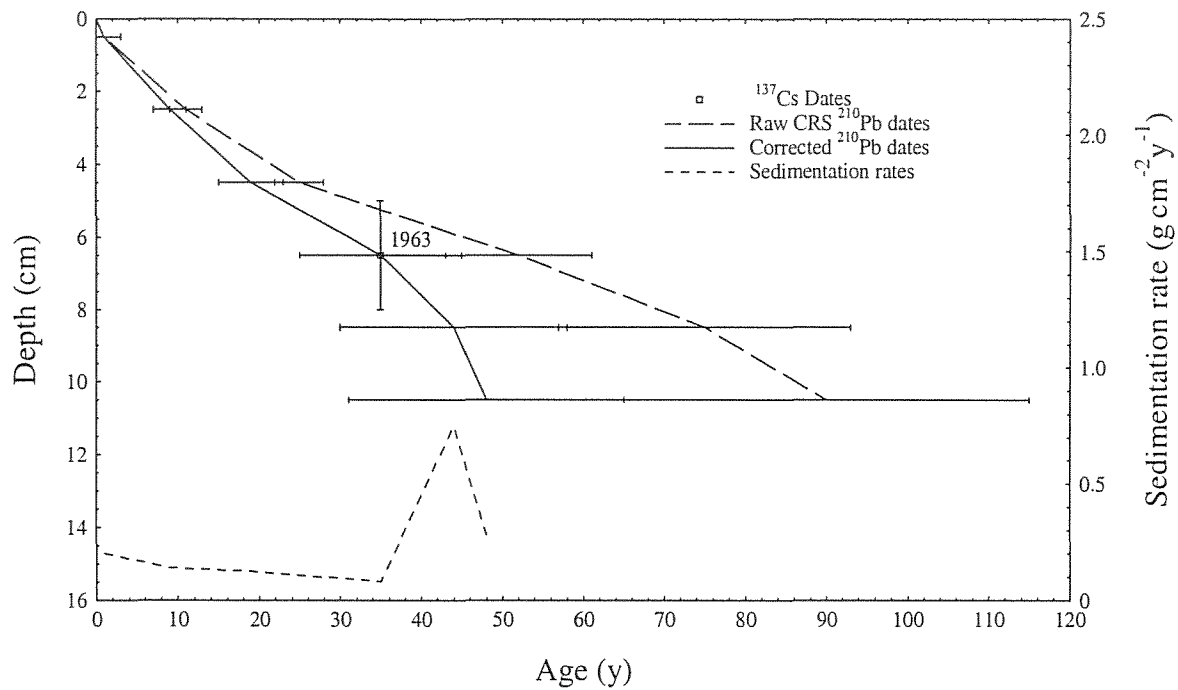


Figure 4.ii Radiometric chronology of Taihu core TAI4 showing CRS model  $^{210}\text{Pb}$  dates together with the 1963 depth determined from the  $^{137}\text{Cs}$  stratigraphy. Also shown are corrected  $^{210}\text{Pb}$  dates and sedimentation rates calculated using the  $^{137}\text{Cs}$  date as a reference point.

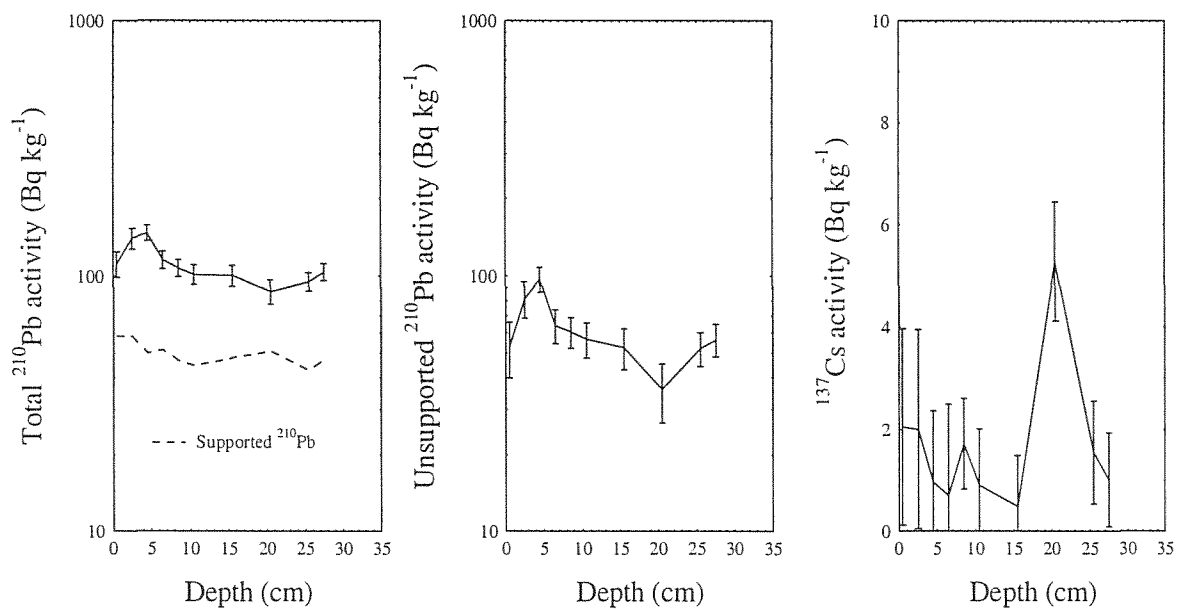


Figure 5.i Fallout radionuclide concentrations in Chenghu core CHEN2 showing (a) total and supported  $^{210}\text{Pb}$ , (b) unsupported  $^{210}\text{Pb}$ , (c)  $^{137}\text{Cs}$ .

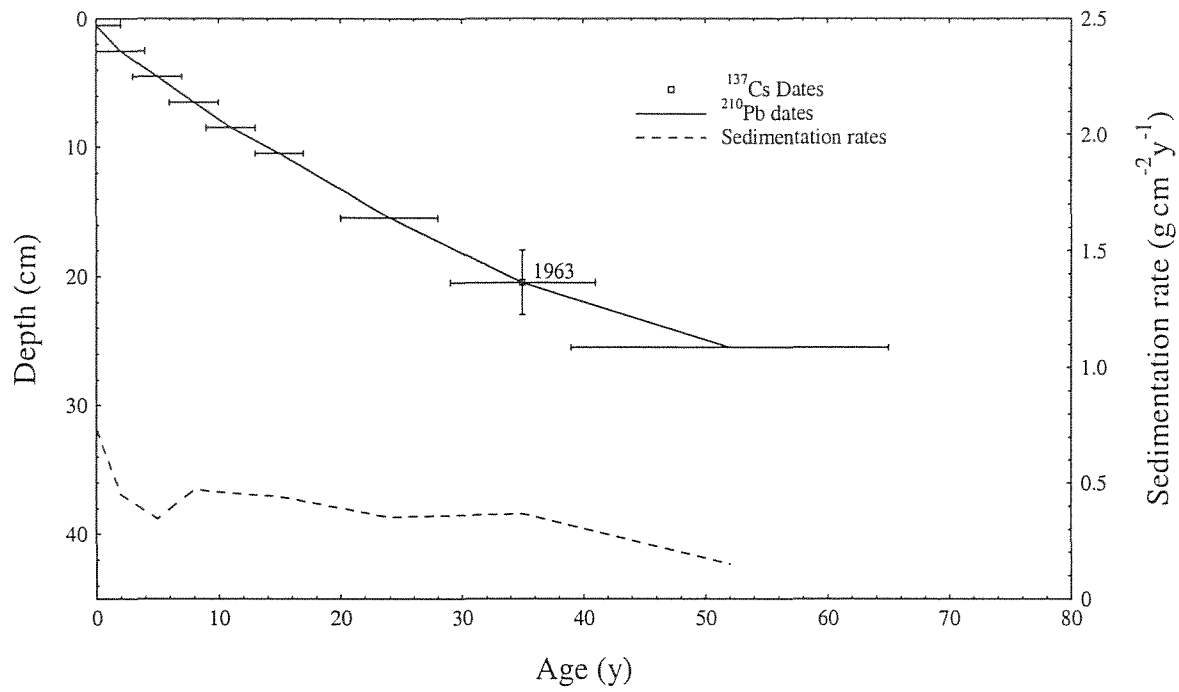


Figure 5.ii Radiometric chronology of Chenghu core CHEN2 showing the 1963 depth determined from the  $^{137}\text{Cs}$  stratigraphy and the CRS model  $^{210}\text{Pb}$  dates and sedimentation rates calculated using the  $^{137}\text{Cs}$  date as a reference point.



## 4. Report on the microfabric properties of lacustrine sediment of Taihu 1, the Taihu Lake, eastern China

Chaolu Yi

### Introduction

Microfabric studies have been performed extensively in marine and delta sediments (Gilbert, 1969; Bennett et al, 1981; Kuehl et al, 1988; Wartel et al, 1991; Reynolds and Gorsline, 1991) and in glacial sediments (van der Meer, 1993; Yi, 1997). In lacustrine sediment studies, the scanning electronic microscope (SEM) has been used to identify the mineral properties (Tang et al, 1994; Peter, et al, 1994; Sack and Last, 1994) and diatom shapes (Edund and Stoermer, 1993) and to describe the sedimentary environment. The thin section method has been used to study laminations in Holocene lacustrine sediments (Valero-Garcés and Kelts, 1995). The micromorphology of lacustrine sediment has also been studied to explain the sediment genesis (George, 1986; Mees and Stoops, 1990; Goldberg and Macphail, 1990; Defarge et al, 1996; Lamoureux and Bradly, 1996). The microfabric method is particularly useful in the studies of lacustrine sediments because of the fine sediment size. In the project of lacustrine record along the Yangtze River supported by Royal Society and NNSFC and Chinese Academy of Sciences, we chose Taihu Lake in the eastern China for preliminary study of lacustrine microfabric.

### Methods

Core Taihu 1, 74 centimetres in length, was taken in Taihu Lake, eastern China. The sample was stored in a plastic tubes and then was cut along the long axis using an electrical osmotic knife. The water in the whole tube was replaced by acetone in order to avoid deformation of the samples.

Subsamples were selected from the core sections in one centimeter interval for study in the SEM. Observation was made in Geology Department, UCL with the help of Jim Davy. One or photos was taken for each subsamples. Grain size and void size were also measured with the amplification of 1200 to 2000 in the images of the SEM. More than ten grains and voids for each sample were measured for size statistics.

### Results

#### 1. Types of microfabric

The following microfabrics were observed in the samples:

#### Contacting pattern of particles

The mineral grains in all samples displayed an edge-to-edge or face-to-face contacting pattern.

#### Surface Textures of Aggregates and Particles

Aggregates tend to have a spherical or elliptical shape without an angular edge. Their sphericity was about 2-3. Most particles had subangular shape (sphericity=2). Some quartz grains displayed an angular shape (sphericity=1). The grains of hydromica and sericite had subrounded shape (sphericities=3).

#### Microvoids

The microvoids were observed. They were intergranular and irregular among mineral grains. The average mode size was smaller, about 19 $\mu$ m, compared with the particle mode size of 54 $\mu$ m.

#### Bioframework

Plant fibre remains were observed within the depth of 12 and diatoms were found at depth of 9-12 cm.

## **Agglutinational Texture**

This type of texture is generated by the flocculation of suspending clay to form pellets (aggregation of small particles). This type of texture has low orientation. Some researchers have ascribed the origin of the physico-chemical flocs to electrostatic attraction (Wang et al, 1986; Reynolds and Gorsline, 1991). The pH value of the water in the lakes in this region is usually 7.8 to 8.6 and is moderately alkaline. The clay ions with positive charges are easily counteracted by OH<sup>-</sup> and deposited at the bottom of lakes.

## **2. Size Change in Depth**

The mode sizes of particles and voids have tendency to decrease with the depth (Fig. 1). The sizes of particles and microvoids have apparent relationship. Their coefficient is 0.807202 (significant level is 99.9%, freedom degree is 44). The ratio of particle size to void size also has tendency to decrease with the depth (Fig. 1). The particle size and this ratio also has strong positive relationship. The coefficient is 0.524146 (significant level = 99.9%. Freedom degree is 44). However, the void size and the ratio do not have apparent relationship (significant level = -0.04326. Freedom degree is 44).

## **Discussion**

The microfabric types observed in Taihu 1 are the common ones in lacustrine sediments. The significant phenomena are that Taihu 1 was lack of lamination structures and the particles did not display preferred orientation. It is suggested that wave actions or human activities disturbed the lamination formation. Some plant remains and diatoms were observed with the depth of 12 cm and below it the coarse plant fibre was seldom found. This implies that aquatic vascular bundle plant, which is harder to be decomposed and whose coarse fibre is easier to be preserved, was rare.

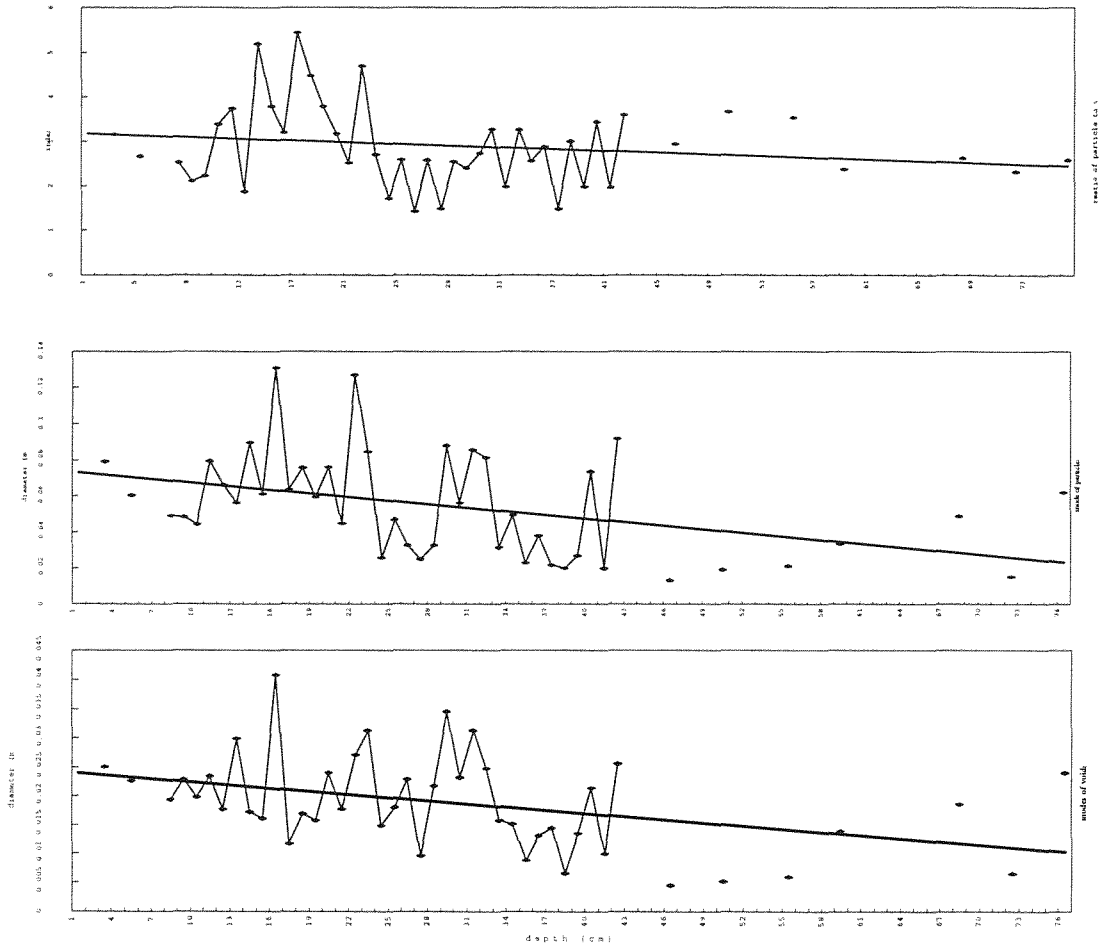
Relatively lower sphericities suggest that sediment did not suffer long-time erosion. The sediment might not come from big rivers, such as the Yangtze River, and also might not come from marine sediment, for these sediments from big river and marine genesis usually have higher sphericitates. So the sediment may come from small rivers around the lake.

The p/v ratio tends to decrease with the depth. This implies that the decrease of void with the depth is also related with other factors. Two of them might be sedimentary load and time periods.

## **Conclusions and suggestions**

The microfabric properties of Taihu 1 indicates that the sediment came from surrounding small rivers. That sizes of particles and voids change with depth seems to suggest that sediment supplies were not stable. That ratio of particle size to void size has tendency to decrease with the depth seems to indicate this property can be used to estimate the sedimentary time beyond <sup>210</sup>Pb dating. Therefore, more observation should be done and more photos should be taken to measure particles and voids for statistical studies.

Figure 1. (a) Ratio of particle size to void size with depth (b) diameter of particles and (c) voids for Taihu 1



## 5. Report of Preliminary Results of Grainsize Analysis of Lacustrine Sediments in Taihu Lake and Chenhu Lake, eastern China

Chaolu Yi

### Introduction

Grain-size analysis is a very useful tool in determining the sedimentary environment (Folk and Wüörd, 1932; .....). In the project of lacustrine record along the Yangtze River supported by Royal Society and NSFC and Chinese Academy of Sciences (?), we chose two lakes, Taihu Lake and Chenhu Lake, in the eastern China for grainsize analysis. The results indicate that the modern lacustrine sedimentary environment in all four sites in Taihu Lake is similar, but is a little different from that of Chenhu Lake. There are variations of sedimentary environment with the depth.

### Sample taking

The cores were taken using plastic tubes with outside diameter of 50 mm and inside diameter of 48 mm. Four cores from Taihu Lake with an area of more than two thousands of square kilometres, and one core from Chenhu Lake with an area of several tens of square kilometres, Jiangsu Province, eastern China, were taken for grainsize analysis in October of 1998. The samples from Taihu were sliced at 2 cm interval and those from Chenhu were selected according to lithographic properties.

### Methods

The organic matter in the samples was removed by hydrogen peroxide. Two grams (dried weight) of each of organic-free samples was used for determination of grainsize. Two ml Calgon (1 litre of such solution contains 33 grams of  $(\text{NaPO}_3)_6$  and 7 grams of  $\text{Na}_2\text{CO}_3$ ) was added to the sample in a small plastic tube, which was made up to 20 ml with double distilled. The tubes were shaken at 150 times per minute in a mechanical shaker for 12 hours to disperse the sediment. About 4 ml suspended sediment was put into the cylinder of the Laser grainsize analyser (Coulter L5130) for grainsize analysis. The size range for analysis is between 0.1 and 900  $\mu\text{m}$  146 samples were analysed. The measurement was made in January at the Geography Department, University of Liverpool

Grainsize parameters of mean size, median size, mode size, standard deviation(S.D.), coefficient of variation (C.V.), skewness and kurtosis were calculated based on standard formula.

### Results

All samples display apparent modes in grain-size distribution curves (Fig. 1). The mode size of the samples from Taihu Lake, except lower part of Taihu 3, is about 12-22.5  $\mu\text{m}$  (Fig. 1A to 1G) and 14.3-35.5  $\mu\text{m}$  of those from Chenhu Lake (Fig. 1H). There are second peaks in many samples (Fig. 1A to 1E and 1G), mostly with grainsizes of 60 to 100  $\mu\text{m}$ . But for Taihu 3-1, the second peak in most samples occurs at the size larger than 500  $\mu\text{m}$ , although there are still small peaks at the size of 60-100  $\mu\text{m}$ . The concentration of >500 $\mu\text{m}$  peak is quite high, sometimes even higher than the content of the mode size (Fig. 1D). Some samples in Taihu 4-1, have no second peaks (Fig. 1F). Overall, the grainsize in Taihu 3-1 and Chenhu 1-1 is larger than that of the other cores.

All samples have right-skewed (inclining to coarse fraction) and leptokurtic characteristics, although their values change with depth. Coefficient of variation for most samples is within 120-200%.

Significant changes with depth occur at a depth of 24-26 cm in Taihu 1-1 (Fig. 2) and at the depth of more than 60-64 cm in Taihu 4-1 (Fig. 5), where the grainsizes parameters display peaks. Taihu 3-1 shows abrupt an change in grainsize properties. Above 8 cm, the grainsize properties are similar to

those of the other cores (Fig. 1C), but below 8 cm, the grainsize increases greatly. The values of other parameters also change at that depth (Figs. 1D and 4).

The grainsize parameters in Taihu 2-1 and Chenhu 1-1 show strong changes with the depth. The general trend is that above depth of 39 cm in Taihu 2-1, the grainsizes and coefficient of variation etc., are greater than those below 39 cm (Fig. 3). In Chenhu 1-1 above the depth of 37 cm, the grainsizes are smaller and standard deviation, coefficient of variation etc. are a little larger. Below that depth, the grainsizes are larger but the standard deviation and coefficient of variation are less (Fig. 6).

### **Explanation of sedimentary environments**

#### ***Sedimentary environmental changes from site to site***

Each sample has an apparent mode and the mode in most samples occurs in silt to fine sand size fractions. This suggests that the sediments have been sorted to some extent. High values of standard deviation, coefficient of variation and skewness, which are indications of sediment sorting, suggest that the sorting level is medium to poor. The fine size, leptokurtic kurtosis and high standard deviation and high coefficient of variation suggest that the sediments were formed in a low energy lacustrine environment(...).

Most samples have bimodal distributions. As shown in Figure 1, we can see the silt and fine sand fractions. The former represents saltation load, while the latter represents a fraction load. The grainsizes lower than the silt mode can represent the suspending load. Saltation load and suspension load comprise the bulk of the sediment. The similarity in grainsize properties both between sites and down-core suggests that the lacustrine sedimentary environment in the sampling areas are similar without significant changes from place to place and from past to present. The only exception Chenhu 1-1. Below 8 cm the sediment has a modal size in the fraction of medium to coarse sand (>500  $\mu\text{m}$ ). This suggests that the site where Taihu 3-1 was experienced higher-energy and changeable sedimentary environment.

#### ***Sedimentary environmental changes with the depth***

The sediment flux into the lakes come mainly from their surrounding small rivers. The discharges of these rivers have significant seasonal fluctuations in this monsoon region. In the absence of other natural and artificial processes, the saltation load from the rivers would accumulate in the lake during the summer flooding season and most of suspension load would accumulate after the flooding period. This should lead to the formation of laminae. However, only the sediment below 28 cm in Chenhu 1-1 has laminations and the most samples with suspension load and saltation load in other sampling sites lack of them. A plausible explanation is that wave action and washing of bottom currents have played important roles in the sedimentation, leading to mixing and destruction of laminae. Human activities may be another factor in altering the sediment properties. Because no evidence suggests that the wave action became stronger and water level became lower as the time passed, the lack of lamination at the top of 28 cm in Chenhu 1-1 can be contributed to the disturbance of human activities since the reclamation of wetlands in that area.

**Taihu 1-1** (Figure 2) The sedimentary environment is stable. The mode is approximately uniform through the whole core, but the mean and median sizes have a strong peak at 27-29 cm. It is suggested that the discharge from the river into the site of Taihu 1-1 increased during that time. In the depth interval of 30 to 56 cm, the mean and median sizes became lower which suggests a smaller discharge from the river or weaker wave actions.

**Taihu 2-1** (Figure 3) The sedimentary environment is different between the top and the bottom. Below 38 cm, the mean and median sizes are smaller than those above that depth. The other parameters of coefficient of variation, standard deviation, skewness and kurtosis also have distinctive changes between the upper and lower parts at that depth. The upper part of the core suggests a larger amount of

discharge with higher energy, while its lower part suggests a small amount of river discharge and weak fluvial and wave actions.

**Taihu 3-1** (Figure 4) Above 8 cm, the sediment properties are similar to the other sites, although the mean, median and mode sizes are finer than most of the. But 8 cm, the sediment is far coarse. The mean size increases from 12 to 100  $\mu\text{m}$ . The medium sand fraction displays the highest or second highest mode. All other parameters have such abrupt change at 8 cm. The sediment at lower part displays three modes in the grainsize distribution (Figure 1D) which represent a mixture of more than one sedimentary environment. These suggest that the lower part of the core was formed by strong washing in bottom currents change occurs at the depth of 60 cm. Below that depth, the grainsize is greater. This suggests the lower part of the sediment was formed in a higher energy environment than the upper. Above 62 cm, there are two small fluctuations. At 46-50 cm, the grainsize is the smallest and at 32-34 cm, grainsize is a little larger. But these differences are not so obvious.

**Chenhu 1-1** (Figure 6) At the bottom part below 39 cm, the grainsize properties are uniform. This suggests that the sedimentary environment was stable. The presence of significant laminations below that depth also suggests that regular transportation and deposition of sediment were undergoing seasonally and annually. Above that depth, the grainsize changes considerably. The sediments at 31-33 and 35-37 cm possess the smallest grainsizes and they at depth of 24.5-26.5 cm possess the largest grainsizes. The surface sediment possesses the finest grainsize. Several periods of reclamation of wetland around the lake have been make since the late of 50th. It is suggested that the modern sedimentary has become unstable because the outlet of river channel has been changed by human activities.

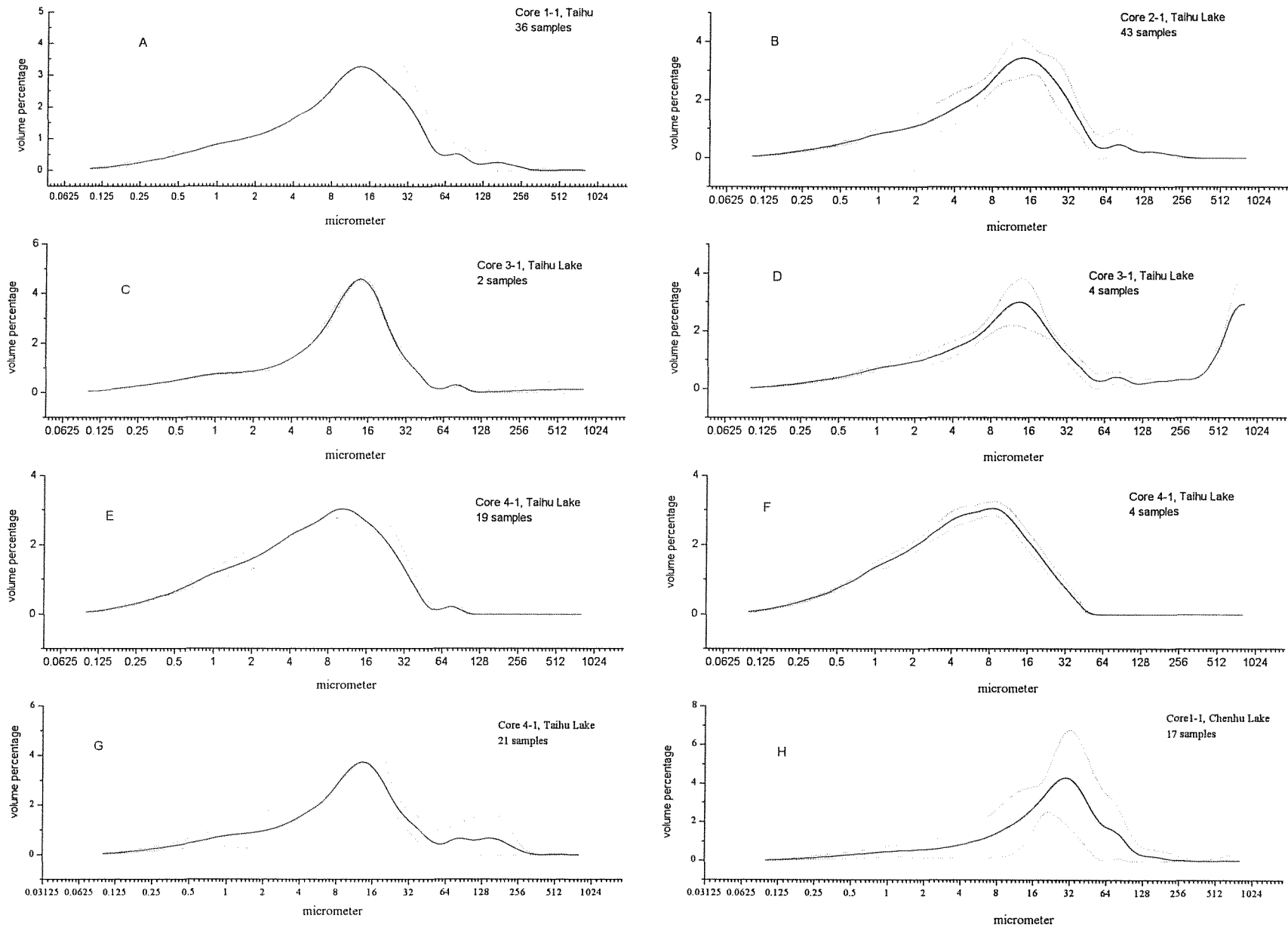


Fig. 1 Grain-size distributions of lacustrine sediment in Taihu Lake and Chenhu Lake. Solid lines represent the average values and dot lines represent the variation range of the values

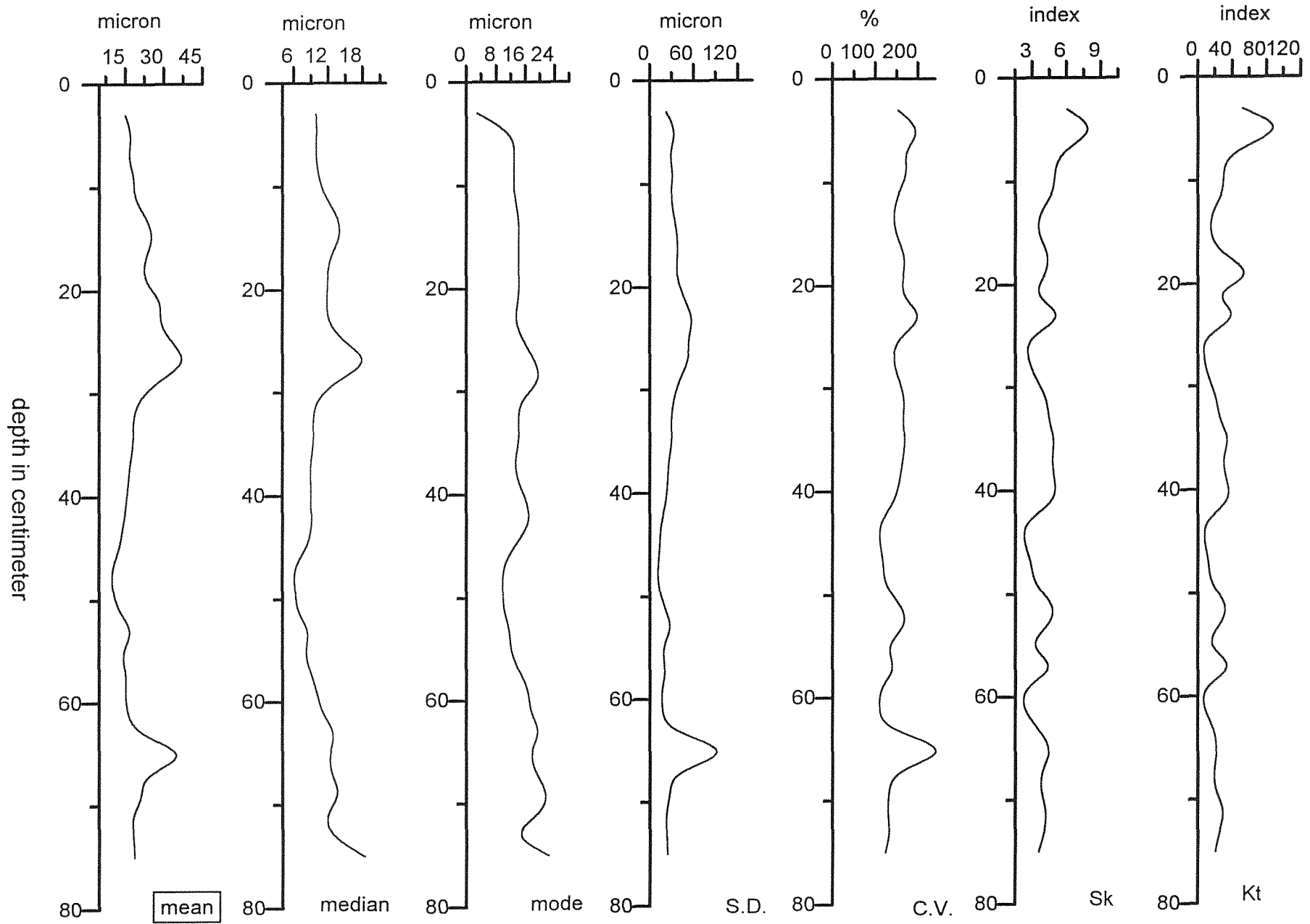


Fig. 2 Variations of grain-size parameters in Core 1-1, Taihu Lake



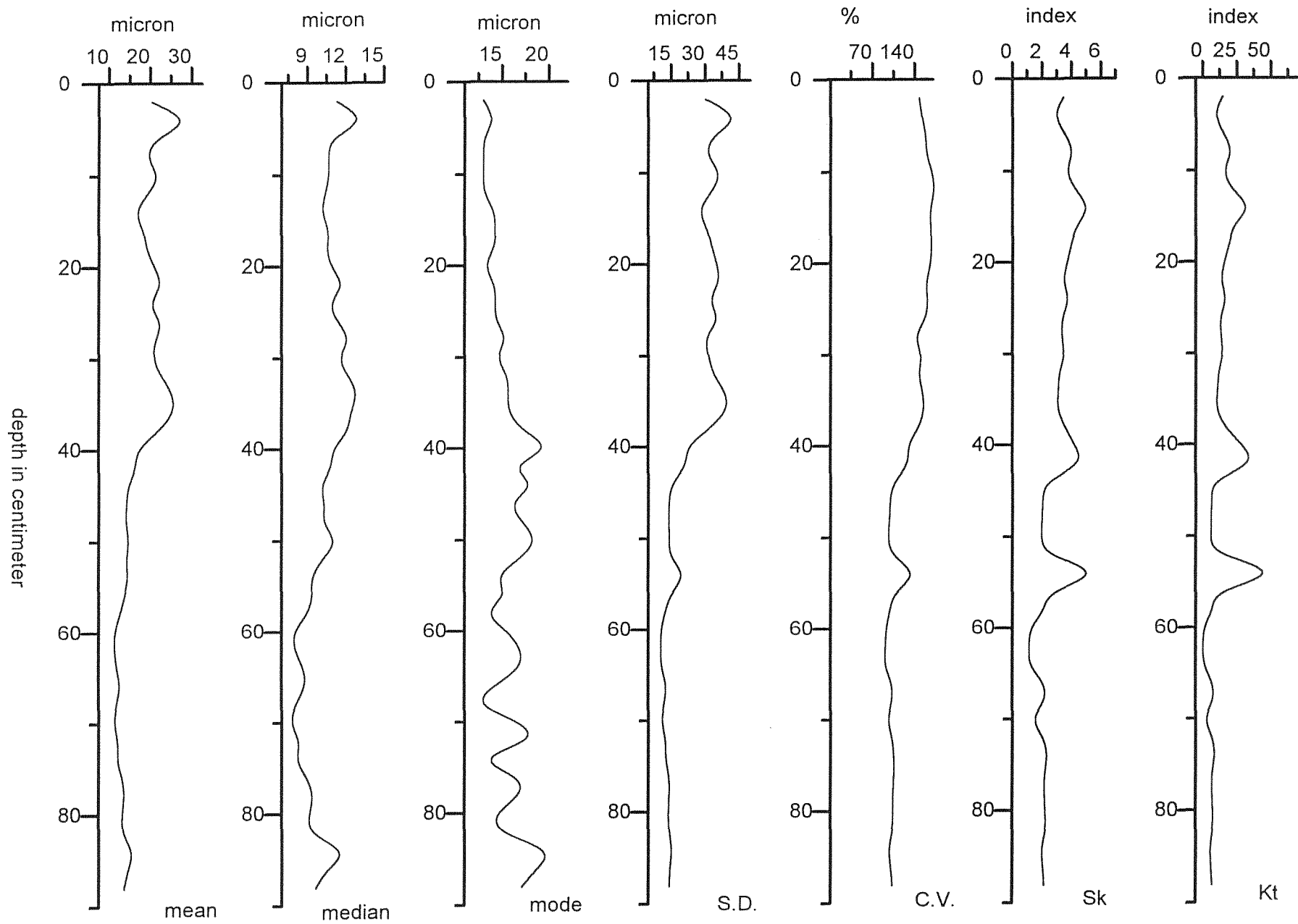


Fig. 3 variations of grain-size parameters in Core 2-1, Taihu Lake

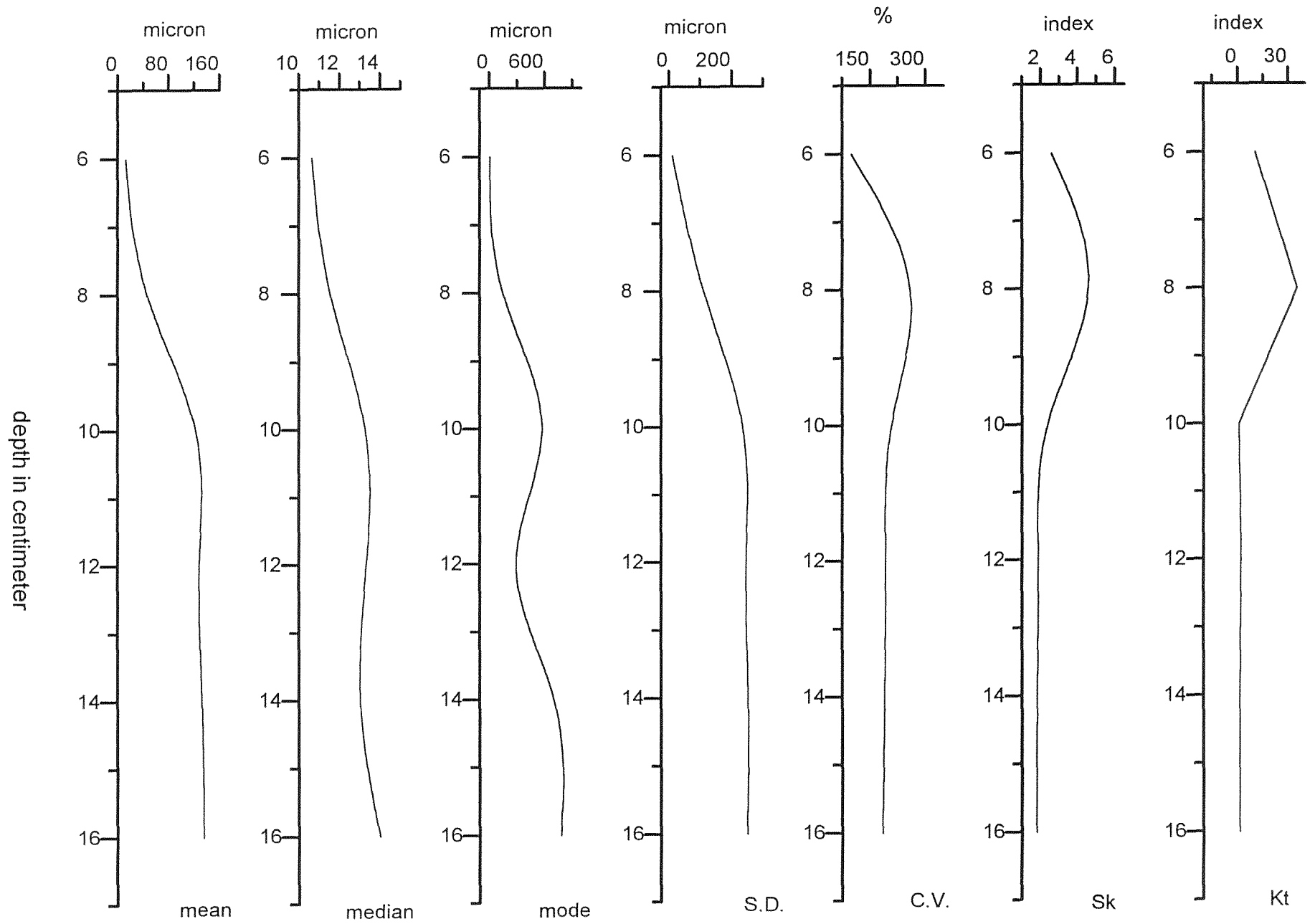


Fig. 4 Variations of grain-size parameters in Core 3-1, Taihu Lake

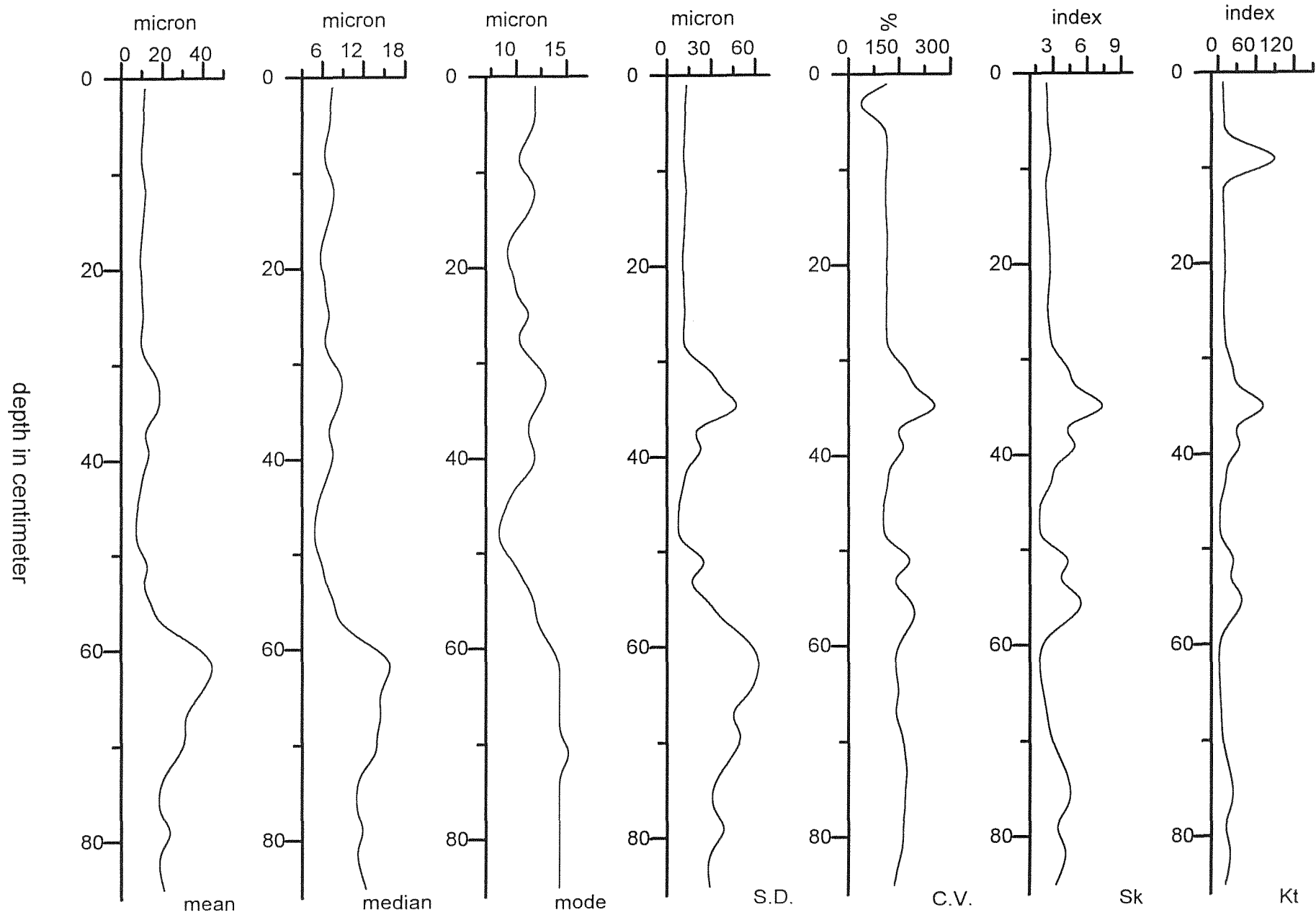


Fig. 5 Variations of grain-size parameters in Core 4-1, Taihu Lake

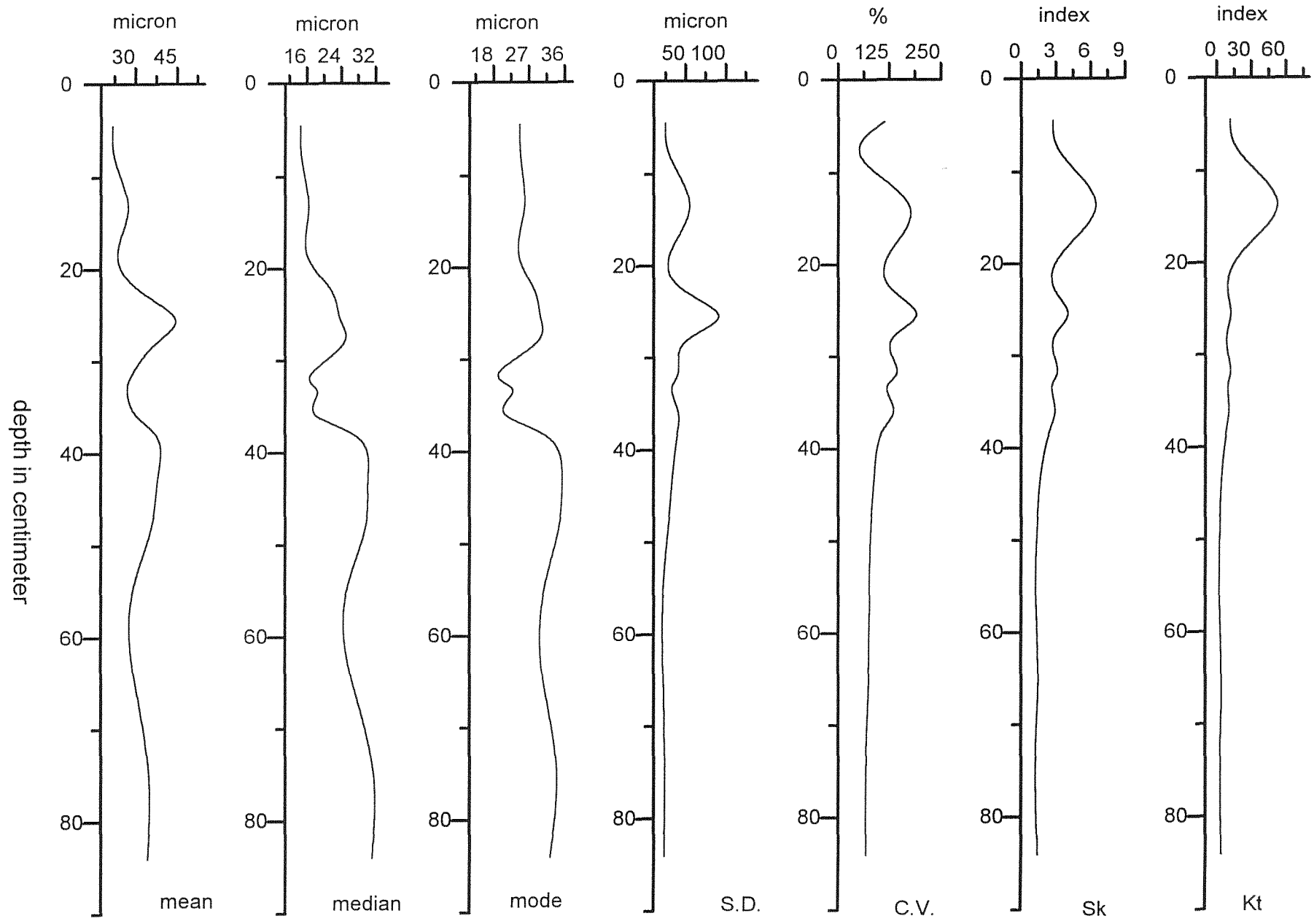


Fig. 6 Variations of grain-size parameters in Core 1-1, Chenhu Lake

## 6. Analyses of Taihu Lake Environmental Magnetic Measurement (I)

Du Yun

A study of lake sediments magnetic properties from Taihu Lake area in Jiangsu province, east China was undertaken at the Department of Geography, Liverpool University by Du Yun from Institute of Geodesy and Geophysics, Chinese Academy of Sciences directed by John Dearing and Bob Jude. The study area lies in the lower reaches of the Yangtze River (Yangtze River delta). Taihu Lake, approximately 2000 km<sup>2</sup> surface area, is one of the largest fresh water lakes in China. Chenghu Lake is a smaller fresh water lake, approximately 40km<sup>2</sup> in an area the east of Taihu Lake. This is one of the fastest developing areas in China. The development of agriculture and industry have a great influence on the lake environment. The research results of this area will be compared with the upper reaches of the Yangtze River, in Yunnan or Sichuan provinces and Tibetan plateau which have less anthropogenic activity.

There are four cores for magnetic measurement, three from Taihu Lake (Taihu 1-2L, 125cm long, Figure 1, Taihu 2-2L, 76cm long, Figure 2, Taihu 3-2L, 20cm long, Figure 3), one from Chenghu Lake (Chenghu 1-2L, 93cm long, Figure 4). Each core was sectioned at 1cm intervals during fieldwork expeditions in October 1998. The water content was determined by drying at 50°C. The samples were packed in 10cm<sup>3</sup> plastic cubes for magnetic measurement.

All the samples from the four cores were subjected to identical mineral magnetic analysis. Magnetic Susceptibility (X) was measured on a Magnetic Susceptibility Meter Model MS2 using a MS2B D.F. sensor (Bartington Instruments LTD.). Anhysteretic Remanent Magnetization (ARM) were created in a peak field to 100 mT with a biasing field of 0.1 mT using a Dtech D.2000A.F Demagnetizer. Saturation IRM (SIRM) in a forward field of 1000 mT was applied with Trilce Pulse Magnetizer (Omitec Instruments LTD.). Isothermal remanent magnetization (IRMs) was applied using Molspin Pulse Magnetizer (including -20, -30, -40, -50, -100, -300). All remanences were measured using a Molspin Portable Fluxgate Spinner Magnetometer.

The following are the main parameters:

Xlf,	Mass Specific Magnetic Susceptibility (in a low magnetic field)
Arm,	Anhysteretic Remanent Magnetization
Xarm,	Susceptibility of Arm
SIRM	Saturation Isothermal Remanent Magnetization
HIRM	High Field Isothermal Remanent Magnetization
Xarm/Xlf	The ratio of Xarm and Xlf
Xarm/SIRM	The ratio of Xarm and SIRM
SIRM/Xlf	The ratio of SIRM and Xlf
Fd (%)	(Xlf-Xhf)/Xlf
HARD (%)	100-(-300mT)
SOFT	SIRM-(-20mT)
IRM Reverse	-20mT, -30mT, -40mT, -50mT, -100mT, -300mT

Figure 1 shows the magnetic stratigraphy of core Taihu 1-2L (125 cm long) from west Taihu Lake. There are three different boundaries which can be seen clearly. The susceptibility, SIRM, HIRM, SOFT is high between 125 and 66 cm, and the ratios of Xarm/ SIRM, Xarm/Xlf are low. Sediment between 65 and 25 cm has reduced in susceptibility, SIRM, HIRM, SOFT values and higher ratios of Xarm/SIRM, Xarm/Xlf. From 24 cm to the top of the core, the values of susceptibility, SIRM, HIRM, SOFT increase and the ratios of Xarm/SIRM, Xarm/Xlf decrease. Figure 2 shows the magnetic stratigraphy of core Taihu 2-2L (76 cm long) approximately 4 km to the north east of core

Taihu1-2L. The profiles are similar to core Taihu 1-2L. It can also be divided into 3 stages. Sediment between 76 and 46 cm possesses high susceptibility, SIRM, HIRM, SOFT and low  $X_{arm}/SIRM$ ,  $X_{arm}/X_{lf}$  ratios. At 45 cm an abrupt decrease in magnetic concentration occurs. Sediment from 7 cm to the top of the core, the susceptibility, SIRM, HIRM, SOFT increases, and the ratios of  $X_{arm}/SIRM$ ,  $X_{arm}/X_{lf}$  is lower.

The magnetic properties of lake sediments are influenced by many factors, such as bacterial, magnetosome, authigenic iron sulphides, such as greigite and reductive dissolution of ferrimagnetic grains. The susceptibility responds to the magnetite grain size, antiferrimagnetic minerals (e.g., hematite), paramagnetic minerals. SIRM generally reflects the Stable Single-Domain (SSD), Multi-Domain (MD) grains and imperfect antiferromagnetic minerals.  $X_{arm}$  is sensitive to the SSD minerals. The high values of susceptibility, SIRM and the low ratios of  $X_{arm}/SIRM$  in lower and upper parts of two cores reflect the hematite and MD grains concentration, and the low values of susceptibility and SIRM and high ratios of  $X_{arm}/SIRM$  in the middle parts of cores reflect the SSD grains concentration. This can also be seen from the values of HIRM and SOFT. HIRM is mostly sensitive to the imperfect antiferromagnetic minerals (e.g., hematite) or ferrimagnetic minerals (e.g., magnetite). SOFT reflects the Multi-Domain grains. High values of HIRM and SOFT in the lower and upper parts of cores show the high hematite and magnetite, MD grains concentration. The ratio of  $X_{arm}/X_{lf}$  influenced by magnetic grain size, the high values in the lower and upper parts indicate the high SD and MD grains concentration.

Core Chenghu 1-2L shows a different magnetic stratigraphy from Taihu Lake. Sediment samples between 93 and 42 cm, have high values of susceptibility, SIRM, HIRM and SOFT, and low values of  $X_{arm}$ ,  $F_d$  and  $X_{arm}/SIRM$  ratio. This indicates MD grains minerals, hematite and magnetite dominate the mineralogy in this part. From 41 to 21 cm, susceptibility, SIRM, HIRM, SOFT decrease quickly and there is a rise in  $F_d$ ,  $X_{arm}/SIRM$ ,  $X_{arm}/X_{lf}$ . This reflects the Stable Single-Domain, Superparamagnetic minerals concentration. From 21 cm to the top of the core, susceptibility,  $X_{arm}$ , SOFT have a little rise slightly, which may indicate pollution.

Taihu Lake area is in proximity to rapidly developing cities such as Shanghai, Suzhou, Wuxi and Changzhou, and about 500 local industries occur around the lake. There is a very serious pollution problem and eutrophication has developed during the past fifty years in the Taihu lake area. Sedimentary magnetic records may be dominated by pollution particles. The most common magnetic component is fly-ash from coal burning, but other metal dusts may be also important. Figure 5 shows the elements spectrum of core Taihu 1-2L by XRF (LEPS, 2172, Metorex, directed by John Boyle), the values of susceptibility and the SOFT ( $SIRM-IRM_{20mT}$ ) covarying with Pb and Zn showing a link between magnetites and heavy metal pollution.



$\chi_{LF}$   
 $10^{-8} \text{m}^3 \text{kg}^{-1}$

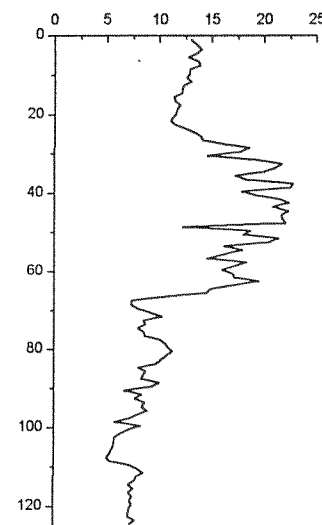
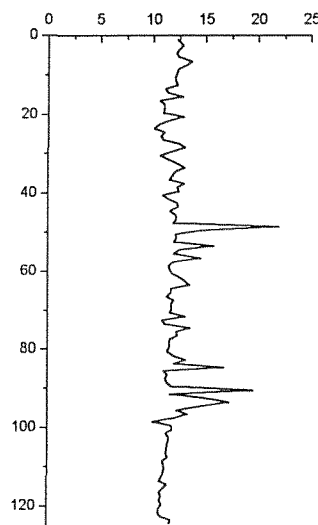
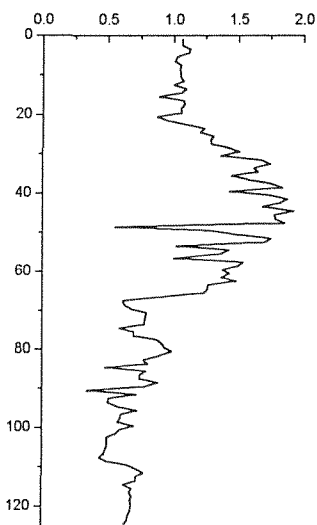
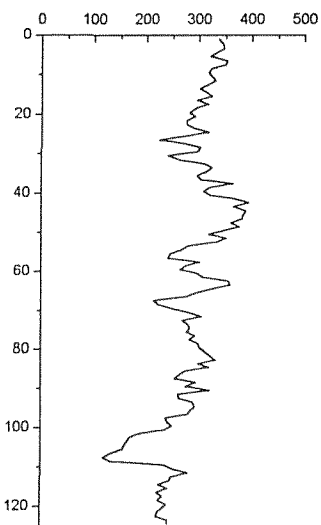
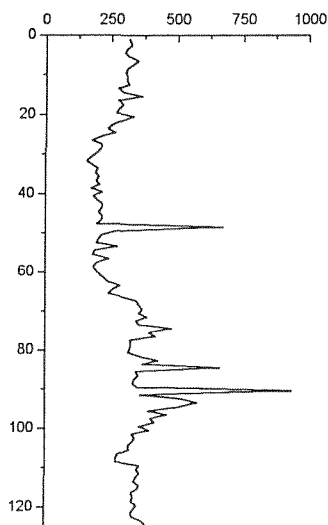
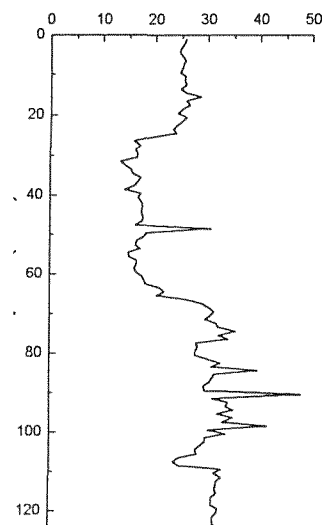
SIRM  
 $10^{-5} \text{Am}^2 \text{kg}^{-1}$

$\chi_{ARM}$   
 $10^{-8} \text{m}^3 \text{kg}^{-1}$

$\chi_{ARM}/\text{SIRM}$   
 $10^{-3} \text{mA}^{-1}$

SIRM/ $\chi_{LF}$   
 $10^3 \text{Am}^{-1}$

$\chi_{ARM}/\chi_{LF}$



HIRM  
 $10^{-5} \text{Am}^2 \text{kg}^{-1}$

HARD %

FD (%)

SOFT  
 $10^{-5} \text{Am}^2 \text{kg}^{-1}$

IRM REVERSE (%)

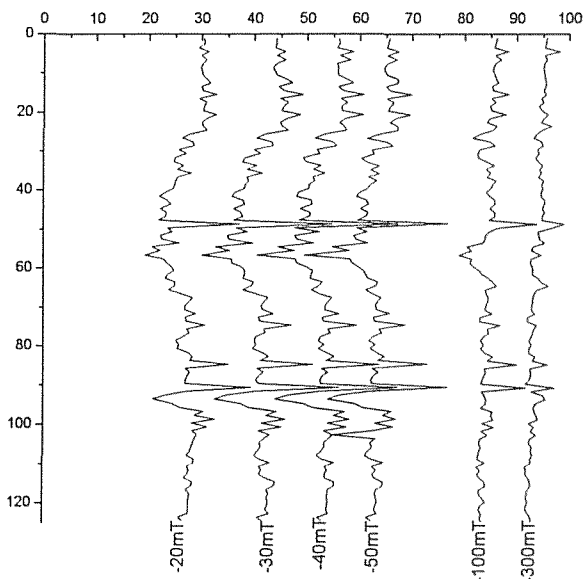
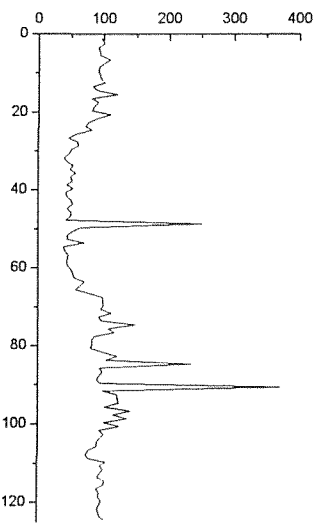
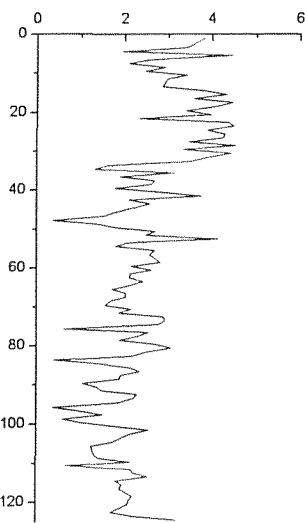
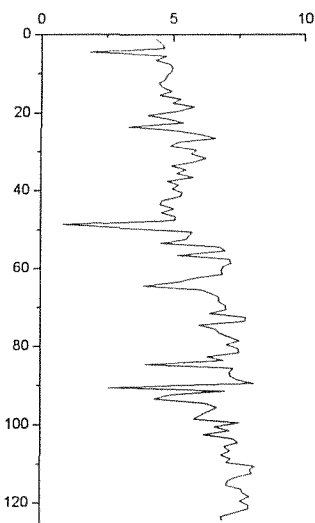
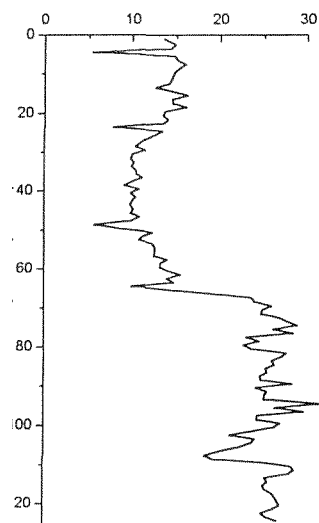


Figure 1 Taihu 1-2 L (125cm)

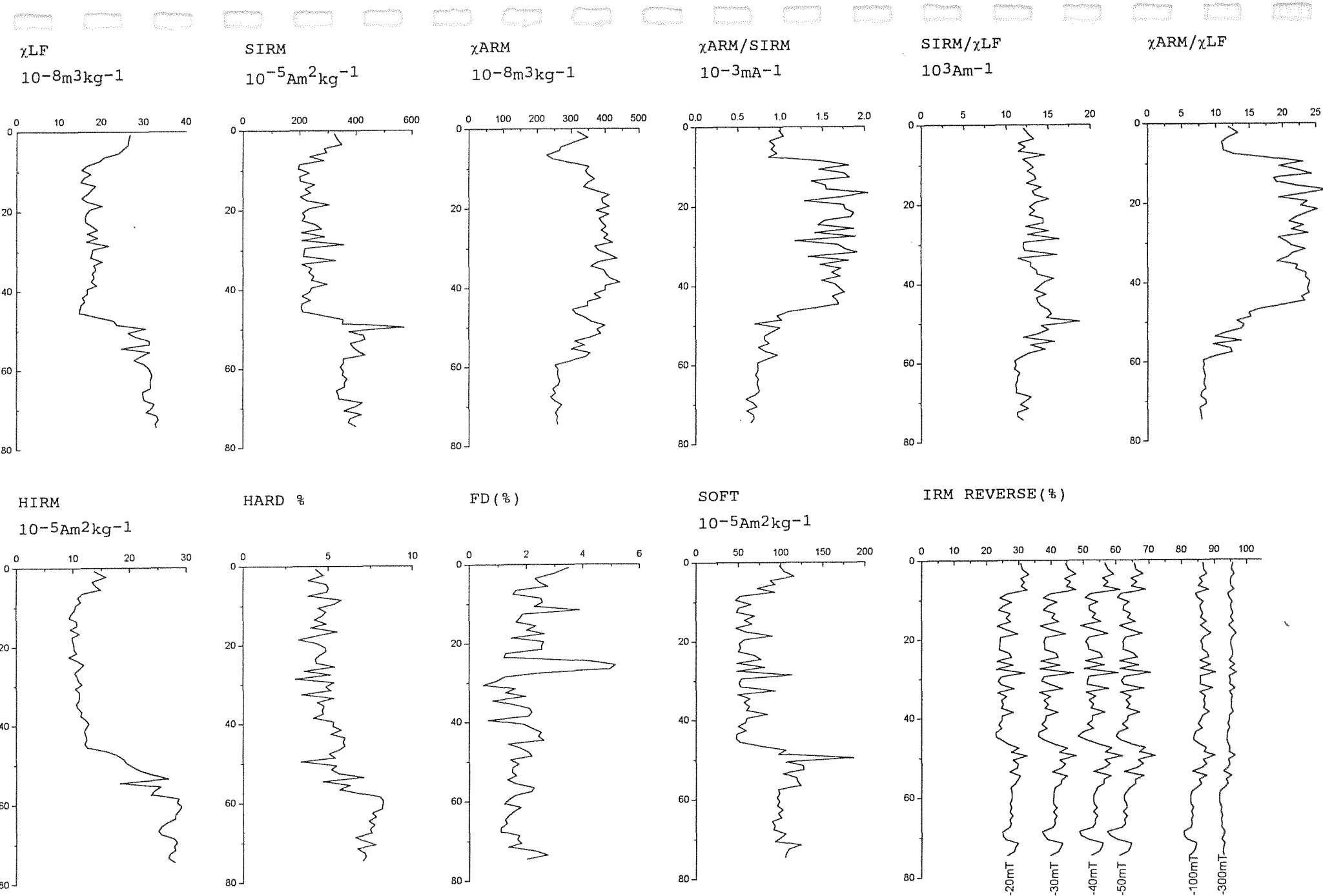


Figure 2 Taihu 2-2 L (76cm)



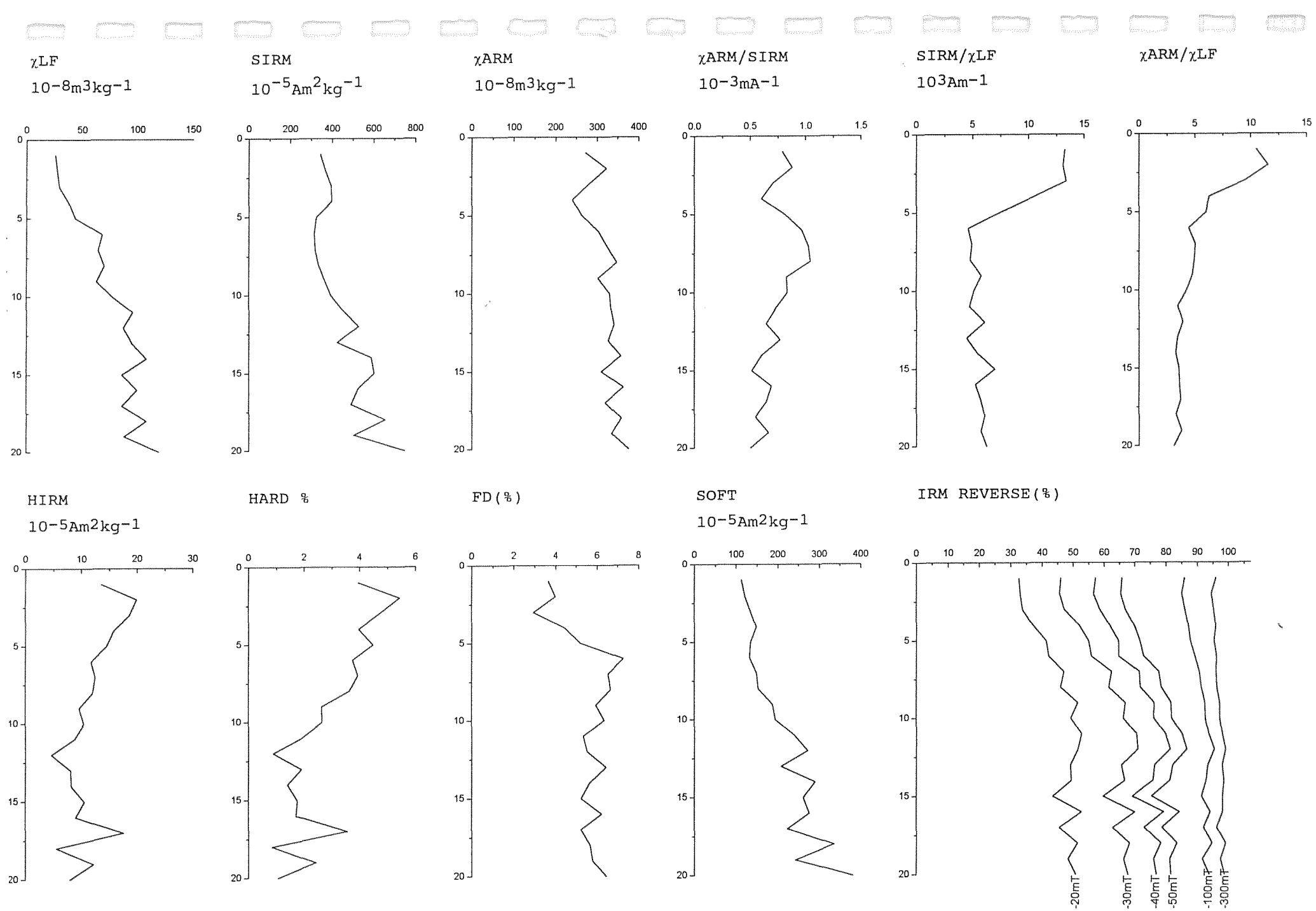


Figure 3 Taihu 3-2 (20cm)

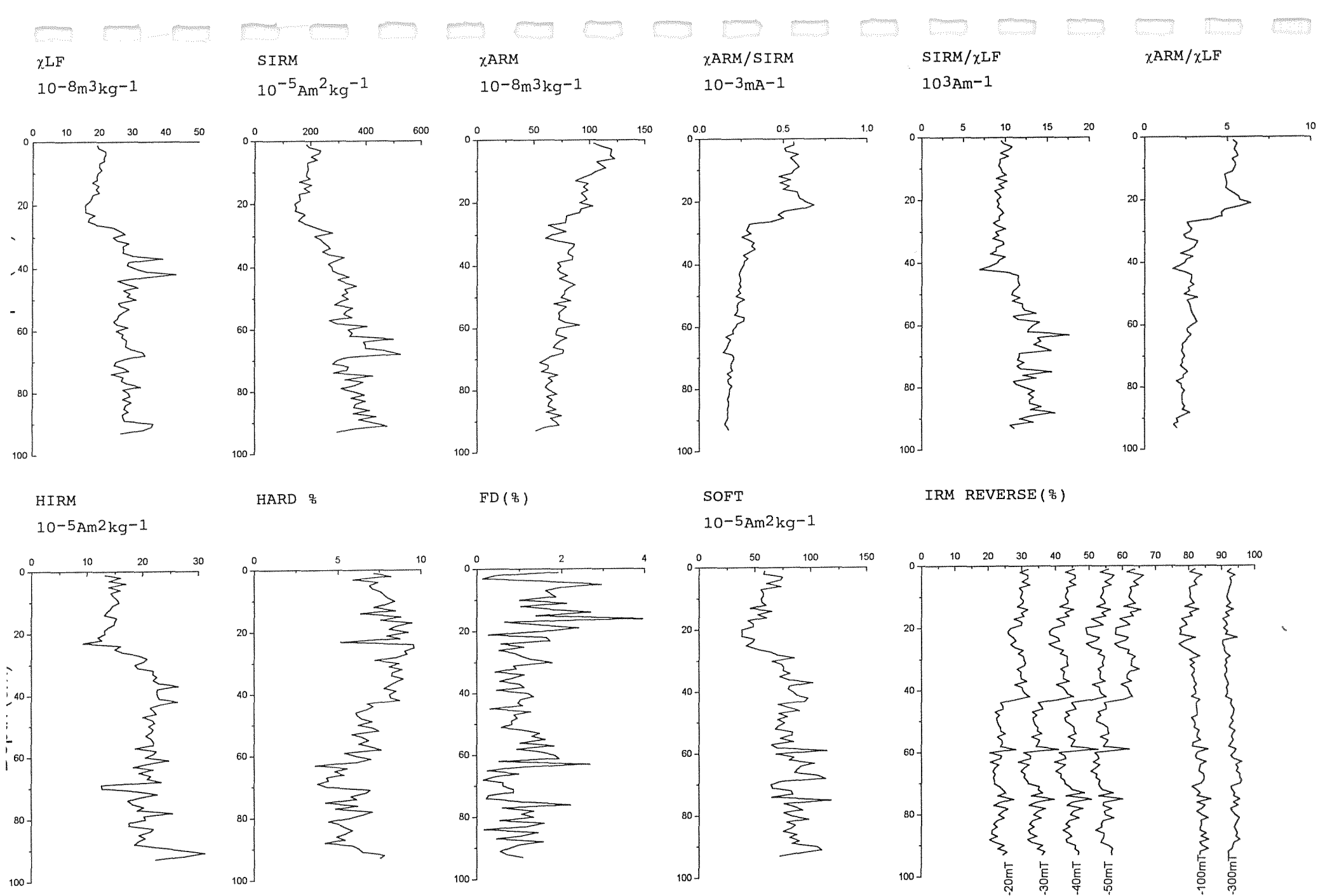


Figure 4 Chenghu 1-2 L (93cm)

## 7. Magnetic measurements (II), nitrogen and phosphorus analyses.

Dai Xue Rong

# 摘 要

这是一个由伦敦、利物蒲、武昌和上海的四所高校和科研机构合作研究的项目，得到了英国皇家学会（Joint Project Q741）和中国国家自然科学基金委的资助。试图通过对中国长江流域东部、中部和西部湖泊沉积记录的研究来探讨在自然和人为因素共同作用下环境变化和大气污染的历史、现状及上、中、下游之间的差异等。按照合作项目总的要求和年度进展计划，第一年的主要任务是对位于中国东部长江下游（江苏省境内）的代表性湖泊进行系统采样。紧接着，合作四方按照各自的分工同时开展各项分析、测试工作。最后向项目的资助机构递交年度工作报告。

野外采样是在上海华东师范大学的主持下于 1998 年 10 月完成的。从太湖（Tai）、滬湖（Gehu）和澄湖（Chen）的表层沉积物中共采得样芯 18 根，其中短样芯 7 根，每根长约 15~30cm；长样芯 11 根，每根长约 60~200cm。此外，在环太湖湖滨低洼地采得土壤样芯 4 根，长约 20~40cm。全部短样芯（Gehu 1 除外）在用特制的取样器取出水面之后当场进行了 1cm 等厚的连续分割，共 137 块。每一块样的 2/3 由英方带回国内分析，另外的 1/3 则留给上海（华东师大）。样品全部用塑料袋封装，以保持原有的水分状态。长样芯在太湖和澄湖都采了双份样，一份分割为散样，另一份作为原状样封存。

实验分析内容包括粒度、微结构、磁性测量、微量元素、含水量、硅藻、放射性测年、球体碳颗粒及氮磷 9 个方面。按照分工，上海方面的任务是：（1）对 6 个短样芯（137 个样品）进行含水量和磁性参数的测量，并将结果与英方所测的结果作比较；（2）从太湖和澄湖的样芯中各选出一个具有代表性和连续性的样芯（后选定为 Tai 1 和 Chen 2，共 58 个样品）做氮、磷元素的分析；（3）选出与两个短样芯在层位上一致的长样芯样品做并行的放射性测年（实际运作中此样品一直没有提供）。到目前为止，除测年工作（现改测短样芯）还在进行外，其它分析项目均已完成。此报告是上述工作的一个阶段性总结，旨在为下一步合作四方之间的资料协调、初步成果发表以及分析测试项目的进一步遴选提供依据。

但存在的问题是样芯还没有实际年代控制，时间序列尚未建立，难以把环境变化同人类活动对环境的影响历史结合起来；由于短样芯跨年时间较短，磁性参数曲线所能反映的古环境信息比较单调；氮磷营养元素的含量变化比较明显，但目前英国方面的 SCP 分析还没有结果，无法做对比分析。因此建议下阶段的工作一方面应加强样芯的测年，另一方面要着重研究由人类活动而引起的环境变化（恶化）问题。

野外工作得到了华东师大地理系郑祥民教授、陈振楼博士和陈满荣、王少平博士研究生们的指导和帮助。师育新副研究员参与了全部实验分析过程。许羽、张卫国、陆敏、沈铭能等在实验技术方面提供了最大的帮助，在此深表感谢！

# 一、野外采样及研究分工

野外采样工作是在华东师范大学俞立中教授的组织 and 安排下开展的，包括课题组中外宾客的接待、车船租用、野外用具（品）准备和采样路线设计等。采样用时 5 天，其中太湖 3 天，滬湖和澄湖各 1 天。所采样品的详细情况列于表 1。

表 1 长江下游湖泊沉积物采样详细地点及样芯记录

样型	采样地点 (经度和纬度)		短样芯长度 (cm)	长样芯编号 (cm)	水深 (m)
湖泊沉积物样芯	太湖	Tai 1: 31° 27.522' N, 120° 08.901' E	Tai 1, 30	Tai1-1L,-2L	(暂缺)
		Tai 2: 31° 29.386' N, 120° 11.024' E	Tai 2, 19	Tai2-1L,-2L	2.8
		Tai 3: 31° 18.119' N, 120° 03.033' E	Tai 3, 20	Tai3-1L,-2L	2.8
		Tai 4: 31° 19.917' N, 120° 04.791' E	Tai 4, 25	Tai4-1L	2.5
	滬湖	Gehu 1: 31° 31.872' N, 119° 48.344' E	Gehu 1, 20	Gehu 1-1L	1.7
	澄湖	Chen 1: 31° 14.675' N, 120° 48.794' E	Chen 1, 15	Chen1-1L	2.3
Chen 2: 31° 13.683' N, 120° 52.004' E		Chen 2, 28	Chen2-2L,	2.5	
土壤样芯	太湖西岸	THS 1: 31° 25.372' N, 120° 07.575' E	THS 1		(岸滩)
		THS 2: 31° 25.204' N, 120° 07.606' E	THS 2		(岸滩)
		THS 3: 31° 10.408' N, 119° 54.819' E	THS 3		(岸滩)
		THS 4: (同上)	THS 4		(岸滩)

- 注：(1) 经纬度数据是由我系的袖珍 GPS 仪测定的；  
 (2) 滬湖样芯 (Gehu 1) 由于太靠近岸边，受到的扰动比较大，故在野外时就决定放弃分样，由英方全部带走；  
 (3) 短样芯采用特制采样器采集，处于悬浮状态的最表层样品保存了原始的状态。而长样芯采用塑制管所取，最表层样可能会受到一定的影响，如水分和细小颗粒的流失等；  
 (4) 在短样芯中 Tai 3 比较特殊，沉积物中含有较多的湖底硬质泥块，很不均匀。推测可能受到较大幅度的扰动。在实验室需作更详细的观察和代用指标确认。

野外采样采取三种方式。(1) 短样芯采用的是特制的采样器 (Glew core)，直径 7cm，最长可采到 40cm。此方式的最大优点是能够保证最表层样的完整性。同一个地点只采 1 根，太湖设 4 个点，滬湖 1 个点，澄湖 2 个点，共 7 个点 7 根短样芯。当短样芯取出水面之后现场就进行了 1cm 等厚的连续分割，6 个样芯共分为 137 块样品。每一块样又大致按 2:1 的比例分为两部分，大部分由英方带回国内做分析，少部分留在上海做分析。样品同时全部用塑料袋封装、标号，以确保样品的原有状态和完整性 (包括刚刚取出时所带的水分)。

(2) 长样芯是采用普通脆塑管 (建材品种) 插取的，可任意长，直径 4.6cm。此方

式的优点是在采样是一直可以软泥的底部，以获得尽可能长（深）的样芯。在 Tai 1、Tai 2、Tai 3 和 Chen 1 点均采 2 根样，在 Tai 4 和 Chen 2 点各采 1 根样。采有两根样芯的其中 1 根在野外就分割成小样（散样），另一根则保留作微结构等分析。所有长样芯均由武昌方面运回并带到英国分析。

（3）岸滩低洼地的土壤样芯是采用硬塑管通过锤击方式采集的。主要采自太湖西岸，共 4 根，每根长约 20~40cm。用于放射性元素  $^{210}\text{Pb}$ 、 $^{226}\text{Ra}$  和  $^{137}\text{Cs}$  的检测。全部样品由英方带回国内（按照最初的安排，也要给上海留样同时作测量，然后相互比较所测结果）。

野外采样结束后通过讨论，决定下一步实验阶段的分工为：

#### （1）英国方面

- UCL：含水量（所有短样芯）、有机碳、硅藻、碳颗粒、岩性等；
- Liverpool：放射性测年（选择 2 个短样芯）、粒度、微量元素、磁性测量（选择 2 个长样芯）；

#### （2）中国方面

- 武昌（IGG）：含水量、微结构、粒度分析、磁性测量（选择 2 个长样芯）；
- 上海（ECNU）：含水量（所有短样芯）、磁性测量（所有短样芯）、地球化学——N、P 指标（太湖、澄湖各选一代表性样芯）、放射性测年（选择 2 个长样芯，层位与短样芯一致）。

## 二、实验分析

### 1. 含水量测定

*目的和意义：*

沉积物含水量的多少与沉积物物质成分、颗粒粗细和埋藏深浅等因素有关。以机械成分为主沉积物往往比泥炭质沉积物的含水量要高。沉积物颗粒粗，空隙度大，含水就多；反之含水就少。随着埋藏深度的加大和压实作用加强，含水量逐渐降低等等。因此，含水量的大小也可以从一个侧面反映沉积物的性质和特点，并常常作为沉积环境研究的辅助测试项目之一。另外，对于某些化学成分来说，由于它们在水体中的溶解度较高，它们的含量高低和分布状况直接与含水量的高低有关。因此，含水量对于某些元素（包括污染元素）的物源分析来说也是十分重要的。特别是，本项研究以湖泊表层沉积物为研究对象，它是一种介于液相和固相之间的一种特殊产物，除含有沉积物和水外还含有大量与生物活动有关的物质。所以与其说是湖泊表层沉积物还不如说是一种与气溶胶相对应的“水溶胶”。

### 方法及步骤:

通常采用的方法是将野外采回的土壤或沉积物样品在室温条件下统一风干（或晾干）、称重；再将晾干的样品在低温条件下（50℃）烘干和再称重。根据前后两次称得的重量采用公式计算结果。但考虑到这次所采的样品是湖泊表层沉积物——一种特殊类型的“水溶胶”。如果采用常规方法，那么从湿样到晾干后的样品之间的水分就无法定量地反映出来。而这部分水分的多少对于沉积物的化学组成（游离态水中的一些可容物质，包括污染元素）也是至关重要的。也就是说我们必须测出处于原始状态下沉积物的所有水分，为各种元素的物源分析提供依据。（从这个角度来看，应同时采集底层水样做各种分析）。

结果计算： $WC \% = ((W_1 - W_2) / W_1) * 100\%$ 。其中  $W_1$ ——为原始样品的重量（g）； $W_2$ ——为烘干后的样品重量（g）。共测样品 137 个，包括 Tai 1、Tai 2、Tai 3、Tai 4、Chen 1 和 Chen 2 全部 6 个短样芯的样品。

### 测量结果:

结果见表 2（共 1 页）。这一部分的工作可与英国方面作比较，但未见到他们的结果。全部测量数据及图件均附在最后。

## 2. 矿物磁性测量

### 目的和意义:

矿物磁性测量工作目前已较普遍用于对各种沉积物的先导研究。磁性参数一方面有其丰富的内涵，可以反映铁磁性物质的性质、特点、类型和含量，还可以反映亚铁磁性物质、细粘滞性晶粒（FV）、多畴（MD）和假单畴（PSD）、不完整反铁磁性物质的情况。另一方面也有其丰富的外延并已经得到认可，如用作地层的划分和对比、沉积物的物源分析、湖泊氧化—还原环境判断、部分重金属元素的示踪、烟尘和其它污染物的断定、洪水事件的确认以及古地理古气候环境的重建等代用指标。湖泊沉积物它的物质成分比较复杂，磁性测量是一项难以用其它方法替代的优势方法。

### 方法及步骤:

将太湖和澄湖 6 个孔的 137 个样品统一进行低温（50℃）烘干，然后采用木棒碾压成粉末状；准确称样后用塑料薄膜包裹并装入专用的塑料盒内待测。测量步骤包括：（1）低频磁化率（ $\chi_{LF}$ ，0.47KHz）和高频磁化率（ $\chi_{HF}$ ，4.7KHz）；（2）无磁滞剩磁（ARM）；（3）在 20mT、300 mT 磁场中被磁化后所带的剩磁（ $IRM_{20mT}$ ， $IRM_{300mT}$ ）；（4）经 1 T 强度的磁场磁化后所带的饱和等温剩磁（SIRM）；（5）带饱和等温剩磁的样品经不同强度反向磁场磁退后的剩磁（ $IRM_{-20mT}$ ， $IRM_{-40mT}$ ， $IRM_{-100mT}$ ， $IRM_{-300mT}$ ）。根据上述测量数据计

算出不同的磁性参数，如单位质量磁化率 ( $\chi$ )、饱和等温剩磁 (SIRM)、“软”剩磁 (Soft)、“硬”剩磁 (Hard) 以及比值参数  $\chi_{fd}\%$ 、SIRM/ $\chi$ 、 $S_{-xmt}\%$ 和  $F_{-xmt}\%$ 等。

磁性参数的计算包括赋值、计算和再赋值、再计算四个过程。根据已有计算公式设计的程序如下：

Mass (g)  $\rightarrow$  c; Xlf  $\rightarrow$  d; Xhf  $\rightarrow$  e; Arm N  $\rightarrow$  f; Arm E  $\rightarrow$  g, 20mt N  $\rightarrow$  h, 20mt E  $\rightarrow$  i, 300mt N  $\rightarrow$  j, 300mt E  $\rightarrow$  k, 1000mt N  $\rightarrow$  l, 1000mt E  $\rightarrow$  m, -20mt N  $\rightarrow$  n, -20mt E  $\rightarrow$  o, -40mt N  $\rightarrow$  p, -40mt E  $\rightarrow$  q, -100mt N  $\rightarrow$  r, -100mt E  $\rightarrow$  s, -300mt N  $\rightarrow$  t, -300mt E  $\rightarrow$  u,

$$X (\text{Susc}) = d/c \rightarrow w \dots\dots\dots (10^{-8} \text{m}^3 \text{kg}^{-1})$$

$$X_{fd} (\%) = 100 * (d-e)/d \rightarrow x \dots\dots\dots (\%)$$

$$\text{IRM } 20\text{mt} = \sqrt{h*h+i*i} * 12.9 \rightarrow y$$

$$\text{IRM } 300\text{mt} = \sqrt{j*j+k*k} * 12.9 \rightarrow z$$

$$\text{IRM } 1000\text{mt} = \sqrt{l*l+m*m} * 12.9 \rightarrow \text{aa}$$

$$\text{IRM } -20\text{mt} = \sqrt{n*n+o*o} * 12.9 \rightarrow \text{ab}$$

$$\text{IRM } -40\text{mt} = \sqrt{p*p+q*q} * 12.9 \rightarrow \text{ac}$$

$$\text{IRM } -100\text{mt} = \sqrt{r*r+s*s} * 12.9 \rightarrow \text{ad}$$

$$\text{IRM } -300\text{mt} = \sqrt{t*t+u*u} * 12.9 \rightarrow \text{ae}$$

$$\text{SIRM} = \text{aa}/m \rightarrow \text{af} \dots\dots\dots (10^{-6} \text{Am}^2 \text{kg}^{-1})$$

$$\text{SIRM}/X = (\text{af}/w)/10 \dots\dots\dots (\text{KA} \text{m}^{-1})$$

$$\text{Soft} = y/m \dots\dots\dots (10^{-6} \text{Am}^2 \text{kg}^{-1})$$

$$\text{Hard} = (\text{aa}-z)/m \dots\dots\dots (10^{-6} \text{Am}^2 \text{kg}^{-1})$$

$$S_{-20\text{mt}} (\%) = 100 * (\text{aa}-\text{ab}) / (2 * \text{aa}) \dots\dots\dots (\%)$$

$$S_{-40\text{mt}} (\%) = 100 * (\text{aa}-\text{ac} * (-1)) / (2 * \text{aa}) \dots\dots\dots (\%)$$

$$S_{-100\text{mt}} (\%) = 100 * (\text{aa}-\text{ad} * (-1)) / (2 * \text{aa}) \dots\dots\dots (\%)$$

$$S_{-300\text{mt}} (\%) = 100 * (\text{aa}-\text{ae} * (-1)) / (2 * \text{aa}) \dots\dots\dots (\%)$$

$$F_{20\text{mt}} (\%) = 100 * y/\text{aa} \dots\dots\dots (\%)$$

$$F_{300\text{mt}} (\%) = 100 * z/\text{aa} \dots\dots\dots (\%)$$

$$\text{ARM} = \text{ae}/m \dots\dots\dots (10^{-6} \text{Am}^2 \text{kg}^{-1})$$

$$X_{\text{arm}} = \text{ap}/0.3184 \rightarrow \text{aq} \dots\dots\dots (10^{-8} \text{Am}^2 \text{kg}^{-1})$$

$$X_{\text{arm}}/X = \text{aq}/w \dots\dots\dots (\text{Am}^{-1})$$

$$X_{\text{arm}}/M_{\text{rs}} = \text{aq} * 1000/\text{af} \dots\dots\dots (10^{-5} \text{Am}^{-1})$$

**分析结果:**

测量结果见表 3 (共 4 页), 计算结果见表 4 (共 4 页)。

### 3. 氮、磷元素含量分析

#### 目的和意义:

氮、磷是植物重要的营养元素，也是土壤肥力最重要的指标。人类在高强度开发的生产、生活过程中，由于大量化肥、洗涤剂等化学化工产品的使用，氮、磷元素通过地面冲刷和径流不断会向湖泊水体中转移。当湖泊水体较小、换水周期较长而氮、磷元素输入通量较大时往往会引起湖泊水质的恶化和生态系统的破坏。表现为藻类及其他水生生物的大量繁殖、水体透明度下降、溶解氧降低等。它们反过来又会给人类的生产和生活带来巨大的负面影响。因此，氮、磷元素在湖泊水体中的积累程度也是衡量湖泊富营养化的一项重要指标。湖泊的富营养化程度与湖泊的地貌背景、人类活动的强度是密切相关的。位于中国东部、长江下游三角洲地区的太湖由于地势平坦，水深平均不足 2 m，换水周期又较长（平均 288d），加上这一地区人类的高强度开发，湖泊富营养化问题十分突出。通过湖泊底质（表层沉积物）氮、磷的测定可为湖泊富营养化程度的合理评价和生态系统的修复提供定量依据。

自然界氮、磷的存在形式多种多样。不同状态的氮、磷在不同的环境介质中存在着很大的差异。湖泊表层沉积物是一种介于液相和固体相之间的一种特殊产物，除了液态的水和固态的沉积物外尚有丰富的生物活动物质，可以暂时称之为“水溶胶”。因此，我们在对底质样的氮、磷分析时只选择总氮（TN）和总磷（TP）两项指标，用来反映这种特殊记录中氮、磷的总体含量情况。

#### ●总氮测定方法及步骤:

总氮的测定采用最常用的标准方法——开氏法。

样品消解：首先选择具有一定代表性的样芯。其中太湖选择了 Tai 1 孔，澄湖选择了 chen 2 孔。两孔共计 58 个样品。准确称取通过 100 目筛的风干样品 0.5000g 左右，加入 1.85g 混合催化剂（ $K_2SO_4:CuSO_4:Se=100:10:1$ ）和 5ml 浓  $H_2SO_4$  后置于电炉上微煮，至溶液为淡蓝色。待冷却后定容、澄清作为备用的消煮液。每一批样品都同时做空白试验。

测定过程：扩散定氮法——用 40% 的 NaOH 与一定量的消煮液充分反应，产生的  $NH_3$  被  $H_3BO_3$  吸收，最后再用 0.01N 的标准硫酸滴定被  $H_3BO_3$  吸收的  $NH_3$ 。这一过程在扩散皿中进行。同一个样品并行做三个，用于测定结果的互相校验。

结果计算： $TN\%=(N(V-V_0)*0.014* \text{取用量倍数})W*100\%$ 。其中 N——标准酸当量浓度；V——用去的标准酸（ml）； $V_0$ ——空白实验用去的标准酸（ml）；0.014——每毫克当量氮的重量（g）；W——烘干土重（g）；取用量倍数——消煮液总量/所用消煮液量。

#### 分析结果:

计算结果见表 5。



### ●总磷测定方法及步骤:

总磷的测定采用硫酸—高氯酸消煮法。

样品消解: 准确称取通过 100 目筛的风干样品 0.5000~1.0000g 左右, 加入浓  $H_2SO_4$  和 60~72% 的高氯酸置于电炉上加热消煮, 待溶液转为无色后继续消煮 30~40 分钟。冷却后定容、过滤、澄清作为备用的消煮液。同时做空白试验。

测定过程: 钼锑抗比色法——取 5ml 滤液注入 50ml 容量瓶内用水稀释至 20ml, 加二硝基酚指示剂, 经酸、碱平衡后加入 5ml 钼锑抗和加水定容、摇匀。半小时后采用分光光度计比色 (波长为 700nm), 读出吸收值。——以空白试验的显色液的吸收值为 0。

结果计算:  $TP\% = \text{待测液磷含量 ppm } P \cdot (V/W) \cdot (V_2/V_1) \cdot 10^{-1}$ 。式中  $V$ ——为样品制备溶液的毫升数;  $W$ ——为烘干土样重 (g);  $V_1$ ——为吸取滤液毫升数;  $V_2$ ——为显色的溶液体积;  $10^{-1}$ ——将 ppm 数换算成 % 数的系数。

分析结果:

计算结果见表 5。

## 三、实验结果初步讨论

下面将获得的实验结果作一初步讨论。

### 1、含水量结果讨论

从图 1 看, 无论是太湖还是澄湖的样含水量都比较高, 变化范围为 30~70% 之间, 平均也在 50% 以上。两个湖泊之间的含水量差异不明显。含水量随深度的分布规律明显, 含水量随深度加深而快速降低深度一般在表层的 10cm 范围之内, 由 70% 下降到 50%; 10cm 深度以下含水量基本趋于稳定或下降幅度较小, 含量在 50% 左右——即湖泊沉积物在重量分配上水分与颗粒物呈对等配比。也由此看出水分对于湖泊沉积物的相对重要性。10cm 深度对于湖泊表层沉积物来说是一个重要的分界。分界线以上部分应属易受扰动的层位, 也是最容易吸收水体中各种元素的层位——水—沉积物界面。这一结论对于将来开展湖泊沉积物底质的污染调查和评价是很有帮助的。

从图 2 的曲线对比来看, 太湖样芯的含水量比较结果是:  $Tai 1 > Tai 2 > Tai 4 > Tai 3$ 。澄湖样芯的含水量比较结果是:  $Chen 2 >> Chen 1$ 。它们含水量的相对高低是否还与其他分析项目有关有待作出进一步的比较。

### 2、磁性测量结果讨论

图 3 至图 8 是太湖和澄湖 6 个样芯的多种磁性参数曲线, 包括磁化率、磁化率频率

系数、无磁滞剩磁、饱和等温剩磁、软剩磁、硬剩磁和比值参数。

从总体来看，各样芯曲线的细节变化都不明显，表明沉积物中的磁性物质具有比较均匀一致的特点，也体现了沉积环境的相对稳定性。由此看出，磁性测量工作虽然在全新世大尺度的湖泊沉积记录研究中取得了较大的成功，但对于那些短尺度样芯的研究来说这种优势并不明显，有其一定的局限性。但都有一个共同的特点，那就是随着年代变新，各曲线都呈微弱的上升趋势。

再从每一个样芯的情况来看，又有所不同。Tai 1 孔在 20cm 深度上所有磁性参数都发生了变化，指示磁界面（也是地层界面）的存在。Tai 2 孔至少有两个界面，8 cm 和 15cm；Tai 3 孔 2 个界面，7cm 和 15cm；Tai 4 孔 1 个界面，8cm；Chen 1 孔 1 个界面，7cm；Chen 2 孔 1 个界面，9cm。这些界面的清晰度、数量、深度位置等因剖面不同而不同，说明不同地点的沉积环境（抑或是人类活动的结果）还有一定的差异。

假如把上述 6 个剖面的各种磁参数按绝对值大小作一比较（图 9），那么可以看出：

（1）Tai 3 孔各磁参数值均明显高于其它五个孔，且波动明显。这是一种十分异常的情况。野外和室内详细观察时都发现沉积物中夹杂着许多硬土层的成分，颜色锈黄、边缘界线清晰，与正常的湖相沉积形成鲜明的对比。因此，推测是经受（人类）较大的扰动而引起的，不宜再作深入的研究。

（2）除 Tai 3 孔外，其它 5 个孔的磁参数都保持在一个比较稳定的分布范围，且可以互相作比较。当然最稳定的还得属 Tai 1 和 Chen 2。它们完全适合作更深入的研究。

### 3、氮、磷分析结果讨论

氮和磷含量都只做了两个孔，Tai 1 和 Chen 2。

从图 10 可以看出，尽管 Tai 1 和 Chen 2 分属两个湖泊，且一大一小。但在氮含量方面明显具有两个相似的特点：

（1）绝对含量比较接近，波动范围为 0~0.12%。反映流域内氮物质含量的

（2）氮含量随深度变化波动的趋势基本可作对比。可以划分为三段：从 10cm 深度位置开始，氮含量发生明显的升高，曲线具有“双峰式”结构；20~10cm 段为氮含量的低值段；20cm 以下又出现偏高的特征。反映流域内氮输入量的阶段性变化。

与氮含量相比，磷含量有所不同。两个孔之间最明显的差别是它们的绝对值大小相差悬殊，Tai 1 孔含量较低，为 0.03~0.06%；而 Chen 2 孔含量较高，为 0.06~0.1%。后者几乎是前者的两倍。而一致的方面是它们都随着深度变浅呈上升的波动趋势。如果作一线性回归分析（图 12），那么这种情况可以看得更为清楚。其中 Tai 1 孔的相关系数为-0.850068，Chen 2 孔的相关系数为-0.644423。



表3 长江下游太湖及澄湖表层沉积物的磁性测量结果

Depth (cm)	Sample No	Mass (g)	$X_{ir}$	$X_{nr}$	arm-N	arm-E	20mt N	20mt E	300mt N	300mt E	1000mt N	1000mt E	-20mt N	-20mt E	-40mt N	-40mt E	-100mt N	-100mt E	-300mt N	-300mt E
1	T1-01	3.61	93.33	93.17	53.5	4.5	250.7	29.1	1325.7	211.2	1433.8	41.5	655.2	54.9	-95.2	-94.9	-981.3	100.1	-1283.1	69.1
2	T1-02	4.15	113.5	111.67	62.9	11.9	314.3	24.5	1528.9	195	1663.3	211.8	693.1	52.7	-120.4	-38.5	-1164.1	6.8	-1493.6	-59.9
3	T1-03	4.5	120.67	119	68.1	6.2	313.7	57.5	1634	129.2	1734.7	67	799.7	57.9	-118.2	5.3	-1174.1	18.2	-1506.9	-347.6
4	T1-04	4.44	109.5	107.83	62.2	13.4	300.8	15.6	1495	13.7	1595.7	14.5	730.7	111.5	240.5	46.7	-1040.7	-309.8	-1426.5	-50.7
5	T1-05	5.49	132.5	130.17	77.2	13.8	361.7	5.1	1799.6	-35.2	1931.1	-84.8	873.3	135.3	278	88.4	-1299.9	-150.7	-1733	0
6	T1-06	6.42	167.33	164.17	93.6	3.3	426.6	4.6	2171.1	128.7	2312.4	263.3	1047.6	211.4	327.2	89	-1573.5	-18.9	-2030.6	-195.5
7	T1-07	5.7	141.5	139.83	79.7	2.6	395.7	16.5	1870.6	159.1	2010	94.5	898.8	90.7	267.2	-49.3	-1330.5	-435.4	-1748	-262.5
8	T1-08	5.44	132.67	130.5	76.5	4	361.6	44	1784.3	8	1917.5	65.9	878.9	81.7	284	75.2	-1293.4	168	-1689.8	-136.4
9	T1-09	7.68	192	189	104.9	18.7	494	62.3	2393.1	202.9	2601.6	106.5	1220.6	95	414.3	46.7	-1747.4	-134.6	-2292.3	109.4
10	T1-10	6.14	153.33	151	86.3	6.8	411.5	6.9	1955.4	-7.4	2112.8	6.4	967.6	11.5	301.7	109.8	-1419.4	216.5	-1839.3	-255.3
11	T1-11	4.65	111.67	110.5	66	8.1	338	26.4	1507.3	33.3	1621.7	-34.3	723.4	112.3	235	-18.9	-1103	-57.2	-1410.5	-28.6
12	T1-12	4.66	115.5	113.5	63	7.4	315.3	8.4	1451.7	309.3	1629.8	19.9	728.8	25.9	221.6	16.2	-1106	-121.4	-1426.9	-113.8
13	T1-13	6.58	173.67	171.33	85.4	12.6	444.4	21.4	2107.2	-140.6	2279	-6.4	1002.8	135.6	286.2	127.9	-1636.2	-300.8	-1951	-489.5
14	T1-14	5.68	149.33	146.17	75.6	17.2	395.9	9.7	1808	507.3	2023	92.9	923.2	142.3	274.8	212.5	-1378.6	-76.6	-1774.3	-317
15	T1-15	6.53	159.17	155	84	11.3	412.2	9.7	1865.7	300.1	2041.7	79.4	924.8	116.7	290.2	-22.4	1367.8	21	-1787.5	-203.3
16	T1-16	6.45	155.67	153.17	80.4	23.6	412.4	16.1	1871.8	122.8	2006.6	83	918.9	126.5	271.1	16.1	1330.8	-345.6	-1773.5	-248.9
17	T1-17	5.24	130	128	70.4	13.5	338.5	67.1	1602.8	134.5	1740.6	-0.2	809.8	35.7	257.4	-79	1167.9	-200.8	-1521.8	-210.4
18	T1-18	6.87	163.8	159.33	86.6	4.4	420.6	22.8	1911.4	9.7	2076.4	150	943.3	139	291	11.5	-1382.4	-109.8	-1826.8	-122.4
19	T1-19	6.02	138	136.17	73.9	2.8	366.9	16.8	1678	240.5	1829.8	17.2	841	24.2	278.8	-96.9	-1215	-101.2	-1604.6	-119.8
20	T1-20	6.98	154	150.33	77.4	20.9	389.1	28.6	1777.2	40.6	1927.5	95.7	895.3	180.8	283.2	34.2	1266.7	47.1	-1698.9	26.6
21	T1-21	8.93	183.17	180	85.2	20.5	433.2	9.7	1845.2	470.5	2071.2	238.9	939.2	85.5	357.7	-142.2	1304.3	-156.4	-1780.1	-300.1
22	T1-22	8.45	161.8	158.33	76.1	17.4	357.8	33.2	1674.6	124.9	1846.8	67.1	894.1	91	335.4	146.3	-1105.6	20.6	-1581	-165.7
23	T1-23	8.93	155.33	151.33	78.4	3.1	337.7	-11.8	1615.3	-16.3	1782.7	53.1	885.3	191.9	365.6	-18.9	-1024.6	-89.4	-1517	-27.5
24	T1-24	7.56	111.83	109	56.8	11.1	242	5.9	1187.5	-1.9	1305	47.2	679.6	126.9	312.2	41.3	-711.3	186.5	-1087.8	-73.5
25	T1-25	9.72	117.83	117.17	50.5	16.1	216.7	-1.8	1152.5	127.6	1310.9	64.8	745	136.9	411.5	-0.3	-605.8	-59.3	-1043	-43.3
26	T1-26	10.38	125.17	123.83	63.4	11.7	234.9	17	1290.7	144.6	1465.1	49.4	854.7	135.5	474.2	77.3	-681.1	-78.1	-1175.5	7.2
27	T1-27	8.33	101.17	99.17	59	13.9	200.6	10.8	1039.3	336.2	1228.7	74.4	741.6	25.3	412.5	82.2	-564.7	-224.1	-994.8	33.4
28	T1-28	10.65	152	149.5	100.4	33	347.8	88.3	1782.9	279.3	1966.5	124.9	1040.6	179.2	475.3	-21.1	-1160.1	-322.8	-1665.4	-279.5
29	T1-29	7.74	116.5	114.33	93.4	22.1	305.8	5.1	1493.9	103.5	1626.4	58.2	907.7	8.6	429.5	-6.6	-989.3	-255.1	-1401.8	-171.3
30	T1-30	9.73	135.67	134.17	121	17.1	363.8	-22.5	1738.4	10.2	1893.1	60.7	1084.1	76.2	515.8	152.5	-1162.1	-207.9	-1637.7	-31.6
1	T2-01	3.15	82.33	80	42.9	11.6	218.3	-24.4	1131.6	47.6	1298.5	3.2	701.7	54.3	176	-62.5	-786.2	-250.3	-1074.1	-72.8
2	T2-02	4.98	139.67	134	69.9	11.7	344.1	46.2	1775.6	397.9	1905.7	222.3	880.5	38.5	292.6	-104.8	-1305.6	-127.8	-1728	46.6

Depth (cm)	Sample No	Mass (g)	X <sub>ir</sub>	X <sub>nr</sub>	arm-N	arm-E	20mt N	20mt E	300mt N	300mt E	1000mt N	1000mt E	-20mt N	-20mt E	-40mt N	-40mt E	-100mt N	-100mt E	-300mt N	-300mt E
3	T2-03	5.58	155.33	149	74.5	21.5	377.4	34.6	1885.2	357	2003	208.2	903.5	37.3	264	-31.1	-1362.8	-310.1	-1807.2	213.6
4	T2-04	4.31	118.17	115.33	64.8	5.3	310.2	-45.9	1571.6	105.7	1648.3	155.6	756.7	47	243.2	-46.7	-1136.3	-17.8	-1456.6	-292.3
5	T2-05	6.83	183.33	178.5	86.2	25	455.4	40.3	2387.3	-14.1	2455.4	509.9	1125.7	22.3	343.6	-77.7	-1710.1	58.8	-2240.1	-290.3
6	T2-06	6.22	172.33	168.17	84.9	12.5	439.1	-43.3	2280	222.4	2301.8	285.9	887.8	77.3	166.2	246.9	-1701.8	91.8	-2209	-51.7
7	T2-07	7.42	199.67	196.67	90.3	17.1	479.4	49.3	2326.2	1004.6	2667.2	180.4	1214	43.1	392.6	-169.4	-1777.6	-357.4	-2384.4	-251.8
8	T2-08	7.48	208.17	204.83	97.1	25.4	516.4	-41.5	2573.5	131.7	2707.8	268.4	1176.2	46.9	315.3	-10.3	-1837.3	-429.4	-2456.6	-57.5
9	T2-09	8.12	199.67	196.67	98.8	15.3	458.6	-30.7	2394.3	-237.5	2524	261.8	1172.1	-24	390.4	-173.5	-1661.5	-430.4	-2257.7	-52.1
10	T2-10	7.37	168.67	167	85.3	7.7	385.8	-2	1924.1	-271.6	2043.4	214.2	965.7	3.9	329.4	113.8	-1340	266.4	-1807.9	-158.2
11	T2-11	7.91	168.83	167.17	86.2	30	375.9	40.8	1781.8	135.2	1884.6	185.3	952.2	0	374.4	-105.1	-1205.7	-137.4	-1656.1	-68.8
12	T2-12	9.66	189.5	185.33	106.8	29.3	381.4	156.9	1982.3	-33	2083.4	201.2	1083.6	55	419.2	47.9	-1309	-213.4	-1826.2	-66.8
13	T2-13	8.75	154.67	153.17	103	20.7	344.8	119.7	1641.8	610.3	1851.7	163.2	989.4	102.5	425	-44.4	-1144.9	-214.7	-1606	-72.6
14	T2-14	9.1	155.5	154	121.6	32.4	384.6	89.4	1961.2	218.6	2067.3	185	1149.8	109	494.1	80.2	-1352.2	-92	-1821.8	-31.8
15	T2-15	10.27	193.33	191.33	141.8	22.5	475.3	55.9	2367.9	-140.5	2469.8	210.7	1316.3	145.7	548.5	98	-1644.2	88	-2136.4	594.8
16	T2-16	9.17	174.5	173.5	131.4	17.5	434	93.3	2119.9	531.3	2281.3	184.8	1203.6	150.4	488	74.3	-1504.9	-237.9	-1979.9	-309
17	T2-17	8.13	143.33	141.83	129.2	1.2	391.3	31.2	1893.5	337.4	1977.8	160.4	1098.8	3.3	460.9	-25.6	-1325.5	-279.2	-1751.5	-185.6
18	T2-18	8.67	155.33	154.83	136.1	12.2	408.5	43.1	2081.2	-198.4	2174.4	294.1	1200.2	58	518.3	118.3	-1450.8	-203.9	-1914.9	39.9
19	T2-19	9.23	167.33	166.67	155.8	7.6	440.8	123.4	2321.2	-85.5	2405.1	161.3	1335.7	62.8	567.2	16.6	-1619.9	-236.3	-2121.9	-140.6
1	T3-01	4.28	125.17	121.17	50.7	12.5	242.2	101.6	1436.3	4.4	1544.5	47.3	702	75	287.1	-128	-966.2	-17.5	-1324.1	-101.3
2	T3-02	4.91	137.67	133.83	63.3	4.3	307.9	49	1724.6	-331	1883.7	185.7	880.3	34.8	332.3	11.3	-1179.2	-88.3	-1619.6	-158.1
3	T3-03	5.39	656.5	612.17	109	16.9	1795.4	215.6	3898	731	4310	249	-437.8	193.6	-1512.4	318.7	-3306	-763	-3837	-577
4	T3-04	6.32	244.67	233.83	71.4	10	530.1	96.5	2258.4	296.3	2485	123	848.6	-4.9	138.1	-233.6	-1607.4	-157.7	-2091.8	-337.6
5	T3-05	7.64	221.17	210.5	79.1	6	420.5	88.1	1985	253	2113.2	137	907.3	205.3	287.6	75.4	-1202.6	-487.2	-1177.2	353.7
6	T3-06	9.08	618.67	577	118	33.8	1468.8	107	3518	-285	3675	181	154.3	106.5	-917.6	-373.2	-2784.5	-341.2	-3277	-496
7	T3-07	9.83	495.5	463.67	156.5	19.1	998.3	107.7	3168	301	3348	142	833.5	-95.1	-270.9	-158	-2452.9	-268.8	-2950	-315
8	T3-08	9.12	443.67	416.83	152.5	39.5	1011.5	96.4	3358	-228	3543	347	831.8	-54.6	-384.9	-69.3	-2687.4	-341.1	-2963	-128
9	T3-09	7.54	379.5	355.5	118.5	21.5	805.3	49.4	2695	167	2828	304	669.3	38.7	-296.3	-9.2	-2064.7	-466.7	-2489	-456
10	T3-10	8.2	510.17	480.67	125.5	33.5	1350.4	79.4	3817	220	3897	234	318.3	37.5	-1078.8	-275.6	-3122.6	-81.7	-3549	-88
11	T3-11	7.79	785.33	733.17	137.6	12.1	1758.9	344.8	4873	1066	5108	-103	156.8	-105.7	-1687.7	-451.6	-4200	-48.8	-4696	-315
12	T3-12	7.95	644.83	603.67	122.9	0.5	1356.4	-85.3	4179	239	4300	180	386.2	210.4	-1195.5	-125.3	-3333	-79.3	-3873	-477
13	T3-13	9.5	876.5	819.33	126.9	12.8	1705.5	196.1	5011	296	5259	164	526.6	-553.5	-1468.2	-88.2	-4156	-491	-4721	-608
14	T3-14	8.81	1317	1226.17	152.1	23.8	2481.6	64.1	7664	-1209	7952	124	704.7	341	-2029.2	-483.2	-6480	-829	-7381	-619
15	T3-15	8.31	570.13	536.83	123.8	33.3	1231.6	234.7	4390	-103	4622	132	969.4	-0.1	-562.5	-192	-3497	-646	-4171	-357
16	T3-16	7.5	540.17	511.5	125	19.7	1357.1	-185.5	4353	533	4448	399	517.4	-5.8	-1006.7	-195.2	-3572	-454	-4125	-86
17	T3-17	8.33	615	583	123.3	26	1175.6	-18.3	4622	-410	4745	527	1372	74.7	-110.4	-121.6	-3372	-818	-4175	350
18	T3-18	8.25	578.8	543.17	125.1	14.6	1007.6	-88	5293	-1419	5636	1	2200.9	216.7	819.9	-140.3	-3851	-1100	-5074	-896

Depth (cm)	Sample No	Mass (g)	X <sub>ir</sub>	X <sub>hr</sub>	arm-N	arm-E	20mt N	20mt E	300mt N	300mt E	1000mt N	1000mt E	-20mt N	-20mt E	-40mt N	-40mt E	-100mt N	-100mt E	-300mt N	-300mt E
19	T3-19	7.63	721	672.5	127.2	24.7	1538.8	-23.5	5897	638	6045	11.7	1453	391.4	-398.3	-203.4	-4413	-908	-5492	-444
20	T3-20	7.7	552.5	520.17	105	14.9	1140	164.5	4732	-536	4914	10.3	1402.8	-41.9	-121.4	185.6	-3586	-197	-4442	-406
1	T4-01	3.48	77.17	73	40	5.4	180.9	4.7	1044.9	13.5	1115.3	162.3	513.1	109.9	185.1	2.8	-671.4	-215.5	-970.1	-42.5
2	T4-02	6.15	132.67	127.5	63.4	0.9	306.1	-27.8	1823.7	15.3	1931	193.1	875.2	63.6	320.6	-132.5	-1222.6	-130.1	-1655.8	-324.9
3	T4-03	6.86	151	146.33	73.4	1.5	340.7	-13.2	1996.2	100.8	2130.7	283.5	963.9	85.2	347.9	-100.5	-1282.5	-415.9	-1826.5	-171.5
4	T4-04	9.69	209.33	200.83	99.8	4.2	441.7	16.3	2525.3	343.6	2727.2	281.3	1243.1	105.5	446	-51.9	-1728.8	-83.2	-2342.9	-305
5	T4-05	7.96	182.17	172.83	88.9	10.3	408.5	28.7	2189	476	2376.8	363.4	1064.7	66.7	335.7	-5.5	-1542.3	-100.6	-2065	-276.4
6	T4-06	8.94	203.5	193.17	89.4	10.6	414.5	38.7	2256.3	-305.9	2434.5	338.4	1076.9	94.2	363	-132	-1540.2	-32.7	-2087	-305.5
7	T4-07	8.84	167.17	161	80.7	3.2	320.4	18.1	1744.5	66.4	1861.4	285.4	880.8	79	311.4	21.9	-1126.5	-317.3	-1593.4	-230
8	T4-08	8.44	136.5	131.67	130.1	12.6	367.3	-13.1	1896.8	188.1	1997.8	268.3	1064.7	102.9	466	-15.4	-1303.5	-381.3	-1757.4	-258.9
9	T4-09	8.12	127.67	124.5	125.8	13.5	354.4	18	1748.3	162.1	1846.8	258.1	970.1	81.5	408.6	5.6	-1233.7	-141.8	-1610.2	-227.4
10	T4-10	8.25	121	116.17	101.1	19.8	313.7	-11.7	1643.5	-61.8	1757.1	174.5	922	36.3	379.8	17.5	-1099.2	-194.1	-1507.2	-166.8
11	T4-11	7.85	102.33	97	81.2	3.2	257	-24.8	1339.1	352.5	1476.5	260.6	780.8	37.5	342.6	10	-856.6	-247.1	-1252.8	-122.6
12	T4-12	7.84	113	106.83	106.3	9.5	316	-4.7	1622.5	53.9	1713.1	201.2	897.3	18.6	354.2	54.3	-1125.1	-122.6	-1466.8	-346.4
13	T4-13	8.74	137	131	142.4	11.4	388.7	16	1899.5	447.2	2047.3	230.8	1100.8	71.9	452.1	54.2	-1414.5	-122	-1828	-63.2
14	T4-14	8.27	115.67	112.17	106.9	22.7	316.2	29.7	1622.1	129.5	1690.5	300	899.3	66.1	387.1	-17.2	-1144	39.1	-1608.8	-137.2
15	T4-15	9.89	121.17	116.83	79	1	263.8	-16	1469.8	-54.6	1597.4	187	861.3	94.5	408.4	171.6	-902.9	101.5	-1316.5	-145.3
16	T4-16	8.01	104.17	100.17	82.4	3.8	251	4	1344.2	-113.7	1451.7	190.8	797.9	21	379.6	12.1	-855	-87.4	-1207.3	-242.7
17	T4-17	7.44	103.67	98	81.5	8.4	258	-4.6	1299	412.8	1458.4	172.7	764.1	24.9	323.2	66.7	-886	-113.7	-1245.8	38
18	T4-18	7.79	107.33	103.33	98.2	7.8	283.1	-24.2	1430.2	184.5	1513.6	114.3	803.6	30	357.3	-66.8	-977	-121.3	-1330.6	-138.6
19	T4-19	7.79	116.83	112.67	117.3	34.9	342.1	-0.9	1666.1	-7.5	1743.7	244	908.6	143.7	378.7	94.6	-1183.5	-120.8	-1567.9	-68.4
20	T4-20	8.79	134.8	130.17	135.3	10.1	373.7	-28	1936.9	-6.1	2033.1	292	1100	87.9	462.5	37.9	-1371.8	-241.2	-1821.6	103.6
21	T4-21	8.72	137.33	133.5	133.7	17.9	381.1	-11.1	1934.4	12.7	2016.2	232	1075.6	18.5	432	280.3	-1390.7	153.6	-1824.4	-35.1
22	T4-22	8.6	132.67	128.5	123.6	14.8	350	-22.9	1862.5	162.5	1956	247.3	1058.8	95.6	466.9	28.4	-1308.2	-77.8	-1737.2	-181.5
23	T4-23	8.36	131.83	128.67	121.7	8.4	342.8	-48.7	1949.2	365.7	2078.9	235.8	1161.1	125.9	539.5	115.5	-1382.2	-80.3	-1831.8	-399.8
24	T4-24	8.44	131.33	125.67	110.5	10.6	322.2	-5.6	1739.9	98.6	1831	222.3	969.5	106.8	418.2	-101.3	-1227.6	-197.3	-1630.3	-112.7
25	T4-25	8.58	140.17	137	117.1	11.5	346.4	1.6	1874.9	-35.7	1974	212.8	1041.3	50.5	421.3	25.2	-1340.9	11.1	1743.7	-78.6
1	C1-01	6.13	119.33	114.17	24.1	3.3	189.8	24.4	1123.3	243	1267	147	537.3	18.7	-18.8	-59.1	-689.4	-100.9	-1025.6	102
2	C1-02	8.51	170.33	164	32.9	2.7	253.7	99.3	1535.7	277	1738.7	144.7	734.6	25.5	-22.5	-86.9	-946.5	-47.8	-1384.3	-158.6
3	C1-03	10.63	209.83	205.17	40.1	6.4	304.2	0.5	1778.4	329.2	1988.6	217.1	878	35.9	-13.4	94.2	-1070.2	-10.7	-1547.9	-418.8
4	C1-04	9.28	183	179	35.2	2	262.5	46	1516.8	415.4	1749.2	209.3	762.7	113.7	-6.7	29.5	-956.6	159.7	-1401.4	-201.9
5	C1-05	8.15	169.67	166	29.5	11.1	251.7	21.6	1402.1	417.6	1612.3	223.8	682.9	72.6	-34.4	73.2	-897.9	16.9	-1304.4	-130.7
6	C1-06	7.16	145.33	143.17	30.2	2.5	221.1	40.2	1313.3	263.7	1487	135.8	650.5	-17.2	-31.2	82.1	-818.4	-79	-1206.1	-91.4
7	C1-07	9.46	212.5	209.83	33.8	9.4	294	101.2	1837.5	-228.2	2040	247.4	855.3	-20.4	-58.8	-49.5	-1108.7	-359.1	-1650.1	-194.5
8	C1-08	7.58	159.5	156.67	29	8.5	245.1	47.2	1403.7	344.9	1574.1	183.2	680.3	-70.3	-38.3	-80.3	-886.2	-91.9	-1272.6	-242.1

Depth (cm)	Sample No	Mass (g)	X <sub>ir</sub>	X <sub>ir</sub>	arm-N	arm-E	20mt N	20mt E	300mt N	300mt E	1000mt N	1000mt E	-20mt N	-20mt E	-40mt N	-40mt E	-100mt N	-100mt E	-300mt N	-300mt E
9	C1-09	7.02	139.5	136.5	29.4	2.8	215.4	27.6	1270.8	214	1439	131.8	620.7	81.2	-9.3	-73.6	-785.1	-20.4	-1136.4	-246.8
10	C1-10	9.35	185.33	181.83	37.2	5.7	288.4	-8.1	1616.3	12.3	1793.8	208.5	793.5	3.3	-1.1	-32.8	-975.6	-105.7	-1430.9	-245.6
11	C1-11	8.14	166.17	162	34.1	3.8	249.7	23.6	1501.4	-25.3	1657.8	180.9	739	132.5	-21.8	132.6	-902.6	-223.4	-1347.8	-85.8
12	C1-12	8.82	176.67	172.83	34.2	7.7	259.6	23.4	1412.5	616	1719.3	253.1	768	64.8	11.4	-76.1	-924.8	-147.1	-1389	11.2
13	C1-13	6.96	136.67	133.83	28.2	2.5	211.7	10.5	1264	144.5	1403.1	138.7	630.4	65.7	13.3	-71.8	-725.1	-127.2	-1143.8	-98.3
14	C1-14	8.82	168.83	163.83	33.1	6.3	246.7	3.7	1461.2	-92.7	1632.8	148.8	735.9	76.7	25.9	-75.4	-881.3	-25.7	-1322.1	28.8
15	C1-15	8.73	158	154.17	31.4	0	229	-4.7	1335.9	157	1500.8	168.6	690.3	96.3	64	-128.1	-756.4	-203.2	-1202.1	-57.7
1	C2-01	3.25	60.83	57.83	16.8	1.6	97.6	-5	570.8	95.3	633	72.2	297.8	17.4	17.4	0.7	-344.3	-5.9	-525.2	-36.7
2	C2-02	5.02	84	81.67	17.2	-0.3	115.7	-6.9	738.7	66.2	827.1	94.7	408.5	9.2	55.6	18.9	-379.7	-135.5	-637.9	-117.1
3	C2-03	5.72	95.83	92.5	24.8	-3.2	144.8	-10.1	897.6	78.4	995.1	138.1	478.1	69.8	50.9	57.3	-489.6	-158.7	-796.4	19.3
4	C2-04	5.29	96.17	93.17	24.8	-0.2	149.7	19.8	901.8	119.5	1008.5	108.9	473.9	57.2	39.8	-23.2	-530.8	-54.8	-811.4	-151
5	C2-05	9.11	164.33	160.67	41.5	0.2	226.8	33.3	1381.3	234	1559	140.3	760.5	83.2	78.6	86	-785.9	-139.7	-1245	-138.9
6	C2-06	5.99	107.67	103.5	27.9	5	159.4	0.6	957.1	40.3	1071	107.9	520.7	39.8	57.9	12.1	-549.4	-1.4	-841.9	-193.1
7	C2-07	6.81	116.33	112.17	31.2	1	174.3	-10.6	1048.3	180.7	1162.4	211.1	582.4	48.4	53.6	50.5	-590.5	-109.6	-942	-159.7
8	C2-08	8.59	146.5	144	36	0.3	215	-14.5	1279.6	-71.8	1447.5	64.3	697.8	92	36.4	-33.1	-739.6	-174.7	-1158.3	-123.7
9	C2-09	10.21	175.83	172	40.2	6	243	24.5	1420.6	313.5	1646.2	202	814.1	88	106	-20.5	-806.3	-174.5	-1284.6	-293.5
10	C2-10	7.72	134	131.33	33.6	3.5	197.4	25.1	1131.4	335	1329.3	165	649.5	112.7	71.2	13.2	-665.6	-108.8	-1041.1	-224.6
11	C2-11	7.69	132.5	128	33.3	5.3	195.6	9	1161.8	68.1	1302.9	132.8	631.2	-12.3	78.1	-25	-629.9	-223	-1049.4	-84
12	C2-12	7.87	135.83	132.67	33.7	3.4	198	18.4	1154.7	283.6	1349.2	159.1	656.7	105.4	74.7	32.9	-669.6	-103.7	-1034.8	-275.8
13	C2-13	7.89	133.67	130.5	33.7	1.5	191.7	0	1167.4	30.9	1316.7	135.7	631.4	174.8	70.9	59.4	-647.6	-103.1	-1031.2	-181
14	C2-14	9.48	161.5	157.83	39.7	3.1	221.9	24.1	1341.6	245.7	1539.6	184	771.8	30.1	121.9	-62.3	-749.3	-120.6	-1224.5	4.7
15	C2-15	9.39	162.17	158.67	38.1	9	221.1	33.6	1321.5	303.5	1535.2	149.4	761.2	75.3	91.4	80.5	-765	147	-1213.3	-73.5
16	C2-16	10.23	171.67	167.33	40.3	7	226.1	56.7	1415.2	63.4	1590.4	203.6	775.6	39.1	129.3	-101.5	-780.6	-49	-1245.6	-172.2
17	C2-17	7.21	115.83	113.17	29	4.7	166.4	24.5	1005.1	171.7	1149.6	139.5	569.7	49.6	77.4	3	-567.4	5.2	-912	-68.5
18	C2-18	7.14	116.5	113.17	28.1	11.7	173.2	13.8	1025.3	151.8	1157	58.2	581.4	6.8	67	51.2	-580.6	-55.8	923.8	-152.2
19	C2-19	9.54	156.5	152.5	35.6	0.6	212.4	3.5	1283.9	108.5	1460.6	90.1	732.5	99.5	116.2	-24.2	-703.5	-76.6	-1150.8	-105.5
20	C2-20	9.68	151.17	147.83	30	2.2	203.3	7.6	1285.9	158.6	1465.2	41.3	742.2	71.9	123.7	33.3	-651	-251.5	-1163.4	103.6
21	C2-21	8.94	131.83	128.67	24.9	3.9	183.2	1	1139.8	289.4	1335.1	92.6	676.6	53.1	114	45.5	-618.2	-73.9	-1051.4	-78.7
22	C2-22	9.72	150.33	146.17	28.2	1.5	186.3	34.9	1177.1	304.1	1369.9	162.9	708.7	-10.9	135.9	23.3	-607.6	-188.9	-1071.6	-107
23	C2-23	9.18	147	143.33	31.2	2.5	197.3	10	1236.5	167.6	1406.5	82.9	725.6	123.3	143.3	61.8	-660.3	43.5	-1117.5	-69.5
24	C2-24	8.62	133.16	130.5	26.7	2.3	174.1	19.1	1101.9	25.8	1242.8	158.7	648.4	32.5	130.4	25.1	-547.7	-170.8	-953.4	-198.4
25	C2-25	8.66	148.83	145	34.2	-1.8	208.3	24.5	1288.8	-22	1445.9	39.3	741	98	133.2	62.1	-664.3	-216.5	-1156	-125.8
26	C2-26	9.94	161.83	158.17	34.2	6.7	210	10.4	1312.4	-191.6	1483.6	59.5	782.1	81.5	161.4	29.7	-682.2	-102.8	-1162.6	-163.4
27	C2-27	9.38	155.67	151.5	36.2	5.7	208.2	27.2	1308.5	146.5	1470.9	100.6	794.2	62.6	186.7	-32	-688.6	-106.2	-1173.8	-160.4
28	C2-28	8.52	136.17	133.5	29.2	8.7	149.2	64	1033.9	364	1261.2	30.6	652.1	58.4	118	75.5	-574.8	-78.5	-988	-84

表4 长江下游太湖及澄湖表层沉积物的磁性参数计算结果

Susc	X <sub>fd</sub> (%)	IRM 20mt	IRM 300mt	IRM 1000mt	IRM- 20mt	IRM- 40mt	IRM- 100mt	IRM- 300mt	SIRM	SIRM /X	Soft	Hard	S- 20(%)	S- 40(%)	S- 100(%)	S- 300(%)	F20 (%)	F300(%)	ARM	X <sub>arm</sub>	X <sub>arm</sub> / X	X <sub>arm</sub> /M <sub>s</sub>
25.5056	1.61233	4066.77	19882.6	21629.8	8966.8	1630.63	15017.1	19282.9	4860.64	19.0571	913.881	392.635	29.2721	53.7694	84.7139	94.5748	18.8017	91.9221	4333.24	13609.4	533.585	2799.92
26.8156	1.38394	4114.15	21144.4	22394.3	10343.1	1526.31	15147.7	19949.5	4976.51	18.5583	914.256	277.759	26.9069	53.4078	83.8204	94.5414	18.3714	94.4186	4433.22	13923.4	519.229	2797.82
24.6622	1.52511	3885.53	19286.3	20585.4	9535.14	3160.4	14007.2	18413.5	4636.35	18.7994	875.119	292.586	26.84	57.6763	84.0222	94.7247	18.8752	93.6893	4147.18	13025.1	528.139	2809.35
24.1348	1.75849	4666.39	23219.3	24935.2	11400	3763.14	16881	22355.7	4541.93	18.819	849.98	312.55	27.1407	57.5458	83.8497	94.8276	18.7141	93.1186	4072.08	12789.2	529.906	2815.81
26.0639	1.88848	5503.46	28056.4	30022.7	13786.4	4374.24	20299.6	26315.9	4676.43	17.9422	857.237	306.279	27.04	57.2849	83.8071	93.8267	18.331	93.4506	4099.05	12873.9	493.936	2752.93
24.8246	1.18021	5108.97	24217.9	25957.6	11653.4	3505.06	18059.1	22802	4553.97	18.3446	896.311	305.218	27.553	56.7515	84.7857	93.9216	19.682	93.2978	4000.35	12563.9	506.107	2758.89
24.3879	1.63564	4699.05	23017.7	24750.4	11386.7	3789.86	16825	21869.3	4549.7	18.6556	863.796	318.503	26.9969	57.6562	83.9894	94.1798	18.9858	92.9995	4020.09	12625.9	517.712	2775.11
15	1.5625	6423.08	30981.8	33588.7	15793.4	5378.32	22608.2	29604.3	4373.53	17.4941	836.339	339.446	26.49	58.0061	83.6544	94.0688	19.1227	92.2386	3854.73	12106.6	484.262	2768.15
4.9723	1.5196	5309.1	25224.8	27255.2	12482.9	4141.66	18522	23954.4	4438.96	17.7756	864.674	330.691	27.1	57.5979	83.9788	93.9446	19.4792	92.5503	3901.37	12253	490.665	2760.33
4.0151	1.04773	4373.48	19448.9	20924.6	9443.64	3041.29	14247.8	18199.2	4499.92	18.7379	940.533	317.357	27.4341	57.2673	84.0456	93.4876	20.9011	92.9475	3913.81	12292.1	511.849	2731.63
4.7854	1.7316	4068.81	19147.3	21026	9407.45	2866.27	14353.1	18465.5	4512.01	18.2043	873.135	403.152	27.629	56.816	84.1318	93.9111	19.3513	91.0649	3962.55	12445.2	502.118	2758.24
6.3936	1.34738	5739.4	27243.3	29399.2	13053.9	4043.87	21460.7	25948	4467.97	16.9282	872.249	327.647	27.7989	56.8775	86.4988	94.1304	19.5223	92.6668	3943.47	12385.3	469.252	2772.02
6.2905	2.11612	5108.64	24223.9	26124.2	12049.9	4481.17	17811.4	23250.9	4599.33	17.4943	899.408	334.56	26.9373	58.5767	84.0898	94.5007	19.5552	92.7259	4093.47	12856.4	489.012	2795.28
4.3752	2.61984	5318.85	24376.9	26357.8	12024.5	3754.72	17646.7	23207.4	4036.42	16.5595	814.525	303.36	27.1899	57.1226	83.4752	94.0237	20.1794	92.4844	3553.97	11162	457.923	2765.32
4.1349	1.60596	5324.01	24198.1	25907.3	11965.6	3503.35	17736.8	23102.4	4016.63	16.6424	825.428	264.988	26.9069	56.7613	84.2313	94.5867	20.5503	93.4027	3581.77	11249.3	466.1	2800.68
4.8092	1.53846	4451.62	20748.8	22453.7	10456.6	3473.33	15287	19818	4285.06	17.2721	849.546	325.37	26.7152	57.7344	84.0411	94.1307	19.8257	92.4069	3782.06	11878.3	478.787	2772.02
3.8428	2.72894	5433.71	24657.4	26855.4	12300	3756.83	17889.1	23618.6	3909.08	16.3952	790.933	319.936	27.0995	56.9946	83.3064	93.9737	20.2332	91.8156	3437.93	10797.5	452.863	2762.16
2.9236	1.32609	4737.97	21867.4	23605.5	10853.4	3807.56	15727.8	20757	3921.17	17.1054	787.038	288.715	27.0108	58.065	83.3139	93.9665	20.0715	92.637	3448.01	10829.2	472.403	2761.72
2.063	2.38312	5032.93	22931.9	24895.4	11782.5	3679.82	16351.7	21918.5	3566.67	16.1659	721.05	281.301	26.336	57.3906	82.8408	94.0212	20.2163	92.1131	3140.19	9862.39	447.011	2765.15
2.5118	1.73063	5589.68	24564.7	26895.6	12165.8	4965.58	16946	23287.3	3011.83	14.6834	625.944	261.022	27.3833	59.2312	81.5033	93.292	20.7829	91.3334	2607.76	8190.2	399.292	2719.34
2.1479	2.14462	4635.45	21662.3	23839.4	11593.5	4720.36	14264.7	20506.6	2821.24	14.7339	548.574	257.65	25.6842	59.9003	79.9183	93.0098	19.4445	90.8675	2426.82	7621.91	398.055	2701.62
2.3942	2.57516	4358.99	20838.4	23007	11685.6	4722.54	13267.6	19572.5	2576.38	14.8117	488.129	242.848	24.6043	60.2633	78.8338	92.5359	18.9463	90.5741	2191.77	6883.7	395.747	2671.85
2.7923	2.53063	3122.73	15318.8	16845.5	8918.37	4062.47	9485.93	14064.6	2228.24	15.0635	413.06	201.945	23.5289	62.058	78.1557	91.7458	18.5375	90.937	1860.4	5842.95	395	2622.22
2.1224	0.560129	2795.53	14958.1	16931.3	9771.41	5308.35	7852.17	13466.3	1741.9	14.3693	287.606	203	21.1439	65.6762	73.1884	89.7676	16.5111	88.3461	1385.42	4351.2	358.939	2497.96
2.0588	1.07054	3038.14	16754.2	18910.5	11163.3	6197.92	8843.76	15164.2	1821.82	15.1078	292.692	207.739	20.4839	66.3875	73.3832	90.0946	16.0659	88.5972	1460.91	4588.27	380.492	2518.5
2.1453	1.97687	2591.49	14091	15879.3	9572.21	5425.87	7837.29	12840.2	1906.27	15.6956	311.103	214.677	19.8594	67.0848	74.6778	90.4307	16.32	88.7384	1541.44	4841.21	398.608	2539.62
2.2723	1.64474	4628.96	23279.9	25419	13621.3	6137.41	15533.8	21784.1	2386.76	16.723	434.644	200.851	23.2064	62.0725	80.5555	92.8501	18.2107	91.5848	2045.46	6424.17	450.114	2691.59
2.0517	1.86266	3945.37	19317.5	20994	11709.9	5541.2	13179.4	18217.7	2712.4	18.0206	509.738	216.601	22.1113	63.1971	81.3885	93.3879	18.7929	92.0144	2353.71	7392.3	491.127	2725.37
2.9435	1.10562	4701.99	22425.7	24433.5	14019.4	6938.54	15229.1	21130.3	2511.16	18.0095	483.247	206.356	21.3112	64.1988	81.1643	93.2404	19.244	91.7824	2171.66	6820.56	489.157	2716.1
2.1365	2.83007	2833.61	14610.5	16750.7	9078.99	2409.31	10643.6	13887.7	5317.68	20.3458	899.559	679.429	22.8997	57.1917	81.7706	91.4541	16.9164	87.2232	4408.79	13846.7	529.785	2603.9
2.0462	4.05957	4478.72	23473.3	24750.2	11369.3	4009.34	16922.7	22299.3	4969.92	17.7205	899.341	256.41	27.0319	58.0996	84.187	95.0487	18.0957	94.8408	4477.77	14063.4	501.435	2829.7
2.8369	4.07519	4888.88	24751.3	25977.9	11665.1	3429.15	18029.5	23475.2	4655.54	16.7243	876.143	219.823	27.548	56.6001	84.7016	95.183	18.8194	95.2783	4207.03	13213	474.658	2838.12
2.4176	2.40332	4045.15	20319.4	21357.6	9780.24	3194.6	14660.1	19164.7	4955.36	18.0736	938.55	240.882	27.1036	57.4788	84.3206	94.8662	18.9401	95.139	4446.57	13965.3	509.357	2818.22



Susc	Xfd (%)	IRM 20mt	IRM 300mt	IRM 1000mt	IRM-20mt	IRM-40mt	IRM-100mt	IRM-300mt	SIRM	SIRM /X	Soft	Hard	S-20(%)	S-40(%)	S-100(%)	S-300(%)	F20 (%)	F 300(%)	ARM	Xarm	Xarm/ X	Xarm /Mrs
26.8419	2.63459	5897.62	30796.7	32350.4	14524.4	4544.36	22073.3	29138.9	4736.52	17.646	863.488	227.486	27.5515	57.0236	84.1159	95.0363	18.2304	95.1972	4266.31	13399.2	499.19	2828.91
27.7058	2.41397	5691.86	29551.6	29921.4	11495.9	3839.39	21985.1	28503.9	4810.51	17.3628	915.09	59.4515	30.7898	56.4158	86.7381	97.6313	19.0227	98.7641	4582.62	14392.7	519.482	2991.93
26.9097	1.50248	6216.87	32686.7	34485.5	15670.5	5515.88	23389.9	30929.8	4647.64	17.2712	837.853	242.425	27.2796	57.9974	83.9127	94.8447	18.0275	94.7839	4168.44	13091.8	486.509	2816.87
27.8302	1.60446	6683.04	33241.6	35101.8	15185	4069.54	24339.9	31698.8	4692.75	16.8621	893.455	248.689	28.3701	55.7968	84.6704	95.1527	19.039	94.7006	4237.81	13309.7	478.247	2836.22
24.5899	1.50248	5929.18	31038.1	32734.3	15123.3	5511.1	22140.8	29132.1	4031.32	16.3942	730.195	208.889	26.8999	58.4179	83.819	94.4978	18.1131	94.8183	3587.7	11267.9	458.233	2795.09
22.886	0.990099	4976.89	25067	26504.3	12457.6	4495.7	17624.3	23411	3596.24	15.7137	675.29	195.019	26.4989	58.4811	83.248	94.1645	18.7777	94.5771	3176.53	9976.53	435.923	2774.16
21.3439	0.983238	4877.59	23051.3	24428.6	12283.4	5016.45	15654.2	21382.1	3088.32	14.4693	616.636	174.118	24.8585	60.2676	82.0408	93.7645	19.9667	94.362	2703.17	8489.87	397.765	2749.03
19.617	2.20053	5320.11	25575.2	27000.9	13996.4	5442.87	17109	23573.7	2795.12	14.2485	550.736	147.588	24.0816	60.0791	81.6823	93.6536	19.7035	94.7198	2440.34	7664.39	390.701	2742.06
17.6766	0.969807	4708.33	22595.2	23979.5	12831.6	5512.34	15026.7	20738.6	2740.52	15.5036	538.095	158.209	23.2447	61.4938	81.3324	93.2423	19.6348	94.2271	2370.13	7443.86	421.114	2716.22
17.0879	0.96463	5093.61	25456.2	26774.7	14898.9	6457.31	17483.7	23504.8	2942.28	17.2185	559.737	144.894	22.1773	62.0586	82.6496	93.8936	19.0239	95.0754	2582.95	8112.26	474.737	2757.13
18.8247	1.0345	6173.63	30599.6	31976.1	17084	7187.7	21240.5	28607.7	3113.55	16.5397	601.132	134.036	23.2863	61.2392	83.213	94.7329	19.307	95.6951	2785.56	8748.62	464.741	2809.85
19.0294	0.573066	5726.51	28192.5	29525.2	15647.2	6367.75	19654.3	25849.9	3219.76	16.9199	624.483	145.329	23.5019	60.7836	83.284	93.776	19.3954	95.4863	2818.96	8853.53	465.255	2749.75
17.6298	1.04654	5063.79	24810.9	25597.4	14174.6	5954.77	17474.2	22720.9	3148.51	17.859	622.852	96.7389	22.3124	61.6316	84.1328	94.3813	19.7824	96.9275	2794.7	8777.32	497.868	2787.77
17.9158	0.321895	5298.9	26969.2	28305.2	15500.6	6858.02	18899.3	24707.6	3264.73	18.2226	611.176	154.091	22.6188	62.1144	83.3849	93.645	18.7206	95.2801	2849.78	8950.32	499.577	2741.52
18.1289	0.39443	5904.93	29963.8	31095.5	17249.6	7320.01	21117.9	27432.5	3368.96	18.5834	639.754	122.61	22.2635	61.7702	83.9565	94.1101	18.9897	96.3606	2972.1	9334.49	514.896	2770.73
29.2453	3.19565	3388.15	18528.4	19933.4	9107.34	4055	12466	17130.8	4657.33	15.9251	791.624	328.269	27.1556	60.1714	81.2691	92.9701	16.9974	92.9516	4002.52	12570.7	429.838	2699.12
28.0387	2.78928	4021.89	22653.4	24417.5	11364.7	4289.15	15254.3	20992.1	4973.02	17.7363	819.122	359.292	26.7284	58.7829	81.2364	92.9857	16.4713	92.7752	4275.38	13427.7	478.898	2700.11
121.8	6.75248	23327.1	51160.8	55691.7	6175.18	19938.4	43768.5	50053.8	10332.4	8.4831	4327.85	840.614	44.4559	67.9007	89.2953	94.9383	41.8861	91.8643	9286.42	29165.9	239.457	2822.76
38.7136	4.43046	6950.67	29383	32095.7	10947.1	3500.65	20835	27333.4	5078.44	13.118	1099.79	429.232	32.9462	55.4534	82.4576	92.581	21.656	91.548	4324.91	13583.2	350.865	2674.68
28.949	4.82434	5542.23	25813.7	27317.5	12000.1	3835.42	16738.3	15856.5	3575.59	12.3513	725.423	196.833	28.0359	57.0201	80.6366	79.0226	20.2882	94.4951	2075.46	6518.4	225.168	1823.03
68.1355	6.73542	18997.7	45530.9	47465	2418.56	12778.6	36188.7	42754.8	5227.42	7.67209	2092.26	213.003	47.4523	63.4611	88.1215	95.0383	40.0247	95.9253	4708.68	14788.6	217.046	2829.04
50.4069	6.42381	12952.8	41051.2	43228	10821.9	4045.56	31831.8	38271.3	4397.56	8.72413	1317.68	221.448	37.4828	54.6793	86.8185	94.2668	29.9639	94.9643	3893.32	12227.8	242.581	2780.59
48.648	6.04954	13107.5	43417.9	45923.4	10753.3	5045.05	34945.6	38258.3	5035.46	10.3508	1437.23	274.724	38.2921	55.4929	88.0477	91.6545	28.5421	94.5442	4194.99	13175.2	270.828	2616.48
50.3316	6.32411	10407.9	34832.2	36691.4	8648.39	3824.11	27306.6	32642.5	4866.23	9.66834	1380.36	246.575	38.2147	55.2112	87.2112	94.4825	28.3661	94.9329	4329.24	13596.9	270.146	2794.13
62.2159	5.78239	17450.2	49321	50361.8	4134.47	14363.5	40295.3	45796.2	6141.69	9.87157	2128.07	126.932	45.8952	64.2603	90.0058	95.4672	34.6496	97.9333	5584.9	17540.5	281.93	2855.97
100.813	6.64179	23121.7	64348.2	65906.6	2439.39	22537.3	54183.7	60714.5	8460.41	8.39218	2968.13	200.051	48.1494	67.0979	91.1064	96.061	35.0825	97.6354	7793.9	24478.3	242.809	2893.28
81.1107	6.38308	17532.1	53997.2	55518.6	5673.34	15506.4	43007.9	50339.2	6983.47	8.6098	2205.3	191.368	44.8906	63.9651	88.7329	95.3355	31.5788	97.2597	6331.97	19886.9	245.182	2847.71
92.2632	6.52253	22145.9	64754.6	67874.1	9855.38	18973.9	53985.3	61403.9	7144.64	7.74376	2331.15	328.366	42.74	63.9773	89.7687	95.2337	32.6279	95.404	6463.57	20300.2	220.024	2841.32
149.489	6.89674	32023.3	100088	102593	10099	26908.6	84273.3	95549.1	11645.1	7.78993	3634.88	284.367	45.0781	63.1142	91.0716	96.5669	31.2138	97.5581	10845.5	34062.6	227.86	2925.06
68.6077	5.84077	16173.5	56646.6	59648.1	12505.3	7667.31	45874.6	54002.6	7177.87	10.4622	1946.27	361.193	39.5174	56.4271	88.4544	95.2677	27.1149	94.968	6498.51	20409.9	297.487	2843.45
72.0227	5.30759	17669.4	56573.1	57609.6	6674.88	13228.3	46449.5	53224.1	7681.28	10.6651	2355.92	138.199	44.2068	61.481	90.314	96.1938	30.6709	98.2008	7096.55	22288.1	309.46	2901.61
73.8295	5.20325	15167.1	59857.9	61586.9	17725	2118.69	44760.4	54046.4	7393.38	10.0141	1820.78	207.559	35.6098	51.7201	86.3392	93.8782	24.6272	97.1926	6488.16	20377.4	276.006	2756.17
70.1576	6.15584	13047.5	70690.8	72704.4	28528.9	10730.4	51664.8	66467.3	8812.65	12.5612	1581.52	244.073	30.3802	57.3795	85.5307	95.7106	17.946	97.2304	8056.64	25303.5	360.667	2871.27
94.4954	6.72677	19852.8	76515.2	77980.6	19411.8	5769.26	58120.2	71077.9	10220.3	10.8156	2601.94	192.064	37.5535	53.6992	87.2658	95.5741	25.4586	98.1208	9315.58	29257.5	309.618	2862.69
71.7532	5.85158	14858.3	61433.2	63390.7	18104.2	2860.93	46329.2	57540.7	8232.56	11.4734	1929.65	254.226	35.7202	52.2566	86.5426	95.3857	23.4392	96.9119	7472.82	23469.9	327.092	2850.86

Susc	Xfd (%)	IRM 20mt	IRM 300mt	IRM 1000mt	IRM-20mt	IRM-40mt	IRM-100mt	IRM-300mt	SIRM	SIRM /X	Soft	Hard	S-20(%)	S-40(%)	S-100(%)	S-300(%)	F20 (%)	F 300(%)	ARM	Xarm	Xarm/ X	Xarm /Mrs
22.1753	5.40365	2334.4	13480.3	14538.9	6769.12	2388.06	9096.27	12526.3	4177.85	18.8401	670.805	304.198	26.7207	58.2127	81.2825	93.0785	16.0562	92.7188	3599.51	11305	509.801	2705.9
21.5724	3.89689	3964.94	23526.6	25034.1	11319.9	4475.03	15860.6	21767.1	4070.59	18.8694	644.706	245.128	27.3911	58.9379	81.6779	93.4748	15.8381	93.9781	3539.37	11116.1	515.293	2730.8
22.0117	3.09272	4398.33	25783.8	27728.3	12482.8	4671.42	17392.4	23665.5	4042.02	18.3631	641.156	283.449	27.4908	58.4236	81.3622	92.674	15.8623	92.9874	3449.78	10834.7	492.226	2680.5
21.6027	4.06057	5701.81	32876.5	35367.5	16093.6	5792.22	22327.3	30478.4	3649.9	16.8956	588.422	257.072	27.2481	58.1886	81.5647	93.0881	16.1216	92.9567	3145.35	9878.6	457.285	2706.5
22.8857	5.12708	5282.64	28898	31017	13761.6	4331.11	19937.9	26876.1	3896.61	17.0264	663.648	266.209	27.8161	56.9818	82.1403	93.3248	17.0314	93.1682	3376.39	10604.3	463.357	2721.4
22.7629	5.07617	5370.3	29372.6	31707	13945.1	4982.69	19873.1	27209.2	3546.64	15.5808	600.705	261.118	28.0094	57.8574	81.3387	92.9073	16.9373	92.6376	3043.53	9558.84	419.931	2695.1
18.9106	3.69085	4139.75	22520.3	24292.7	11407.9	4026.98	15097.3	20767.9	2748.04	14.5317	468.298	200.494	26.5199	58.2885	81.0738	92.7452	17.0412	92.7041	2349.31	7378.49	390.177	2685
16.173	3.53846	4741.18	24588.7	26003	13798.6	6014.68	17519.8	22915.1	3080.92	19.0498	561.751	167.57	23.4673	61.5654	83.6881	94.0624	18.2332	94.5611	2715.06	8527.2	527.249	2767.7
15.7229	2.48296	4577.65	22649.8	24055.3	12558.4	5271.44	16019.5	20977.7	2962.47	18.8417	563.75	173.085	23.8968	60.9569	83.2973	93.6032	19.0297	94.1574	2583.46	8113.88	516.055	2738.8
14.6667	3.99174	4049.54	21216.1	22778.1	11903	4904.62	14399.1	19561.6	2760.98	18.8248	490.853	189.333	23.8718	60.7661	81.6073	92.9395	17.7782	93.1426	2371.1	7446.93	507.744	2697.2
13.0357	5.20864	3330.7	17862.9	19341.2	10083.9	4421.42	11500.7	16238.3	2463.85	18.9008	424.293	188.324	23.9316	61.43	79.731	91.9784	17.2207	92.3565	2068.57	6496.78	498.383	2636.8
14.4133	5.46018	4076.85	20941.8	22250.9	11577.7	4622.56	14599.7	19442.2	2838.12	19.691	520.006	166.975	23.9837	60.3874	82.807	93.6886	18.3222	94.1167	2479.87	7788.54	540.372	2744.2
15.6751	4.37956	5018.48	25173.5	26577.5	14230.6	5873.85	18314.8	23595.3	3040.9	19.3996	574.197	160.636	23.2281	61.0504	84.4555	94.3897	18.8825	94.7175	2699.69	8478.93	540.917	2788.3
13.9867	3.02585	4096.93	20991.7	22148.2	11632.3	4998.52	14766.2	20828.9	2678.14	19.1477	495.397	139.84	23.7398	61.2843	83.335	97.0217	18.4978	94.7785	2518.61	7910.21	565.552	2953.6
12.2518	3.58174	3409.27	18973.5	20747.2	11177.4	5714.53	11720.8	17086	2097.79	17.1223	344.719	179.341	23.0628	63.7718	78.2467	91.1767	16.4325	91.451	1727.6	5425.89	442.865	2586.4
13.005	3.83988	3238.31	17402.1	18888	10296.5	4899.33	11087	15885.7	2358.05	18.1319	404.283	185.504	22.7433	62.9694	79.3493	92.0524	17.1448	92.1332	1983.23	6228.75	478.95	2641.4
13.9341	5.46928	3328.73	17582.9	18944.8	9862.12	4257.14	11523.1	16078.3	2546.35	18.2742	447.41	183.052	23.9714	61.2356	80.4123	92.4346	17.5707	92.8112	2161.06	6787.25	487.097	2665.4
13.7779	3.72682	3665.31	18602.5	19581	10373.7	4689.03	12700.1	17257.6	2513.61	18.2438	470.515	125.614	23.5108	61.9734	82.4296	94.0671	18.7187	95.0026	2215.35	6957.77	504.995	2768.0
14.9974	3.56073	4413.11	21492.9	22712.9	11866.6	5035.35	15346.5	20245.1	2915.65	19.441	566.51	156.609	23.8769	61.0848	83.7837	94.5674	19.43	94.6287	2598.86	8162.24	544.244	2799.4
15.3356	3.43472	4834.24	24986.1	26496.1	14235.2	5986.25	17967.7	23536.6	3014.35	19.6559	549.97	171.787	23.1372	61.2965	83.9063	94.4152	18.2451	94.301	2677.66	8409.72	548.379	2789.9
15.7489	2.7889	4918.27	24954.3	26180.6	13877.3	6643.09	18049.1	23539.1	3002.36	19.064	564.022	140.631	23.497	62.687	84.4704	94.9552	18.7859	95.316	2699.44	8478.13	538.332	2823.8
15.4267	3.14314	4524.65	24117.5	25433.3	13714.1	6034.14	16905.6	22531.9	2957.36	19.1704	526.122	152.996	23.0391	61.8627	83.2352	94.2961	17.7903	94.8266	2619.99	8228.61	533.4	2782.4
15.7691	2.39703	4466.52	25583.4	26989.8	15066	7117.25	17860.4	24186.5	3228.44	20.4732	534.273	168.226	22.0894	63.1851	83.0874	94.8068	16.5489	94.7893	2893.12	9086.44	576.218	2814.5
15.5604	4.30975	4157.01	22480.7	23793.3	12582.2	5550.79	16039.3	21081.1	2819.12	18.1172	492.537	155.527	23.5594	61.6646	83.7054	94.3004	17.4713	94.4831	2497.76	7844.73	504.147	2782.6
16.3368	2.26154	4468.61	24190.6	25612.1	13448.6	5444.48	17298.2	22516.6	2985.1	18.2722	520.817	165.68	23.7456	60.6287	83.7695	93.9569	17.4472	94.4498	2624.31	8242.19	504.517	2761.1
19.4666	4.32414	2468.57	14825.8	16453.9	6935.37	800.034	8988.01	13295.5	2684.17	13.7886	402.703	265.602	28.9249	52.4311	77.3126	90.4022	15.0029	90.1049	2168.92	6811.95	349.93	2537.8
20.0153	3.71632	3514.49	20130.2	22506.8	9482.05	1157.98	12225.4	17974.3	2644.74	13.2136	412.984	279.268	28.9351	52.5725	77.1594	89.9309	15.6153	89.4406	2112.14	6633.6	331.427	2508.2
19.7394	2.22085	3924.19	23331.1	25805.4	11335.7	1227.41	13806.3	20685.9	2427.6	12.2982	369.162	232.762	28.0362	52.3782	76.7508	90.0806	15.2069	90.4118	1945.99	6111.79	309.624	2517.6
19.7198	2.18579	3437.85	20287.2	22725.6	9947.56	390.242	12510.9	18264.7	2448.88	12.4184	370.458	262.763	28.1138	50.8586	77.526	90.1852	15.1276	89.2701	1968.18	6181.47	313.465	2524.2
20.8184	2.16302	3258.86	18872.3	20998.1	8859.05	1043.35	11585	16911	2576.45	12.3758	399.86	260.832	28.9051	52.4844	77.5858	90.268	15.5198	89.8763	2074.97	6516.86	313.034	2529.3
20.2975	1.48627	2898.95	17279.7	19262.1	8394.38	1132.99	10606.4	15603.3	2690.24	13.2541	404.881	276.875	28.2101	52.941	77.5317	90.5025	15.05	89.7082	2179.23	6844.32	337.2	2544.1
22.463	1.25647	4011	23885.8	26508.8	11036.5	991.513	15033.7	21433.7	2802.2	12.4747	423.996	277.274	29.1833	51.8702	78.356	90.4275	15.1308	90.1051	2265.72	7115.95	316.785	2539.4
21.0422	1.77429	3219.88	18646.3	20443	8822.6	1147.66	11493.3	16711	2696.96	12.8169	424.786	237.025	28.4214	52.807	78.1107	90.8723	15.7506	91.2114	2204.62	6924.05	329.055	2567.3
19.8718	2.15054	2801.38	16624.1	18640.8	8075.26	956.99	10131.2	15001.3	2655.38	13.3626	399.057	287.279	28.3398	52.5669	77.1748	90.2378	15.0282	89.1813	2136.94	6711.49	337.739	2527.5
19.8214	1.88852	3721.83	20850.9	23295.8	10236.2	423.358	12658.9	18728.5	2491.53	12.5699	398.057	261.488	28.03	50.9087	77.1699	90.1971	15.9764	89.5049	2003.05	6290.98	317.383	2524.9

Susc	Xfd (%)	IRM 20mt	IRM 300mt	IRM 1000mt	IRM-20mt	IRM-40mt	IRM-100mt	IRM-300mt	SIRM	SIRM /X	Soft	Hard	S-20(%)	S-40(%)	S-100(%)	S-300(%)	F20 (%)	F 300(%)	ARM	Xarm	Xarm/ X	Xarm /Mrs
20.414	2.50948	3235.48	19370.8	21512.6	9685.12	1733.5	11994.9	17421.8	2642.82	12.9461	397.479	263.116	27.4896	54.029	77.8788	90.4921	15.04	90.0441	2140.27	6721.95	329.282	2543.48
20.0306	2.17354	3362.42	19878.6	22418	9942.4	992.644	12079.9	17918.7	2541.72	12.6892	381.227	287.914	27.825	52.2139	76.9424	89.965	14.9987	88.6725	2031.6	6380.65	318.545	2510.36
19.6365	2.078	2734.29	16411.8	18188.2	8176.21	941.977	9496.62	14809.4	2613.25	13.3081	392.858	255.231	27.5233	52.5895	76.1065	90.7115	15.0333	90.2332	2127.79	6682.75	340.323	2557.26
19.1417	2.96156	3182.79	18887.4	21150.4	9544.53	1028.44	11373.6	17059.1	2398	12.5276	360.861	256.576	27.4365	52.4313	76.8874	90.3281	15.0484	89.3004	1934.14	6074.56	317.347	2533.17
18.0985	2.42405	2954.72	17351.7	19482.1	8991.1	1847.25	10103.5	15524.9	2231.63	12.3305	338.456	244.032	26.9247	54.7409	75.9302	89.844	15.1663	89.0648	1778.34	5585.24	308.602	2502.77
18.7169	4.93178	1260.69	7465.24	8218.64	3848.17	224.642	4442.12	6791.6	2528.81	13.5109	387.905	231.817	26.5888	51.3667	77.0246	91.3182	15.3394	90.833	2089.72	6563.2	350.656	2595.37
16.7331	2.77381	1495.18	9567.42	10739.3	5270.99	757.546	5200.67	8366.41	2139.3	12.7849	297.845	233.442	25.4593	53.527	74.2133	88.9523	13.9225	89.0879	1666.62	5234.35	312.814	2446.76
16.7535	3.4749	1872.46	11623.1	12959.8	6232.87	988.691	6639.35	10276.6	2265.7	13.5238	327.353	233.692	25.9531	53.8144	75.6151	89.6479	14.4482	89.6857	1796.61	5642.61	336.802	2490.45
18.1796	3.11948	1947.95	11734.9	13085.3	6157.68	594.28	6883.71	10646.8	2473.59	13.6064	368.233	255.27	26.471	52.2708	76.3033	90.6824	14.8866	89.6802	2012.63	6321.07	347.701	2555.43
18.0384	2.22723	2957.09	18072.6	20192.4	9868.98	1502.94	10297	16160.1	2216.51	12.2877	324.598	232.687	25.5626	53.7216	75.4972	90.0154	14.6446	89.5021	1773.89	5571.25	308.855	2513.53
17.975	3.87295	2056.27	12357.5	13885.8	6736.62	763.046	7087.28	11142.5	2318.17	12.8966	343.284	255.148	25.7428	52.7476	75.5198	90.1218	14.8084	88.9935	1860.18	5842.29	325.023	2520.22
17.0822	3.57603	2252.62	13722.5	15240.2	7538.86	949.988	7747.55	12325.2	2237.92	13.1009	330.781	222.868	25.2666	53.1167	75.4181	90.4364	14.7807	90.0413	1809.87	5684.26	332.759	2539.98
17.0547	1.70648	2779.8	16532.8	18691.2	9079.52	634.671	9803.39	15027	2175.92	12.7585	323.609	251.265	25.7117	51.6978	76.2247	90.1981	14.8723	88.4525	1749.36	5494.22	322.153	2525.01
17.2214	2.17824	3150.59	18766.7	21395.3	10563.1	1392.74	10642.1	16998.4	2095.52	12.1681	308.579	257.449	25.3144	53.2548	74.8702	89.7247	14.7256	87.7143	1664.88	5228.89	303.627	2495.27
17.3575	1.99254	2566.96	15221.4	17279.6	8503.75	934.131	8700.19	13739.2	2238.29	12.8952	332.508	266.602	25.3936	52.703	75.1748	89.7556	14.8555	88.089	1779.69	5589.48	322.021	2497.21
17.2302	3.39623	2525.91	15012.9	16894.5	8144.03	1057.85	8619.89	13580.6	2196.94	12.7505	328.467	244.68	25.8974	53.1308	75.5109	90.1924	14.9511	88.8627	1766.01	5546.51	321.906	2524.65
17.2592	2.32644	2565.21	15338.3	17525.3	8579.85	1052.95	8740.81	13814.9	2226.85	12.9024	325.948	277.887	25.5215	53.0041	74.9377	89.4142	14.6372	87.521	1755.39	5513.15	319.433	2475.77
16.9417	2.37151	2472.93	15064.7	17075.4	8451.43	1193.17	8459.25	13505.8	2164.18	12.7743	313.426	254.841	25.2526	53.4938	74.7703	89.5475	14.4824	88.2246	1711.76	5376.14	317.332	2484.14
17.0359	2.27245	2879.34	17594.5	20002.2	9963.79	1765.98	9790.37	15796.2	2109.93	12.3852	303.728	253.974	25.0932	54.4145	74.4733	89.4862	14.3951	87.9629	1666.27	5233.25	307.189	2480.29
17.2705	2.15823	2884.94	17491.2	19897.6	9867.41	1571.17	10049	15680.3	2119.02	12.2696	307.235	256.276	25.2046	53.9481	75.2517	89.4024	14.4989	87.9059	1669.89	5244.64	303.676	2475.03
16.781	2.52811	3007	18274.4	20683.6	10017.9	2120.5	10089.6	16221.1	2021.86	12.0485	293.939	235.503	25.783	55.126	74.3903	89.2125	14.5381	88.3522	1585.64	4980.03	296.766	2463.1
16.0652	2.29647	2169.7	13153.6	14938.6	7376.93	999.21	7319.77	11797.9	2071.93	12.897	300.929	247.576	25.3092	53.3444	74.4995	89.4879	14.5241	88.0509	1636.32	5139.21	319.897	2480.4
16.3165	2.85837	2241.36	13370.5	14944.2	7500.57	1087.77	7524.25	12077.7	2093.02	12.8276	313.916	220.402	24.9047	53.6394	75.1745	90.4094	14.9982	89.4697	1691.55	5312.67	325.601	2538.28
16.4046	2.55591	2740.33	16621.3	18877.6	9536.03	1531.14	9128.79	14907.6	1978.78	12.0623	287.246	236.505	24.7424	54.0555	74.179	89.485	14.5163	88.0479	1562.64	4907.79	299.172	2480.21
15.6167	2.20943	2624.4	16713.8	18908.6	9619.2	1652.54	9002.81	15067.2	1953.37	12.5082	271.116	226.734	24.5639	54.3698	73.8061	89.8422	13.8794	88.3926	1556.53	4888.6	313.036	2502.65
14.7461	2.39703	2363.32	15170	17264.2	8754.98	1583.41	8031.56	13601	1931.11	13.0958	264.353	234.247	24.6441	54.5858	73.2608	89.3908	13.6892	87.8699	1521.36	4778.16	324.028	2474.3
15.466	2.76725	2445.08	15683.1	17796.2	9143.31	1778.69	8208.1	13892.4	1830.89	11.8381	251.551	217.399	24.3111	54.9974	73.0614	89.0319	13.7393	88.126	1429.26	4488.88	290.242	2451.75
16.0131	2.4966	2548.44	16096.7	18175.3	9494.42	2013.15	8536.33	14443.6	1979.88	12.3642	277.608	226.431	23.881	55.5381	73.4833	89.7341	14.0214	88.5634	1573.38	4941.51	308.592	2495.86
15.4478	1.9976	2259.36	14218.4	16162.3	8374.86	1713.04	7400.91	12562.3	1874.98	12.1375	262.107	225.511	24.0914	55.2995	72.8956	88.863	13.9792	87.9726	1457.34	4577.08	296.294	2441.14
17.1859	2.57341	2705.59	16627.9	18659	9642.14	1895.85	9013.09	15000.4	2154.62	12.5371	312.424	234.538	24.1622	55.0803	74.1521	90.1962	14.5002	89.1146	1732.15	5440.16	316.548	2524.88
16.2807	2.26163	2712.32	17109.4	19153.8	10143.7	2117.02	8899.73	15144.9	1926.94	11.8358	272.869	205.677	23.5204	55.5264	73.2323	89.5349	14.1607	89.3263	1523.63	4785.28	293.923	2483.35
16.5959	2.67874	2708.6	16985.1	19018.9	10277	2443.55	8987.96	15282.7	2027.61	12.2175	288.763	216.827	22.9822	56.424	73.629	90.1776	14.2416	89.3063	1629.29	5117.1	308.335	2523.72
5.9824	1.96078	2094.28	14139.7	16274.3	8445.76	1807.12	7483.75	12791.2	1910.13	11.9514	245.808	250.536	24.0518	55.5521	72.9926	89.2988	12.8687	86.8838	1501.31	4715.18	295.024	2468.52

表 5 长江下游太湖 (Tai 1 孔)、澄湖 (Chen 2 孔) 表层沉积物的 N、P 计算结果

样品编号	TN (%)	TP (%)	P <sub>2</sub> O <sub>5</sub> (%)	样品编号	TN (%)	TP (%)	P <sub>2</sub> O <sub>5</sub> (%)
Tai1-1	0.100858	0.0547905	0.12547	Cheng2-1	0.0679818	0.0766361	0.175497
Tai1-2	0.105479	0.0552696	0.126567	Cheng2-2	0.114689	0.0724856	0.165992
Tai1-3	0.109898	0.0505632	0.11579	Cheng2-3	0.0977238	0.0807556	0.18493
Tai1-4	0.10826	0.0458335	0.104959	Cheng2-4	0.0505556	0.0843946	0.193264
Tai1-5	0.100567	0.0527211	0.120731	Cheng2-5	0.035	0.0920074	0.210697
Tai1-6	0.0531646	0.0530042	0.12138	Cheng2-6	0.0403846	0.0955254	0.218753
Tai1-7	0.045	0.0520182	0.119122	Cheng2-7	0.0496774	0.0834926	0.191198
Tai1-8	0.0271845	0.0503176	0.115227	Cheng2-8	0.0434415	0.075321	0.172485
Tai1-9	0.0689655	0.0534902	0.122492	Cheng2-9	0.0224163	0.0733277	0.16792
Tai1-10	0.0575342	0.0490044	0.11222	Cheng2-10	0.00833333	0.0731893	0.167603
Tai1-11	0.00738137	0.0445258	0.101964	Cheng2-11	0.00789845	0.0795695	0.182214
Tai1-12	0.0160305	0.0487074	0.11154	Cheng2-12	0.0144543	0.0741596	0.169826
Tai1-13	0.00876296	0.0504394	0.115506	Cheng2-13	0.0345679	0.0778756	0.178335
Tai1-14	0.0322086	0.052957	0.121272	Cheng2-14	0.00773481	0.0800953	0.183418
Tai1-15	0.0095498	0.0508075	0.116349	Cheng2-15	0.0300268	0.0776808	0.177889
Tai1-16	0.0182344	0.0496744	0.113754	Cheng2-16	0.034	0.0757624	0.173496
Tai1-17	0.0110236	0.0471508	0.107975	Cheng2-17	0.0162791	0.0705653	0.161594
Tai1-18	0.00435459	0.0463824	0.106216	Cheng2-18	0.0191518	0.0802514	0.183776
Tai1-19	0.012963	0.0460108	0.105365	Cheng2-19	0.0195743	0.0741389	0.169778
Tai1-20	0.00434783	0.0446019	0.102138	Cheng2-20	0.0155772	0.073454	0.16821
Tai1-21	0.0255319	0.0464471	0.106364	Cheng2-21	0.0145617	0.0615879	0.141036
Tai1-22	0.0165436	0.0484017	0.11084	Cheng2-22	0.0289513	0.0642424	0.147115
Tai1-23	0.018806	0.0460067	0.105355	Cheng2-23	0.0262248	0.0659428	0.151009
Tai1-24	0.00796586	0.0423918	0.0970773	Cheng2-24	0.0456973	0.0707631	0.162048
Tai1-25	0.0019774	0.0389765	0.0892563	Cheng2-25	0.0603269	0.0740354	0.169541
Tai1-26	0.0268126	0.0386563	0.088523	Cheng2-26	0.0433231	0.0697563	0.159742
Tai1-27	0.0103321	0.0357111	0.0817784	Cheng2-27	0.0384146	0.0696706	0.159546
Tai1-28	0.0332117	0.034399	0.0787736	Cheng2-28	0.0305593	0.0684349	0.156716
Tai1-29	0.0396601	0.0347018	0.0794672	---	NaN	NaN	NaN
Tai1-30	0.0157746	0.0304344	0.0696948	---	NaN	NaN	NaN

# Water content /%

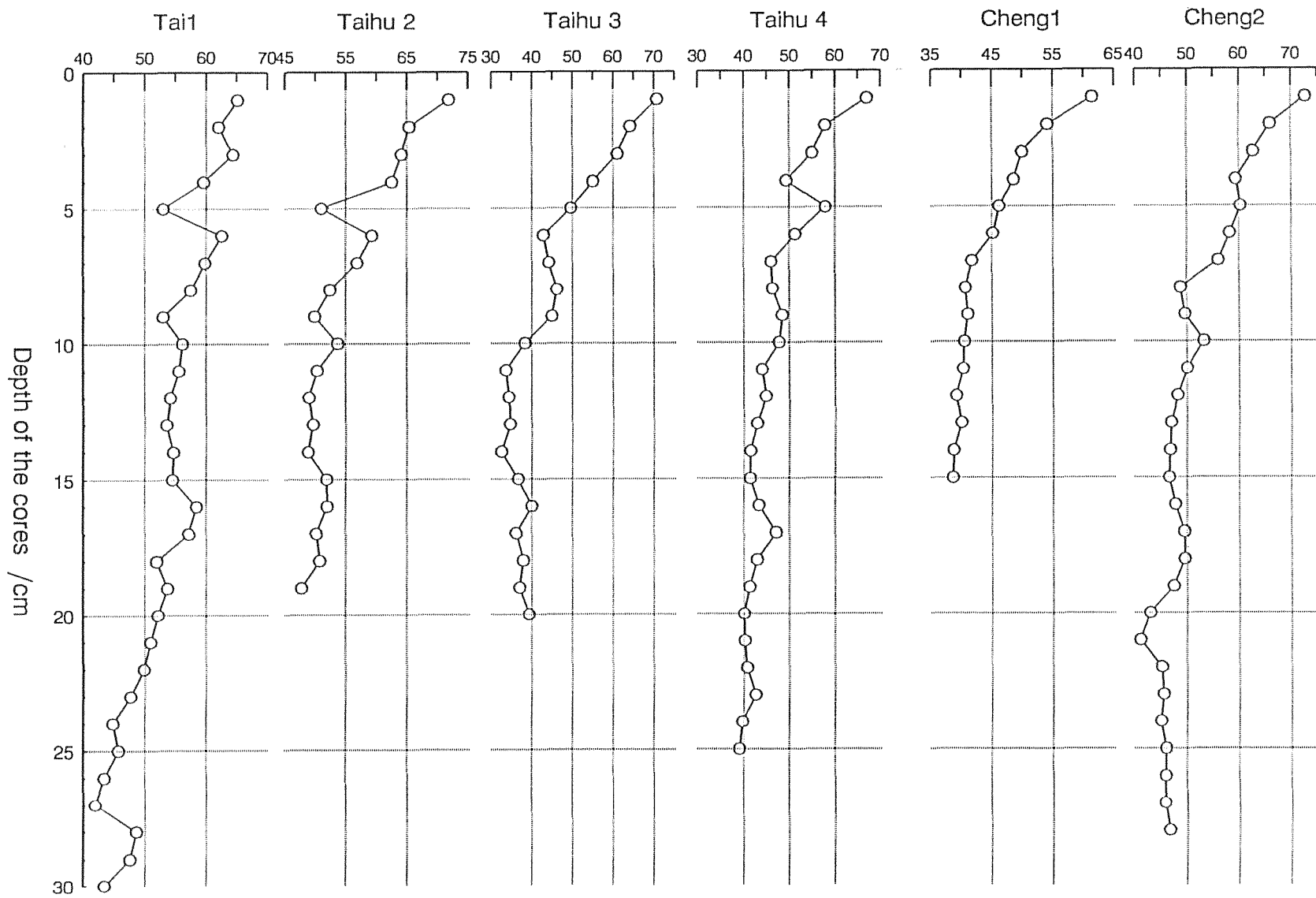


图 1 长江下游太湖及澄湖表层沉积物的含水量随深度分布曲线

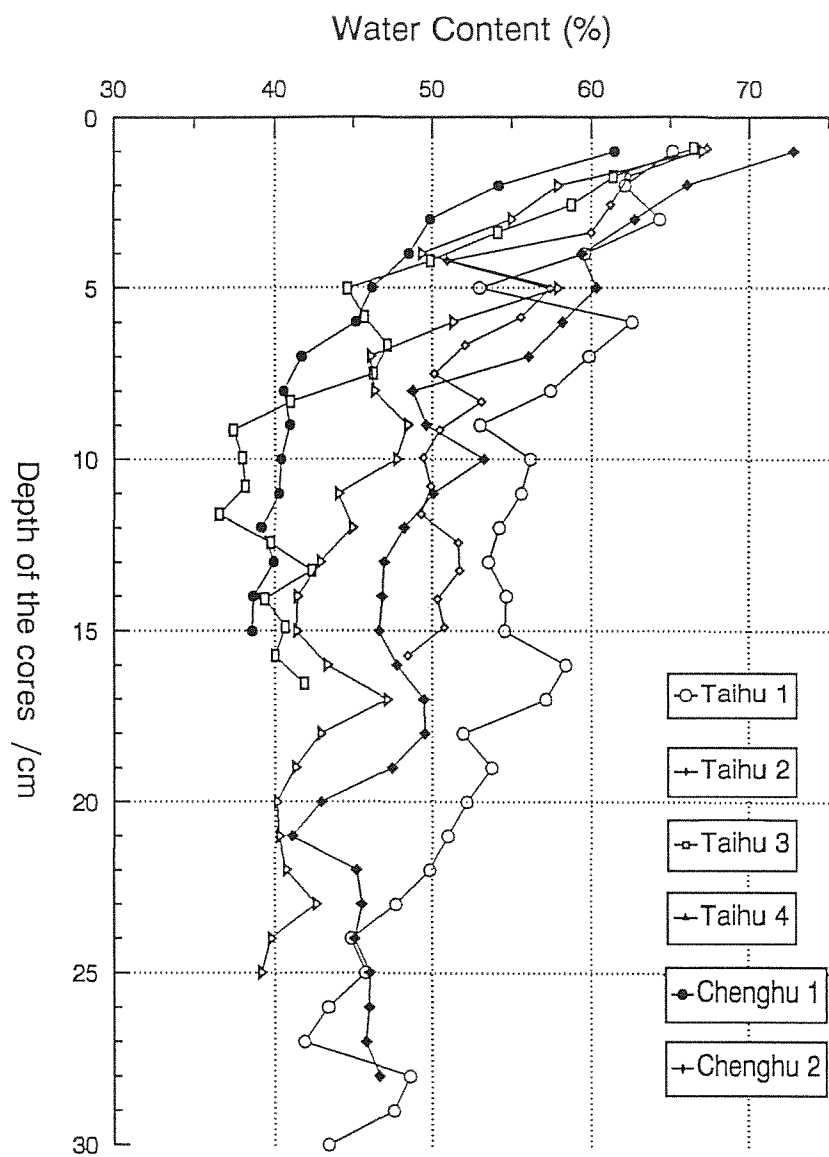


图 2 长江下游太湖及澄湖不同地点表层沉积物的  
深度—含水量曲线比较

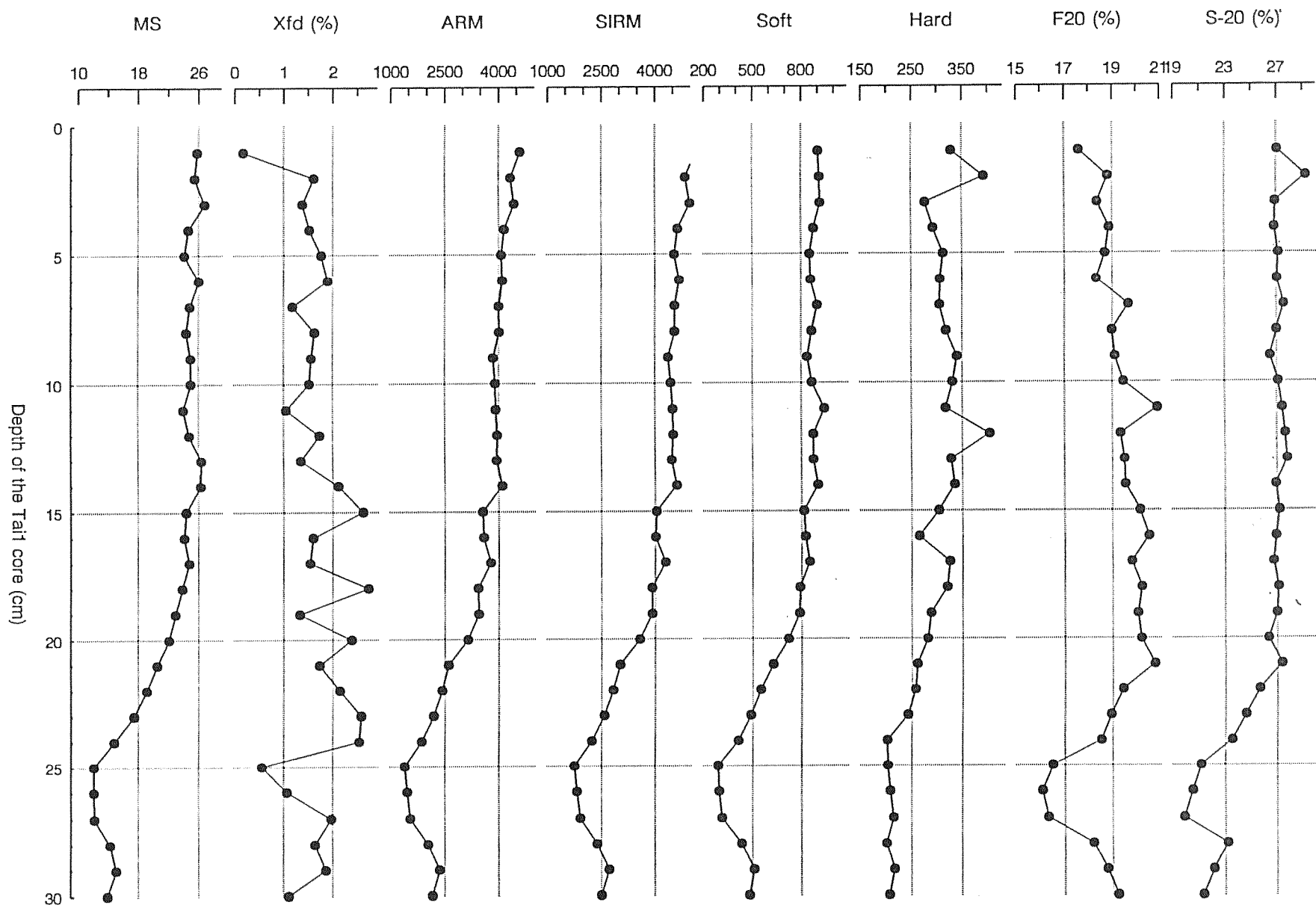


图 3 长江下游太湖表层沉积物 Tai 1 孔深度—磁参数曲线

图 4 长江下游太湖表层沉积物 Tai2 孔深度—磁参数曲线

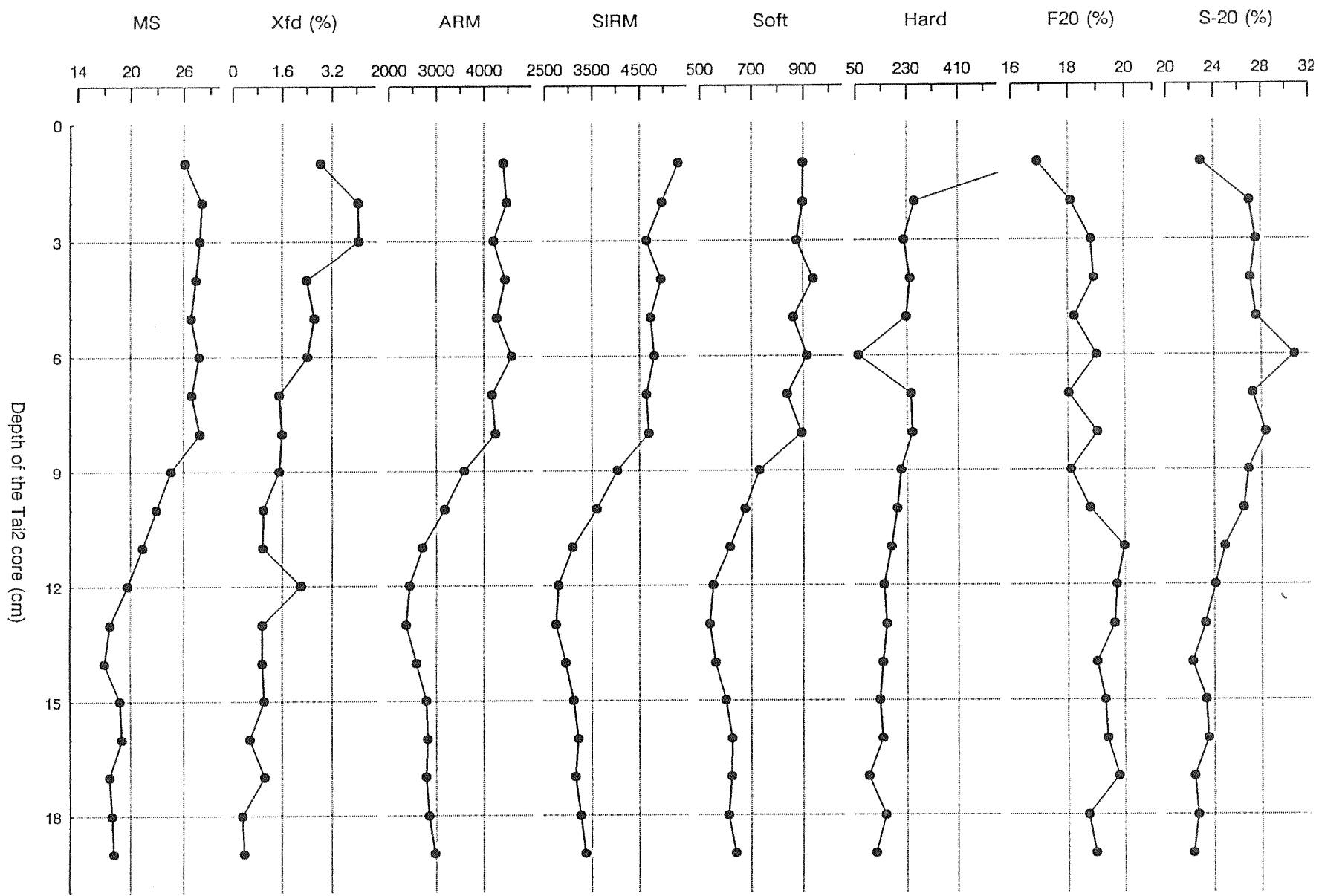




图 5 长江下游太湖表层沉积物 Tai3 孔深度—磁参数曲线

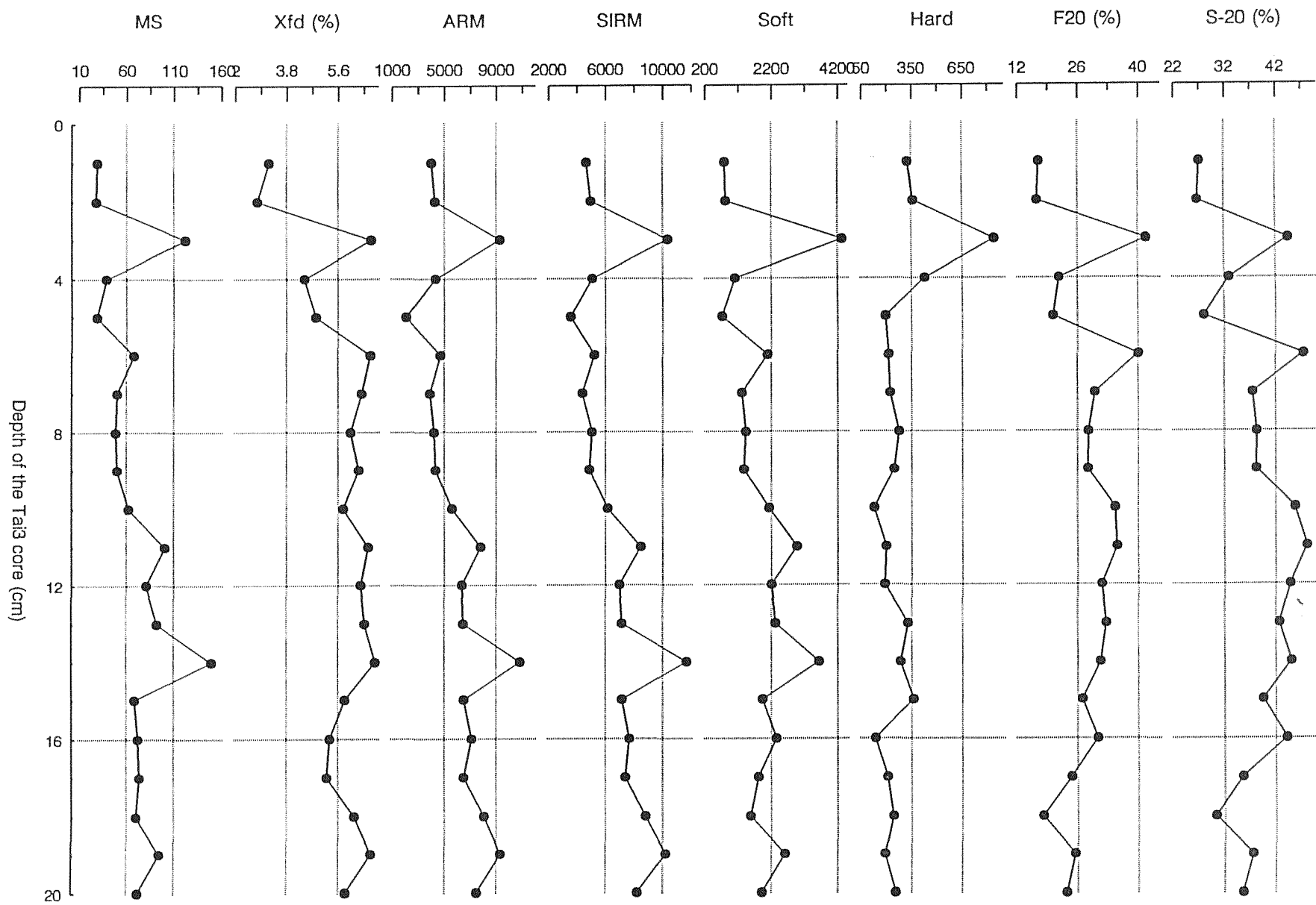


图 6 长江下游太湖表层沉积物 Tai 4 孔深度—磁参数曲线

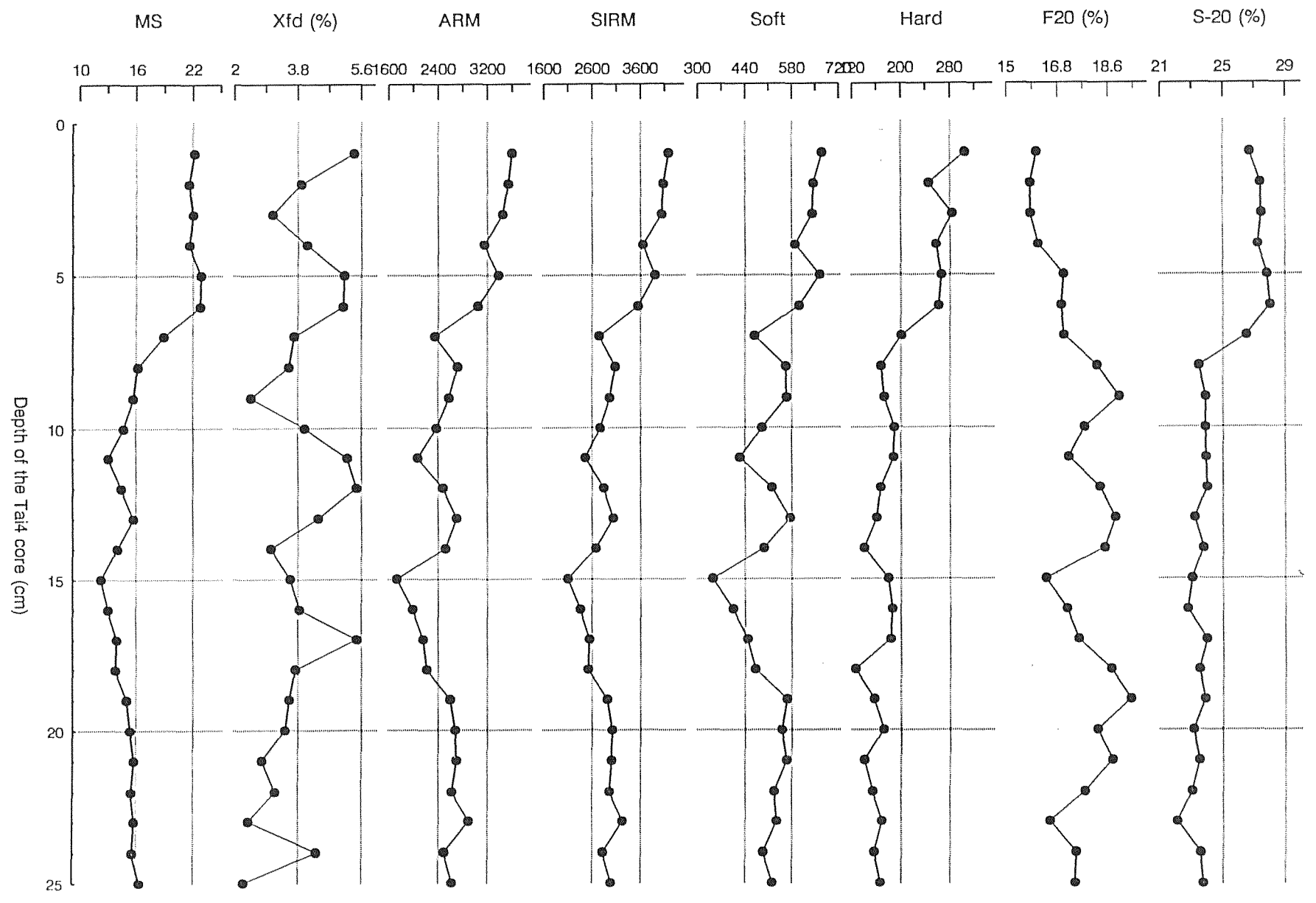


图 7 长江下游澄湖表层沉积物 Chen 1 孔深度—磁参数曲线

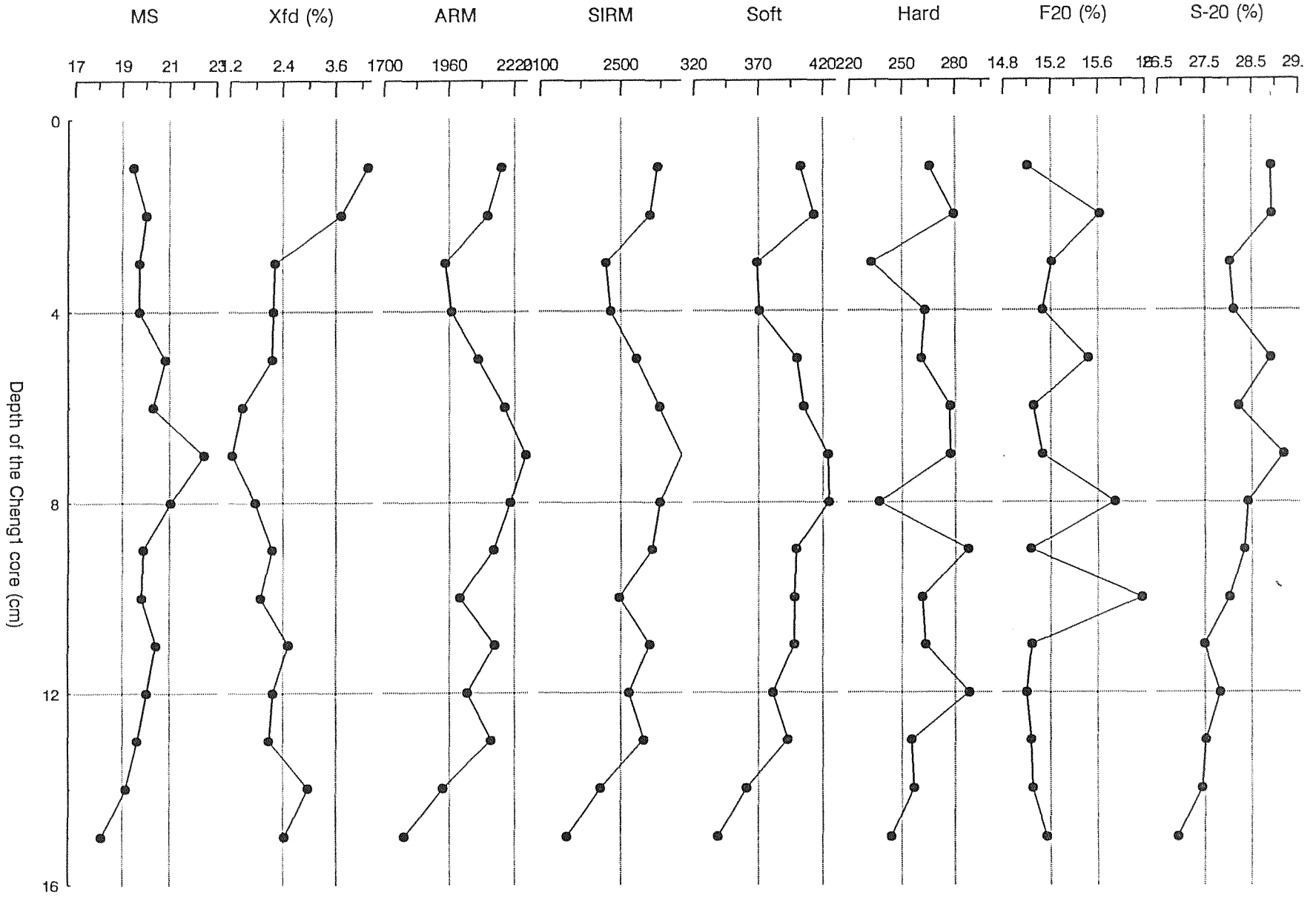
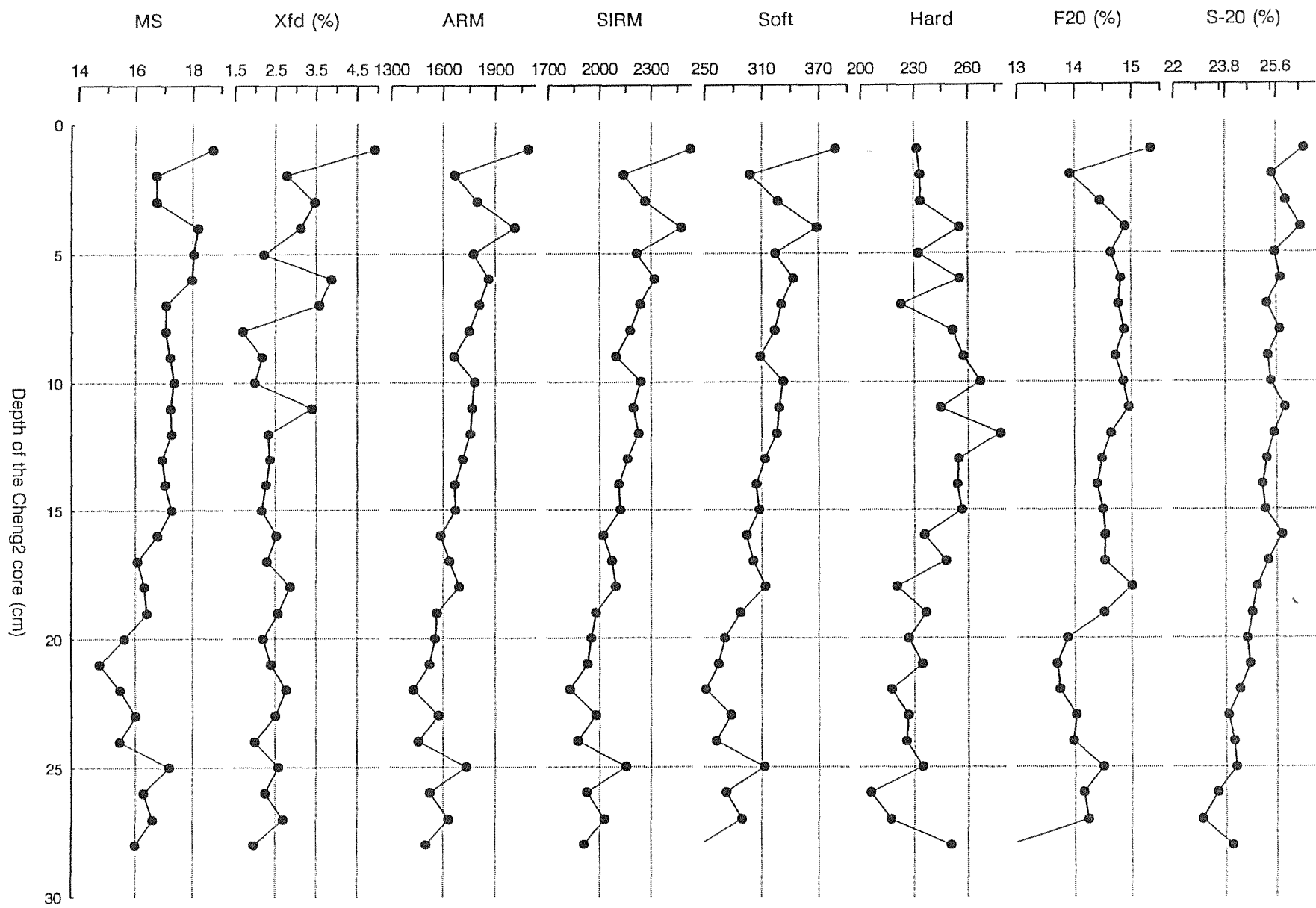


图 8 长江下游澄湖表层沉积物 Chen 2 孔深度—磁参数曲线



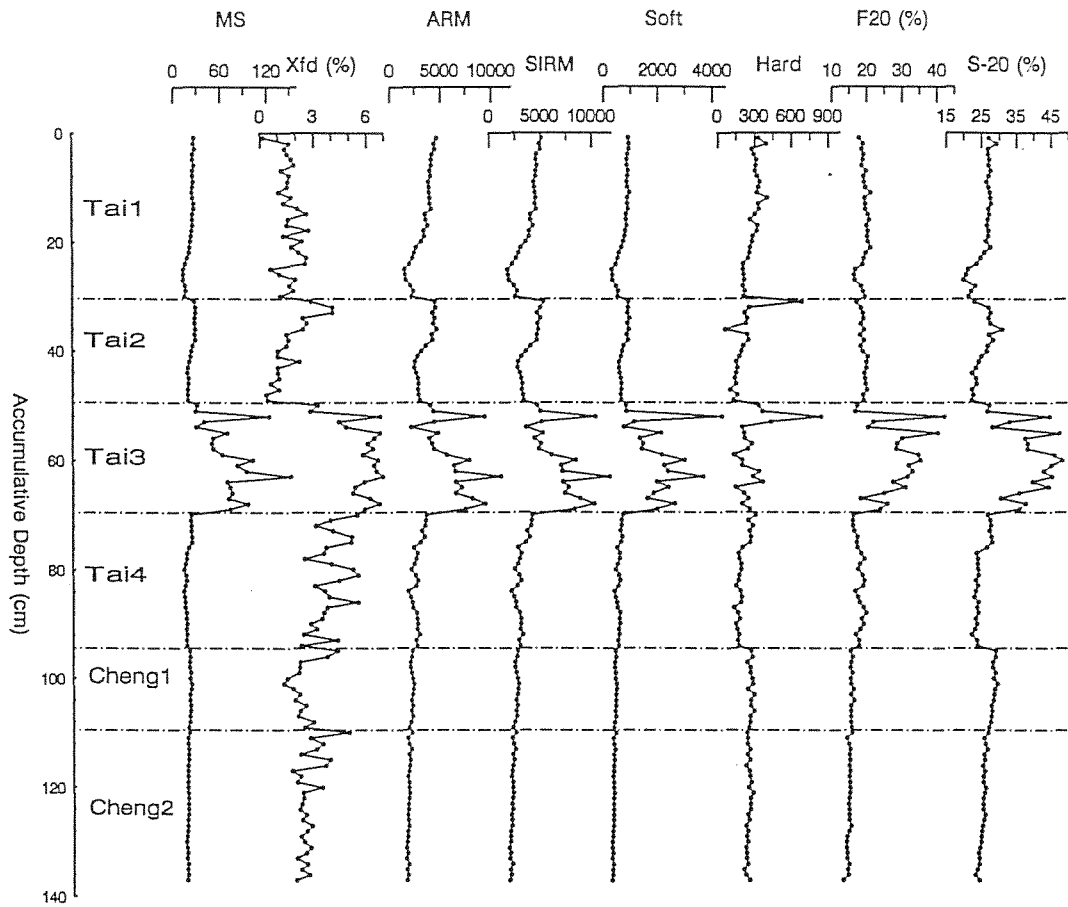


图 9 长江下游太湖及澄湖不同地点表层沉积物的  
累积深度—磁参数曲线比较

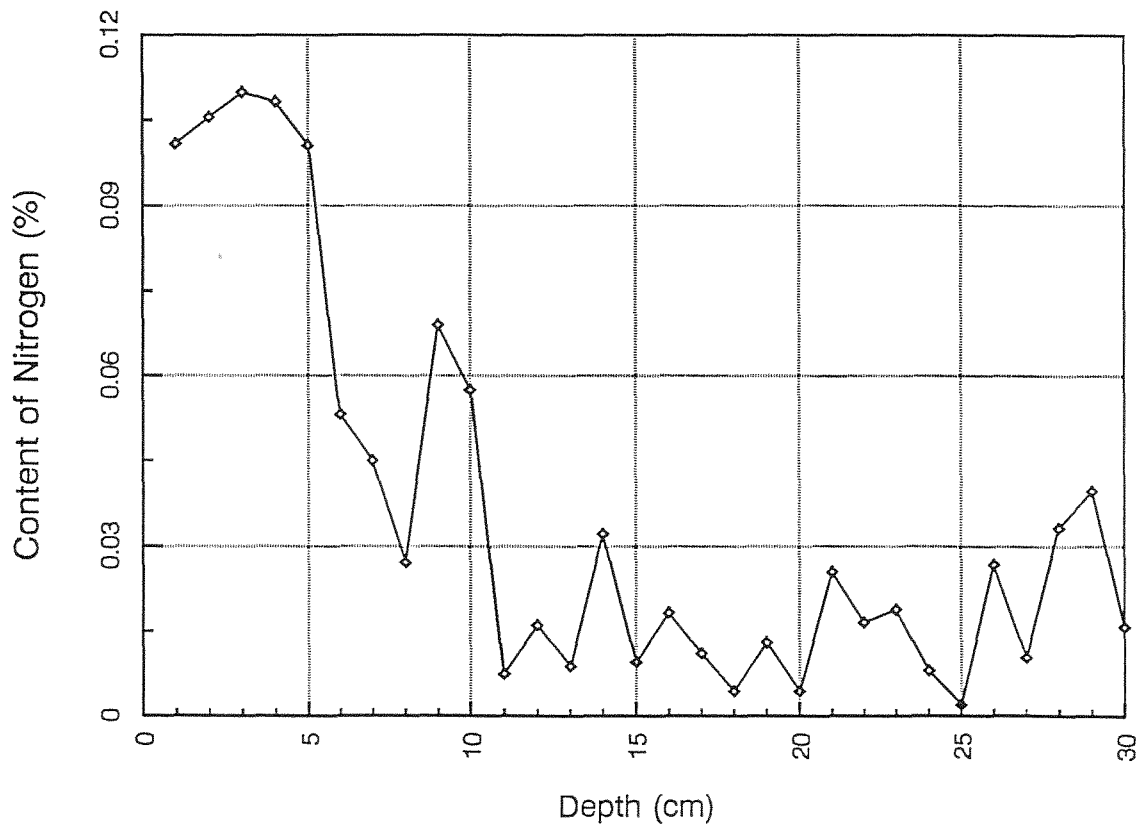
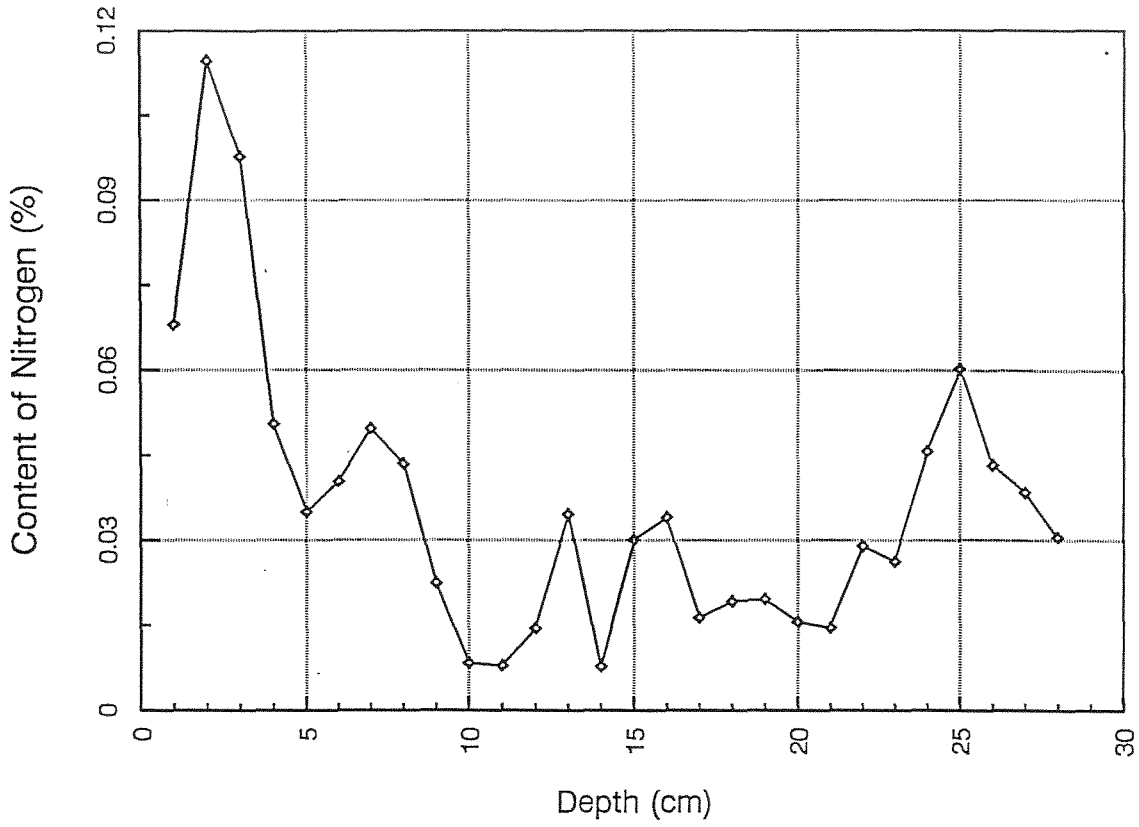


图 10 长江下游太湖 (Tai 1 孔) 及澄湖 (Chen 2 孔) 表层沉积物的氮含量及随深度的分布

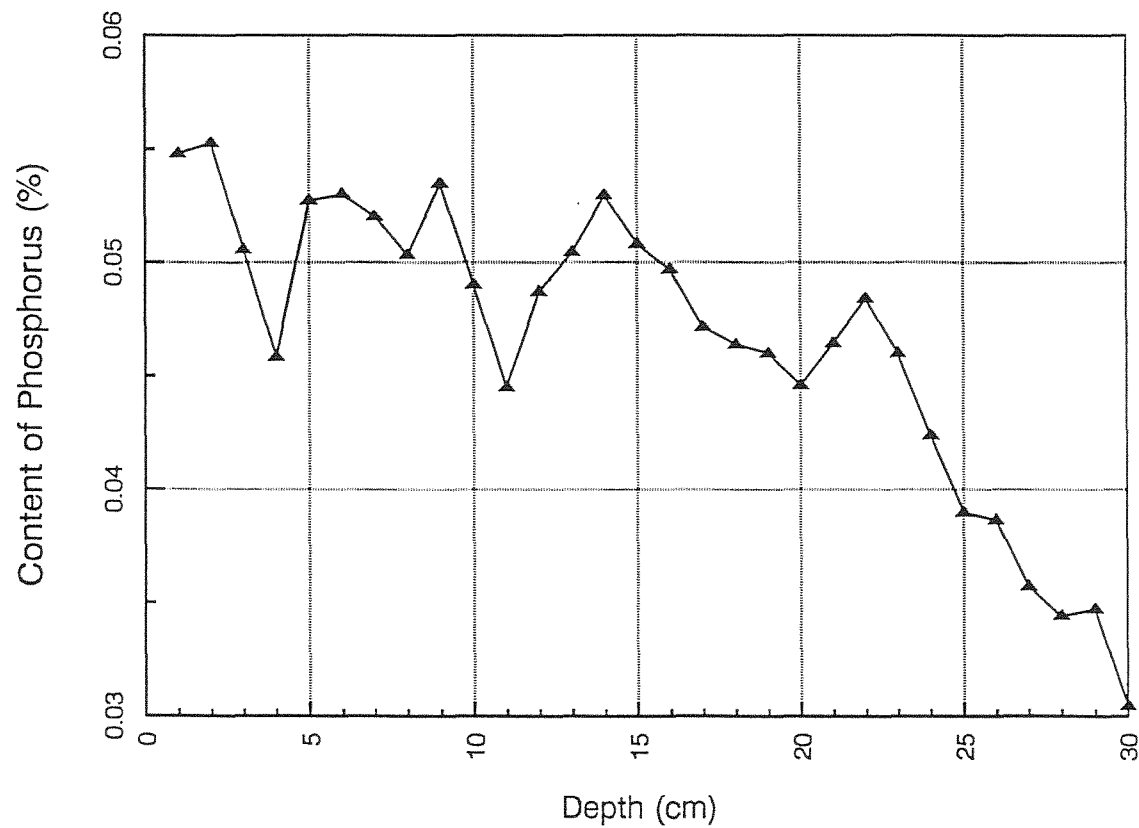
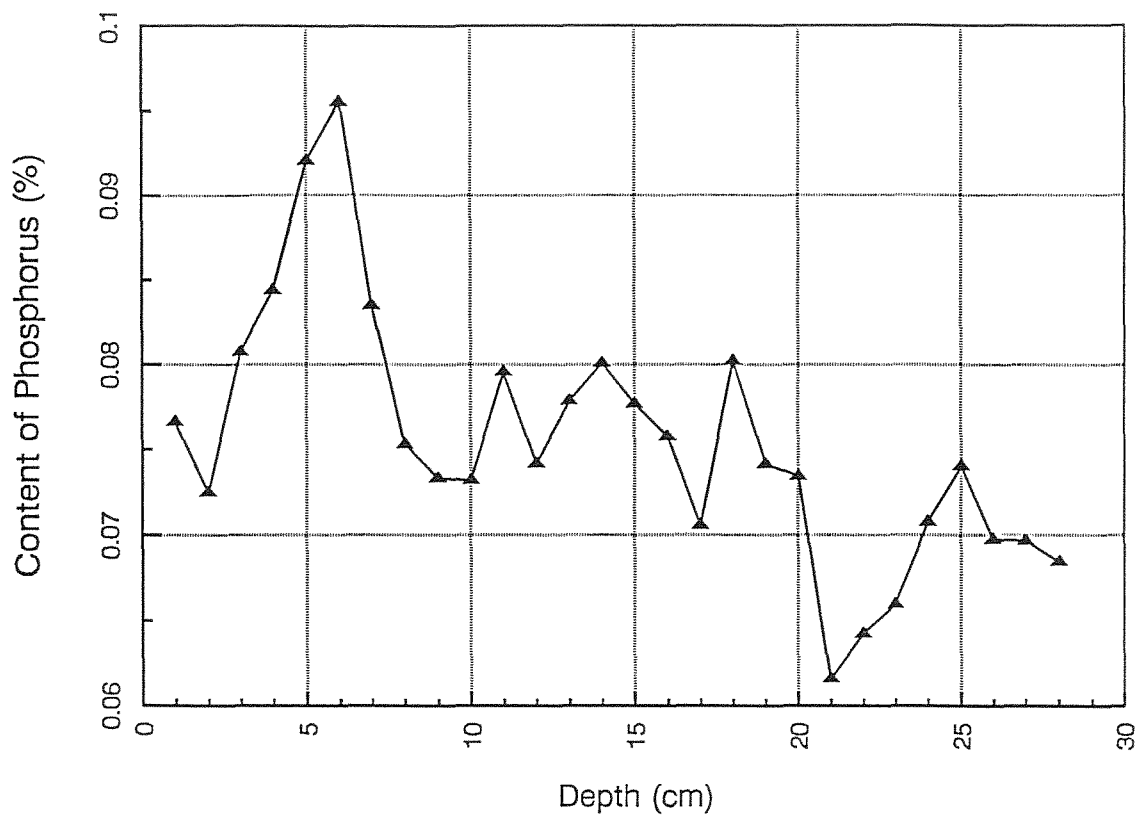


图 11 长江下游太湖 (Tai 1 孔) 及澄湖 (Chen 2 孔) 表层沉积物的磷含量及随深度的分布

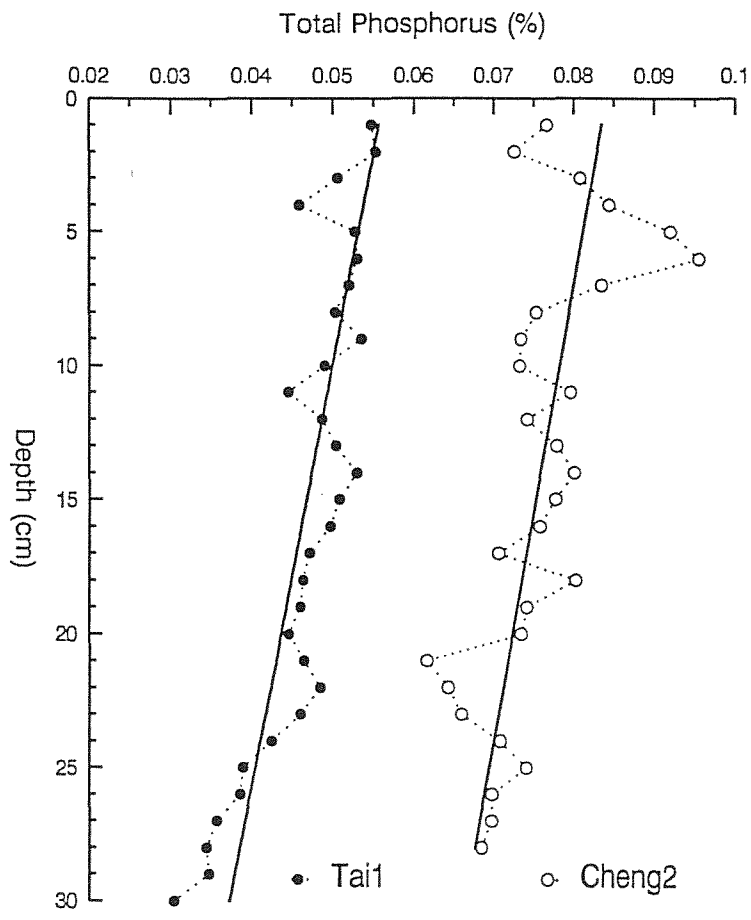


图 12 长江下游太湖 (Tai 1 孔) 与澄湖 (Chen 2 孔) 表层沉积物中磷含量的趋势分析及比较



## 8. Sediment geochemistry of lakes near Shanghi.

John Boyle

The sediments in six cores from 3 lakes (Tai Hu, Chen Hu and Ge Hu) have been chemically analysed using isotope source XRF (Figure 1). Heavy metals have been determined by flame atomic absorption analysis in four of the cores from (Figure 2a,b).

### **Tai Hu cores TAI 1-2L, TAI 2-2L and TAI 1-1 – Major elements**

The cores TAI 1-2L, and TAI 1-1 have been analysed for a wide range of elements. In the case of TAI 2-2L few samples were measured, and these only by XRF. The purpose was to compare this with TAI 1-2L, and the results in Figure 1 show them to be strikingly similar. Both show that two fundamentally different sediment types are present. The lower part of each core is a chemically immature, base-rich sediment, very different from typical lake sediment. It is likely that this represent old wind, blown sediment. Above this sediment is base-poor sediment, typical of mineral-rich lake sediment. The date of the contact is uncertain, but it is likely that a large hiatus is present within it.

The upper half of the sediment can be divided into two parts, as is made clear in Figure 2. Below 25-28 cm in TAI 1-2L and TAI 1-1 the sediment is rich in Si and Zr and depleted (relatively) in the other major and minor elements. The correlation of Zr with Si suggests that this is silt dominated. A profound change in the Fe and Mn signal occurs within this lower part. The Mn concentration is relatively high at the base of the unit, but falls sharply at 50 cm. A sharp increase in the Fe concentration slightly predates this event. The Fe concentration then falls again, at 40 cm. The most likely explanation for the Mn fall at 50 cm is declining oxygen in the sediment.

At 25-28 cm the proportion of clay (indicated by Ti and K) increases sharply.

### **Chen Hu – Major elements**

The two cores from Chen Hu are not as similar to each other as those from Tai Hu. The 70 cm of CHEN 2-2L are monotonous, whereas a sharp break is present in CHEN 1-2L at 30 cm. Superficially, the compositional variation in CHEN 1-2L resembles that in Tai Hu. However, there are great differences, particularly in the case of the basal sediment.

### **Ge Hu – Major elements**

A single short core from Ge Hu has been analysed. This shows little variation, and is similar to the other surficial sediments.

### **Taihu – trace elements**

The two TAI 1 cores both show the same strong trace metal enrichment in the upper layers (20 cm in TAI 1-1 short, and 28 cm in TAI 1-2L). Cd, Cu, Pb and Zn all show the same pattern, increasing in concentration sharply at first, and then flattening off. Cd and Pb appear to have levelled off, while there is some sign that Cu continues to increase. However, these effects are subtle, and really the concentrations are fairly constant in the upper 10-20 cm.

In Taihu the initial rise in all of the trace metals is accompanied by an increase in Ti and K, and a decrease in Si and Zr. The correlation of Si with Zr points to a silt association, and decoupling of K and Ti from this suggests that they are present in a different size class; clay is most likely. Thus, the initiation of industrial contamination of the lake sediments coincides with a pulse in clay supply. This pulse is quite short lived, though the Ti and K concentrations do not return to pre event values entirely.

Shortly after the clay pulse and trace metal enrichment there is an increase in the sediment sulphur concentration. This, like the clay pulse, is short lived. It could represent organic matter concentration, and thus possibly enhanced productivity. The pulse in Ca might be associated with such as eutrophication.

### **Chenhu - trace elements**

CHEN 2-2 shows no such clear trace metal signal as is seen in Taihu. Cd, Pb and Zn all increase in concentration slightly up-core. However, the effect is subtle, and is to some extent matched by the K and Ti curves, suggesting that natural clay supply variations could explain any trends. The absolute concentrations are far higher than is seen at the base of the two Taihu cores. Perhaps this is related to the higher K content, and to higher clay concentrations.

All of the trace metals shows a peak in concentration at 4-5 cm. This is accompanied by peaks in Mn, Fe, Ti and K. A clay explanation seem unlikely as the trace metals are more strongly enriched than either K or Ti. Some kind of supply association with Mn and Fe is more likely. The high accumulation rate makes a diagenetic cause unlikely.

### **Gehu- trace elements**

Gehu has generally low trace metal concentration, with the sediment superficially resembling the basal sediment of Taihu. There is some sign of a subsurface increase in Cd, Zn and possibly Cu at 4-5 cm. This is particularly marked if we consider the Ti and K concentration profiles, but of which decrease up-core. If we take TAI 1-1 as a model, then for a 5 ppm increase in Zn, we should get 1.5 ppm increases in Pb and Cu, and 0.02 ppm increase in Cd. This plausibly fits the observed data.

Figure 1. Major elements in all cores

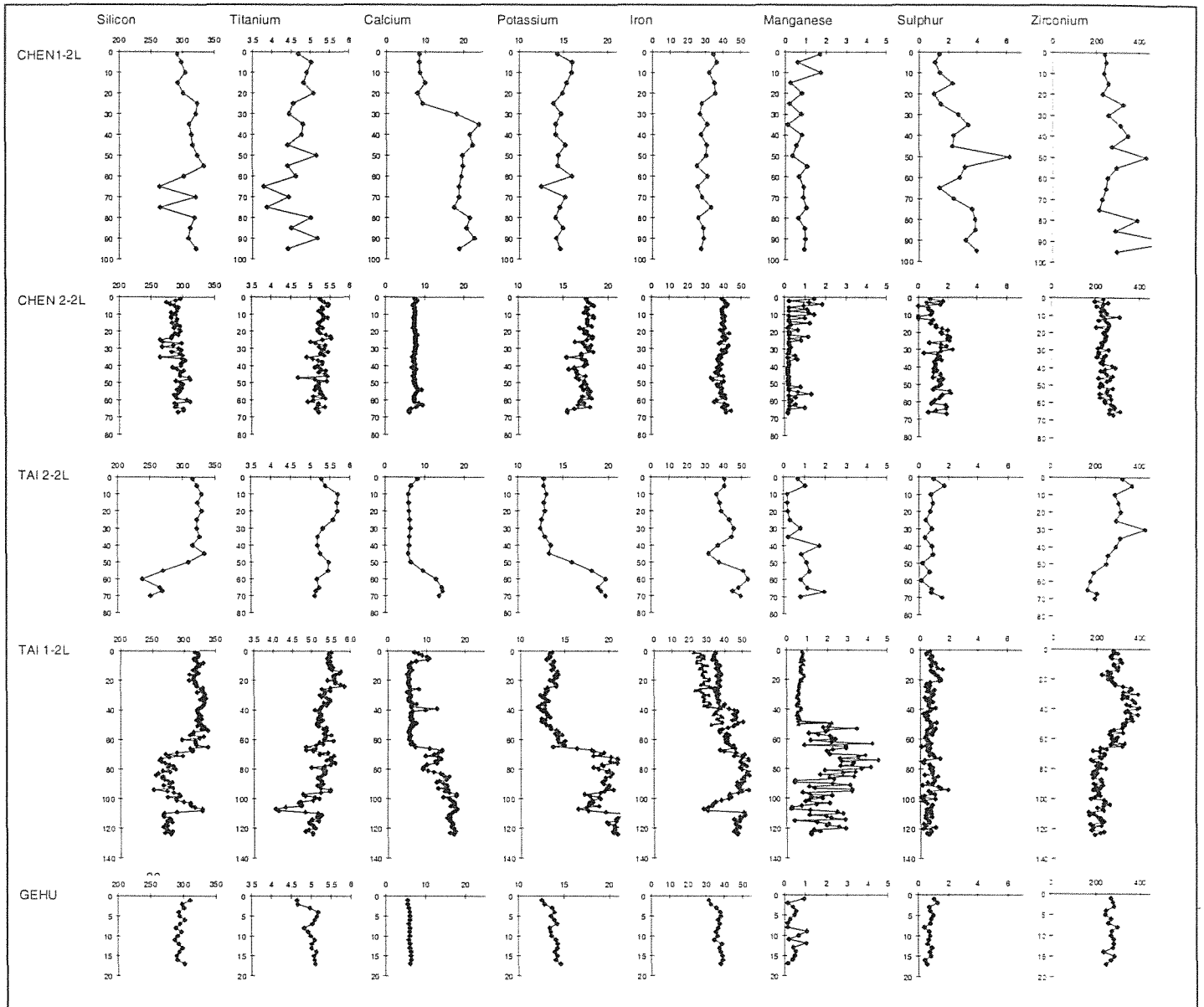


Figure 2 a. Major elements in the upper parts of 4 cores

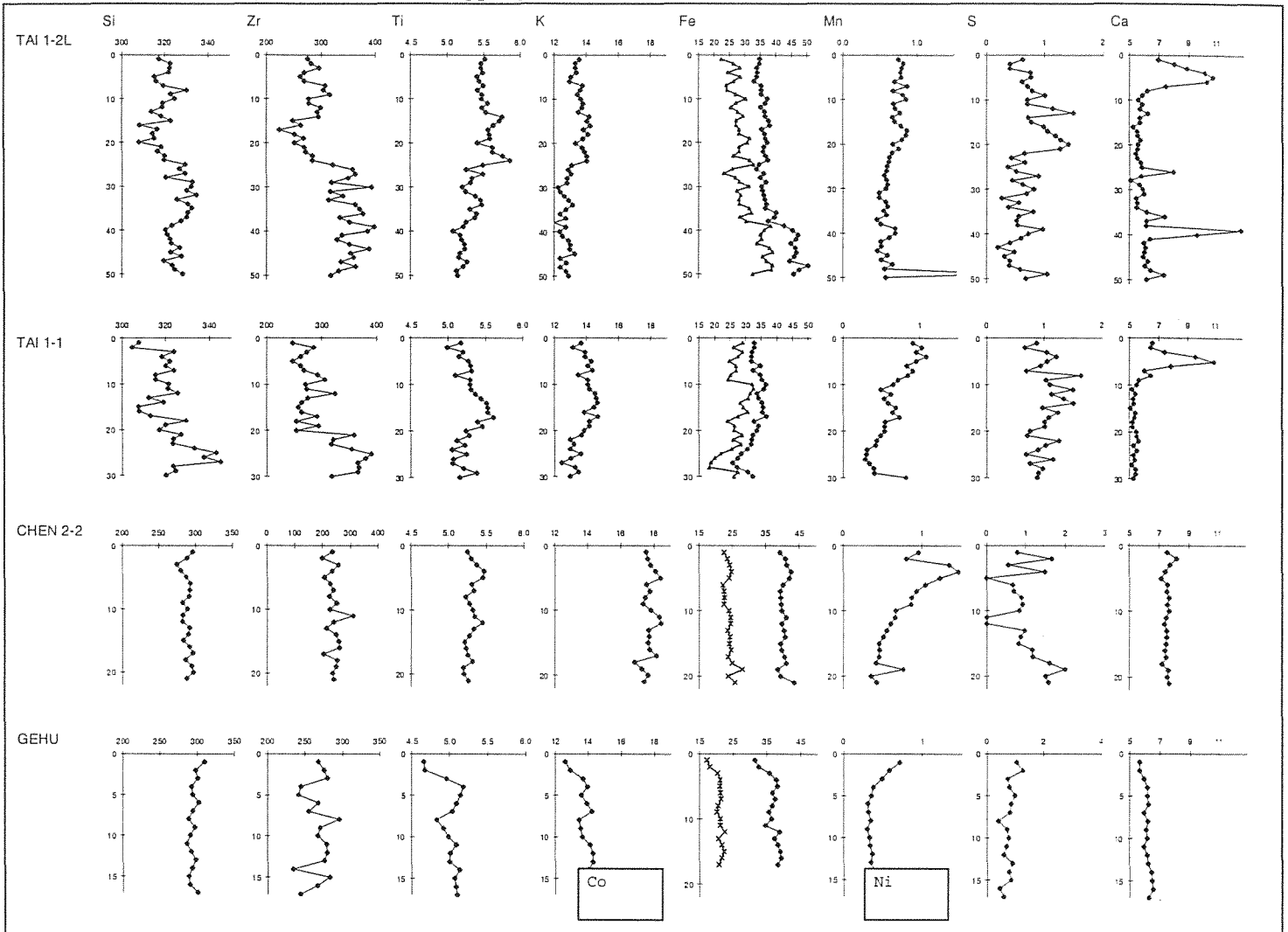
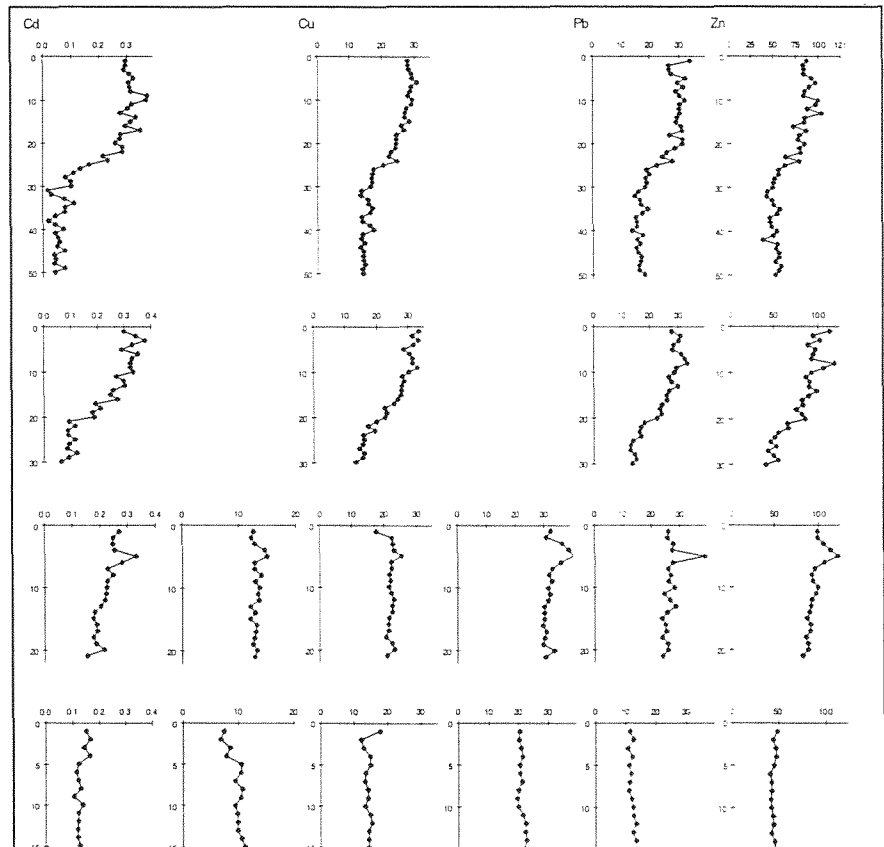


Figure 2b  
Trace element concentration profiles



## 9. Report on short core lithostratigraphy and diatom analyses

Helen Bennion

### Dry weight and loss on ignition results

A short sediment core from each of the seven sites was extruded in the field and sliced at 1 cm intervals to the core base. The percentage dry weight (% DW) for each sample was calculated by weighing approximately 1g of wet sediment in a pre-weighed crucible, from each pre-homogenised sediment layer, drying the sediment at 105°C for at least 16 hours, then reweighing the crucible. Approximate organic matter content was then determined as a percentage loss on ignition (% LOI) by placing the crucible containing the dried sediment in a muffle furnace at 550°C for two hours and then reweighing.

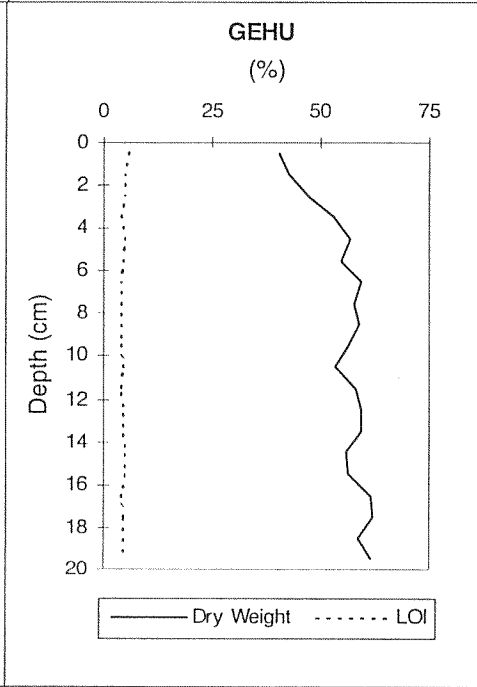
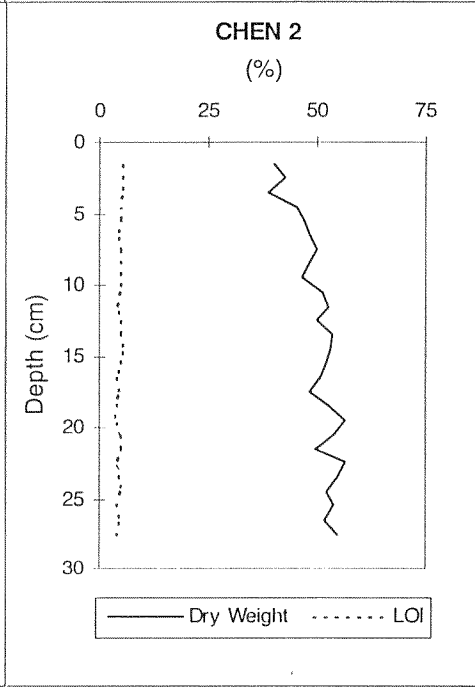
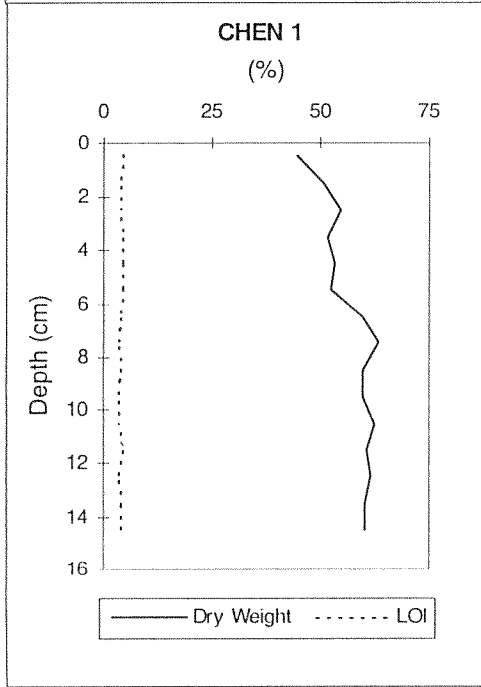
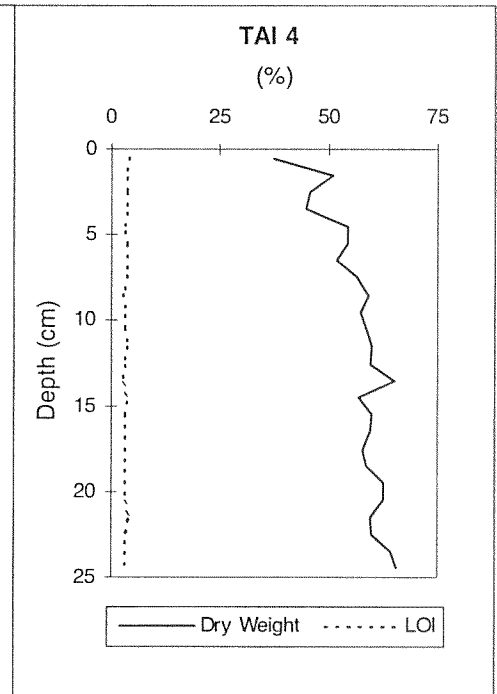
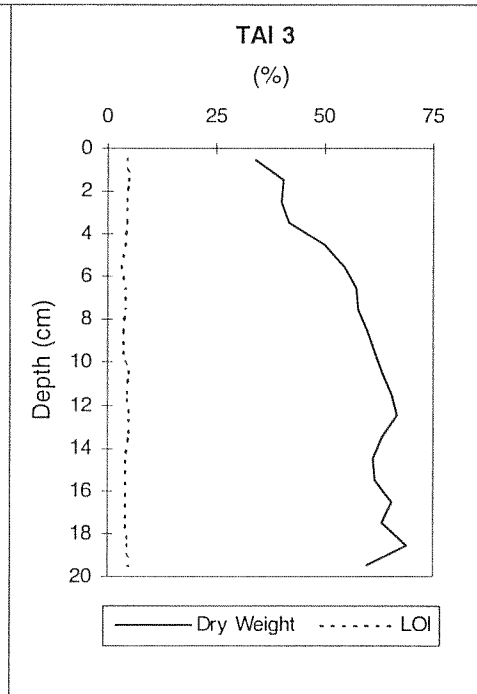
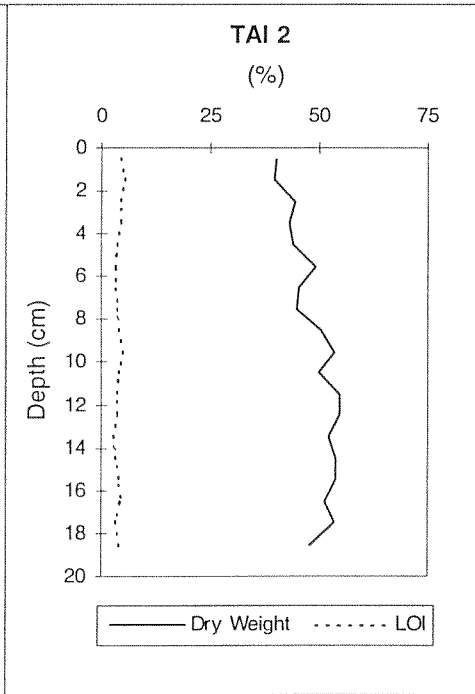
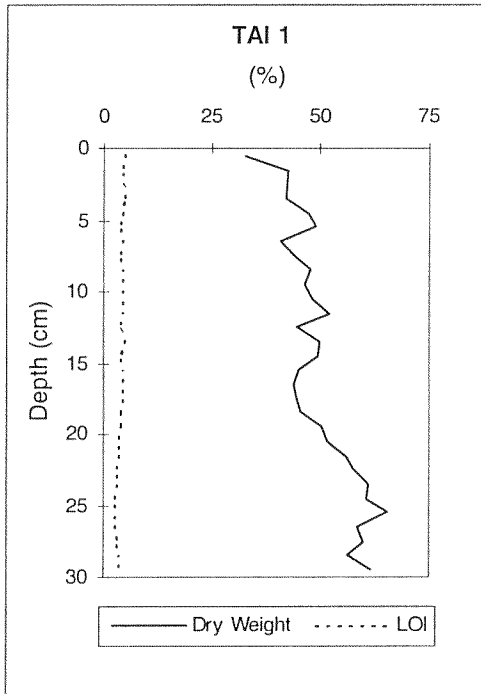
The results are shown in Figure 1. The four cores from Tai Hu all had similar profiles with extremely low %LOI values throughout the cores of approximately 3-4%, and high % DW values of c. 50-60% in the lower core sections, decreasing slightly to c. 30-40% in the upper part of the cores. These data suggest that the material is very low in organic matter content and appears to contain a high clay fraction. The cores from Cheng Hu and Ge Hu exhibited similar % DW and % LOI profiles to those from Tai Hu with very low % LOI values of c. 4% and high % DW values of c. 50-60% in the lower core sections declining to c. 40% towards the top of the cores.

### Diatom results

Three samples from each of the short sediment cores were prepared and analysed for diatoms using standard techniques. Diatom preservation was extremely poor in all of the cores from Tai Hu. The surface sediments contained largely planktonic diatoms, most commonly *Aulacoseira granulata*, with some *Cyclotella meneghiniana*, *Stephanodiscus* spp, *Navicula* spp. and *Nitzschia* spp. These taxa are indicative of nutrient-rich, alkaline waters. The samples lower in the cores appeared to have a high clay fraction and contained only a few fragments of *A. granulata*. The samples from the Cheng Hu cores were remarkably similar to those from the four Tai Hu cores. Ge Hu was markedly different, however, and the surface sediment assemblage was comprised of non-planktonic taxa such as *Fragilaria brevistriata*, *Cocconeis placentula*, *Achnanthes* spp., and *Cymbella* spp, all taxa found attached to plants or the sediment surface. This reflects the greater light penetration and dominance of submerged macrophytes at Ge Hu compared with the poor water clarity at Tai Hu and Cheng Hu. Fragments of *Fragilaria* spp. only were found in the downcore samples from the Ge Hu core.

### Long cores

Further to the screening of the Tai Hu short cores, a number of samples from lower in the core TAI 1L were prepared to examine whether there was preservation of diatom valves in the older core sections (30 - 80cm). Unfortunately, the material was highly minerogenic (largely clay particles) and contained no traces of diatom remains.



## 10. Spheroidal Carbonaceous Particle report

Neil Rose

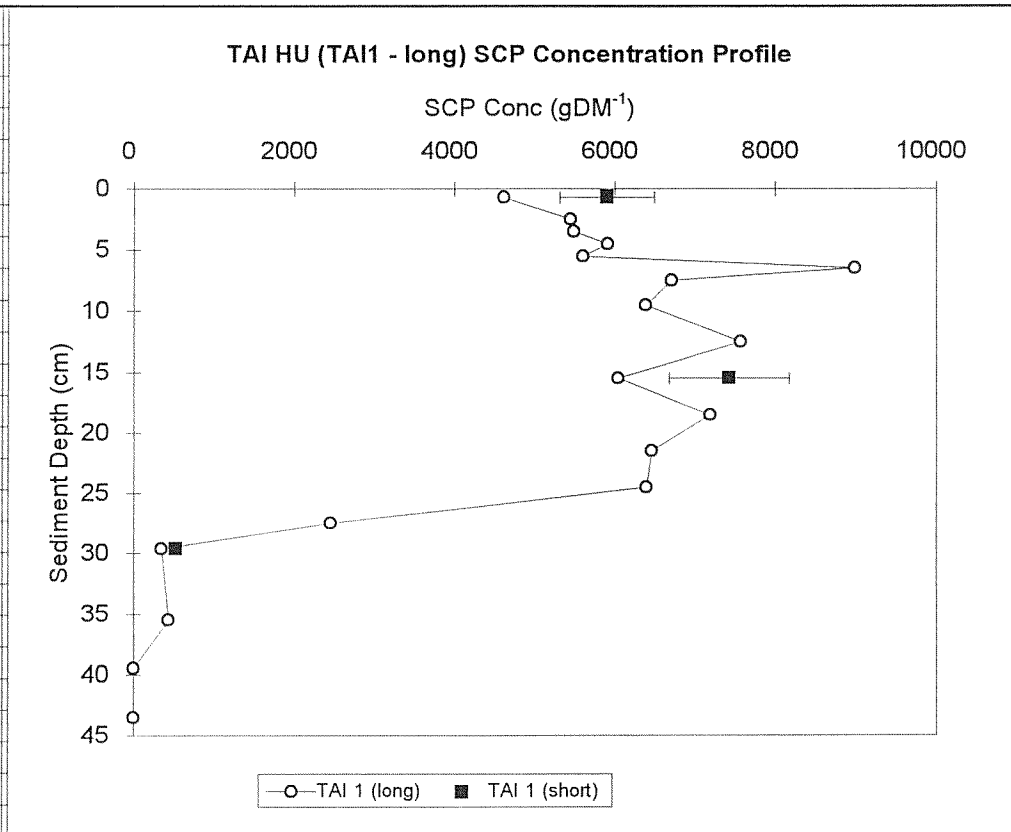
Spheroidal carbonaceous particles (SCPs) are produced from the high temperature combustion of fossil-fuels and are emitted to the atmosphere along with the flue-gases. They are not produced from any natural source and therefore act as unambiguous indicators of atmospheric deposition from this industrial source.

All seven short cores from the 1998 coring of Taihu, Chenghu and Gehu were screened for SCPs. Full analyses of the TAI 1 (long), TAI 4 (short), CHEN 2 (long), and the GEHU 1 cores were undertaken and the results and data are given in tables and figures on the following pages. The screened data from the short cores from TAI 1 and CHEN 2 are also shown on the profiles and confirm a reasonable agreement between the records of the respective cores.

The Tai Hu cores appear to show recognisable SCP profiles with features (rapid increase in concentration, sub-surface concentration peak) in common with many cores analysed from other areas of the world. Here,  $^{210}\text{Pb}$  chronologies suggest that the rapid increase feature in TAI 1 and TAI 4 occur in the 1940s and 1950s respectively, while the concentration peaks occur in c.1990 and the mid-1980s respectively.

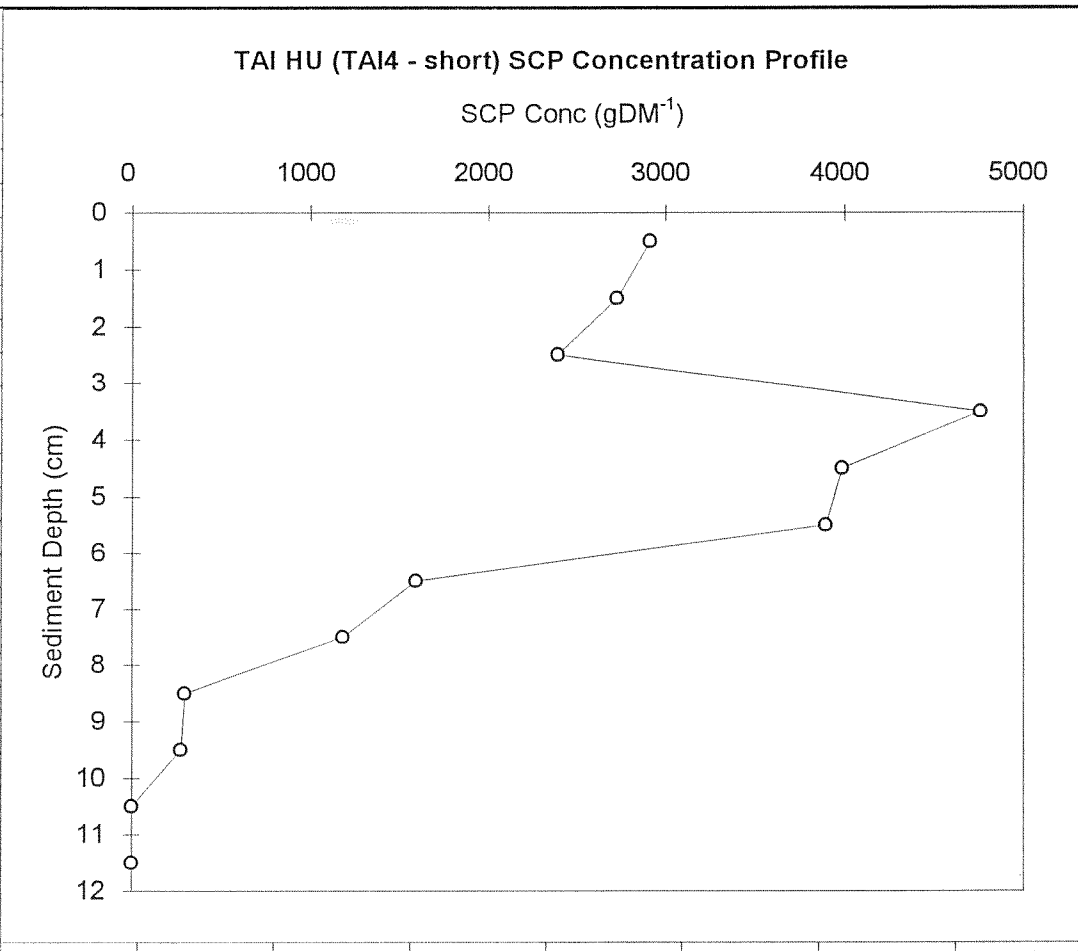
The CHEN 2 core shows a rapid increase from zero at 66-67cm to over  $3000 \text{ gDM}^{-1}$  at 54 - 55cm. This is below the reach of the  $^{210}\text{Pb}$  chronology but extrapolated data would suggest that this might be around the start of the 20th century or late-19th century. Above this depth, concentrations fluctuate considerably without any real trend except for a significant trough at 16 - 18cm (late 1960s - early 1970s). The explanations for these trends are currently unclear. The SCP profile for Gehu shows no real trends.

TAI HU			
TAI 1 (long)			
Mid-depth (cm)	SCP Conc (gDM <sup>-1</sup> )	90% C.L. (gDM <sup>-1</sup> )	(short)
1	4618	5630 - 3606	5903 (0-1)
2.5	5451	6306 - 4595	
3.5	5491	6245 - 4738	
4.5	5910	6876 - 4945	
5.5	5605	6406 - 4804	
6.5	8987	10048 - 7927	
7.5	6710	7566 - 5854	
9.5	6387	7300 - 5474	
12.5	7567	8377 - 6758	
15.5	6041	6847 - 5236	7424 (15-16)
18.5	7193	8054 - 6322	
21.5	6458	7220 - 5696	
24.5	6397	7220 - 5574	
27.5	2460	2942 - 1978	
31.5	351	523 - 179	530 (29-30)
35.5	438	686 - 190	
39.5	0	0 - 0	
43.5	0	0 - 0	





TAI HU		
TAI 4 (SHORT)		
Mid-depth (cm)	SCP Conc (gDM <sup>-1</sup> )	90 % C.L. (gDM <sup>-1</sup> )
0.5	2913	3627 - 2200
1.5	2727	3172 - 2281
2.5	2392	2944 - 1839
3.5	4759	5656 - 3861
4.5	3986	4963 - 3009
5.5	3892	4461 - 3324
6.5	1593	2044 - 1142
7.5	1182	1517 - 848
8.5	296	441 - 151
9.5	272	461 - 84
10.5	0	0 - 0
11.5	0	0 - 0



CHENG HU			
CHEN 2 (long)			
Mid-depth (cm)	SCP Conc (gDM <sup>-1</sup> )	90% C.L. (gDM <sup>-1</sup> )	(short)
0.5	2949	3751 - 2147	3136
1.5	2726	3338 - 2113	
2.5	3164	3825 - 2503	
3.5	3223	3968 - 2479	
4.5	2594	3298 - 1889	
5.5	3626	4420 - 2831	
6.5	3620	4413 - 2827	
8.5	3051	3704 - 2399	
10.5	3622	4483 - 2761	
12.5	2997	3710 - 2285	
14.5	1933	2532 - 1334	1565
16.5	1350	1850 - 850	
17.5	1343	1932 - 755	
18.5	3091	3805 - 2377	
19.5	2551	3158 - 1945	
22.5	3359	4135 - 2583	
24.5	3211	3897 - 2524	
27.5	3241	4011 - 2470	2973
29.5	3415	4203 - 2626	
32.5	2907	3489 - 2326	
34.5	2307	2779 - 1836	
37.5	2611	3198 - 2024	
39.5	3581	4329 - 2833	
42.5	2170	2719 - 1621	
45.5	1813	2374 - 1251	
48.5	2401	2972 - 1830	
54.5	3016	3677 - 2355	
57.5	2132	2671 - 1592	
60.5	1067	1415 - 718	
66.5	0	0 - 0	

